5-2011

Development of an Autonomous Mammalian *lux* Reporter System

Daniel Michael Close
dclose@utk.edu

To the Graduate Council:

I am submitting herewith a dissertation written by Daniel Michael Close entitled "Development of an Autonomous Mammalian *lux* Reporter System." I have examined the final electronic copy of this dissertation for form and content and recommend that it be accepted in partial fulfillment of the requirements for the degree of Doctor of Philosophy, with a major in Life Sciences.

Gary S. Sayler, Major Professor

We have read this dissertation and recommend its acceptance:

Mitch Doktycz, Cynthia Peterson, Todd Reynolds, Dan Roberts

Accepted for the Council:

Carolyn R. Hodges

Vice Provost and Dean of the Graduate School

(Original signatures are on file with official student records.)

Development of an Autonomous Mammalian *lux* Reporter System

A Dissertation Presented for the

Doctor of Philosophy Degree

The University of Tennessee, Knoxville

Daniel Michael Close

May 2011

Acknowledgements

I would like to acknowledge the guidance and support of my major professor Dr. Gary Sayler, who provided me with experiences and opportunities beyond those afforded to most students during my tenure in his laboratory. I would like to express my gratitude to Dr. Steven Ripp, who contributed significantly to the scholarly merit of this dissertation and provided me with invaluable experience and advice towards the preparation of scientific papers and grant applications. I would like to thank all of my colleagues at the Center for Environmental Biotechnology, who shared with me their time and expertise in order to provide a solid foundation upon which to frame my research. I would also like to acknowledge all of my fellow graduate students, who provided me with the motivation to work hard and achieve my goals.

Finally, I would like to thank my family for instilling in me the wonder of the world around me and providing me with the encouragement that has constantly fueled my ability to investigate and explore that wonder. Without their support little of what I have accomplished, academically or otherwise, would have been possible.

Abstract

Since its characterization, the definitive shortcoming of the bacterial luciferase (*lux*) bioluminescent reporter system has been its inability to express at a functional level in the eukaryotic cellular background. While recent developments have allowed for *lux* function in the lower eukaryote *Saccharomyces cerevisiae*, they have not provided for autonomous function in higher eukaryotes capable of serving as human biomedical proxies. Here it is reported for the first time that, through a process of poly-bicistronic expression of human codon-optimized *lux* genes, it is possible to autonomously produce a bioluminescent signal directly from mammalian cells. The low background of the bioluminescent signal, along with its characteristic lack of substrate amendment required for bioluminescent production, makes a mammalian-based *lux* reporter system ideal for real-time monitoring of cell culture or murine model systems. The delectability of a *lux*-based system provides for a functionally equivalent process to monitoring firefly luciferase-expressing cells under cell culture or subcutaneous imaging conditions without the well-documented uncertainties stemming from additional substrate introduction. However, the relatively blue-shifted emission wavelength of the *lux* reporter system, along with its low quantum yield, has been shown to reduce its effectiveness for use during deep tissue imaging of animal subjects. Despite these disadvantages, it has been demonstrated that a human cell line expressing the human codon-optimized *lux*

genes can function as a biosensor for determination of human bioavailability of toxic compounds and that, by regulating the production of the *luxC* and *luxE* genes, the *lux* system can be employed as the first mammalian, real-time, fully autonomous bioreporter. These cell lines provide unique and efficient models for the detection and monitoring of human-relevant compounds of interest. The limiting reagent for bioluminescent production in the mammalian cellular background has been determined to be the cytosolic availability of the $FMNH_2$ co-substrate and, in light of this evidence, directions for future optimization have been characterized and evaluated in respect to their ability to increase bioluminescent yield under these conditions.

Table Of Contents

List Of Tables

Table Page

List Of Figures

Figure Page

CHAPTER I

Introduction

Background And Research Objectives

Biosensors, with their small size, relative simplicity, rapidity of operation, and continuous, real-time to near real-time monitoring capabilities, possess unique characteristics conducive to the high throughput and remote-based monitoring needs relevant to agricultural, environmental, pharmacological, and clinical sensing. While the most popular biosensors have traditionally incorporated enzymes or antibodies as their biorecognition elements, the development and use of whole-cell biosensors (those housed entirely within a bacterial or eukaryotic cell) has increased greatly in recent history because they possess some interesting advantages over their enzymatic and immuno-dependent counterparts. Primary among these advantages is the indication of bioavailability — the effect and interactions the analyte has on a living system. As opposed to analytical instruments that measure only the total concentration of a target analyte in a sample, whole-cell biosensors that measure bioavailability indicate that the analyte can be assimilated by or directly affect a living organism, thereby exposing possible toxic interactions. Another advantage of whole-cell bioreporters is that they can be designed to produce signal in a constitutive

manner, regardless of the presence of a target analyte. This makes them valuable tools for localization and monitoring of cellular activities under *in vivo*, *in vitro*, or *in situ* conditions in ways not possible with traditional analytical equipment.

One important consequence of bioreporter-based interrogation has been the recent rise of whole animal bioluminescent imaging (BLI). This technique is progressively becoming more widely applied by investigators from diverse backgrounds because of its low cost, high throughput, and relative ease of operation in visualizing a wide variety of *in vivo* cellular events (Baker 2010). The ability to visualize cellular processes or other biological interactions without the requirement for animal subject sacrifice allows for repeated imaging and releases investigators from the constraints of considering their process of interest on a "frame-by-frame" basis using labeled slides. In addition, the ability to continually monitor a single individual reduces the amount of measured variation and can reduce error, leading to higher resolution and less data loss. With continuing advances in the hardware and software required for performing these experiments, it is also becoming easier for researchers with little background in molecular imaging to obtain useful and detailed publication-ready images.

The mainstays of BLI are the light generating luciferase enzymes such as firefly luciferase, *Renilla* luciferase, *Gaussia* luciferase, *Metridia* luciferase, *Vargula* luciferase, or bacterial luciferase (Thompson, Nagata et al. 1989; Wood, Lam et al. 1989; Lorenz, McCann et al. 1991; Meighen 1991; Verhaegen and Christopoulos 2002; Markova, Golz et al. 2004). These bioluminescent proteins

are preferred over their fluorescent counterparts because the lack of endogenous bioluminescent reactions in mammalian tissue allows for near background-free imaging conditions whereas the prevalence of fluorescently active compounds in these tissues can interfere with target resolution upon exposure to the fluorescent excitation wavelengths required for the generation of signal output. Of these luciferase-based reporters, only those based on the bacterial luciferase gene cassette have the potential for development into a fully autonomous reporter system, negating the need for addition of a potentially influential substrate that could create undo error during the data acquisition process. The development of the bacterial luciferase gene cassette into a functional mammalian-based bioreporter has been the focus of this work and has been performed under the following experimental hypotheses:

- **Hypothesis 1**: Through a process of poly-bicistronic expression of *Photorhabdus luminescence* genes codon-optimized for expression in mammalian cells it will be possible to autonomously produce a bioluminescent signal in the human HEK293 cell line.

- **Hypothesis 2**: Bioluminescent expression driven by codon-optimized bacterial luciferase genes will allow improved temporal detection of signal compared to bioluminescent signal from firefly luciferase and fluorescent signal from green fluorescent protein in HEK293 cell culture and nude mouse models.

- **Hypothesis 3**: By regulating the expression of the *luxC* and *luxE* genes from the bacterial luciferase gene cassette it will be possible to construct a bioluminescent reporter capable of responding to changes in target analyte presence autonomously and in a near real-time manner.

- **Hypothesis 4**: HEK293 cells constitutively expressing bioluminescence through expression of the codon-optimized bacterial luciferase genes will be capable of acting as real-time biosensors to determine the mammalian bioavailability of toxic chemicals.

Literature Review

Bacterial luciferase

Bioluminescent bacteria are the most abundant and widely distributed of the light emitting organisms on Earth and can be found in both aquatic (freshwater and marine) and terrestrial environments. Despite the diverse nature of bacterial bioluminescence, the majority of these organisms are classified into three genera: *Vibrio*, *Photobacterium*, and *Photorhabdus* (*Xenorhabdus*). These bacteria often exist as symbiotes of other organisms, although some can be free-living in aquatic environments as well. Of the known genera of bioluminescent

bacteria, only those from the genus *Photorhabdus* have been discovered in terrestrial habitats (Meighen 1991).

Today it is well known that the bacterial bioluminescence reaction is the result of two proteins, LuxA and LuxB, that work together to produce light from the oxidation of a long chain fatty aldehyde in the presence of reduced riboflavin phosphate ($FMNH_2$) and oxygen, while the remaining proteins in the *lux* operon, LuxC, LuxD, and LuxE, function to regenerate the aldehyde substrate required for this reaction (Figure 1A). However, this was not always so evident. The study of bacterial bioluminescence is rooted in the lessons of general bioluminescence. The idea that oxygen was a required substrate for bioluminescent reactions stems from Robert Boyle's early experiments in the mid 1600's showing that removal of oxygen caused the cessation of light from what was either luminescent bacteria or fungi (Boyle 1666). In the late 1880's when it was discovered from work in beetles that bioluminescence required a luciferase and a luciferin for function, this knowledge was applied to the bacterial system as well (McElroy and Strehler 1954).

In 1942 Doudoroff was one of the first to observe and report on the metabolism of bioluminescent bacteria and found that all were able to tolerate oxygen, aiding in the confirmation that oxygen was required for light production (Doudoroff 1942). Although the first published report of a bioluminescent reaction occurring outside of a bacterium occurred in 1920, it could not be reproduced reliably until 1953 when McElroy and colleagues (McElroy, Hastings et al. 1953)

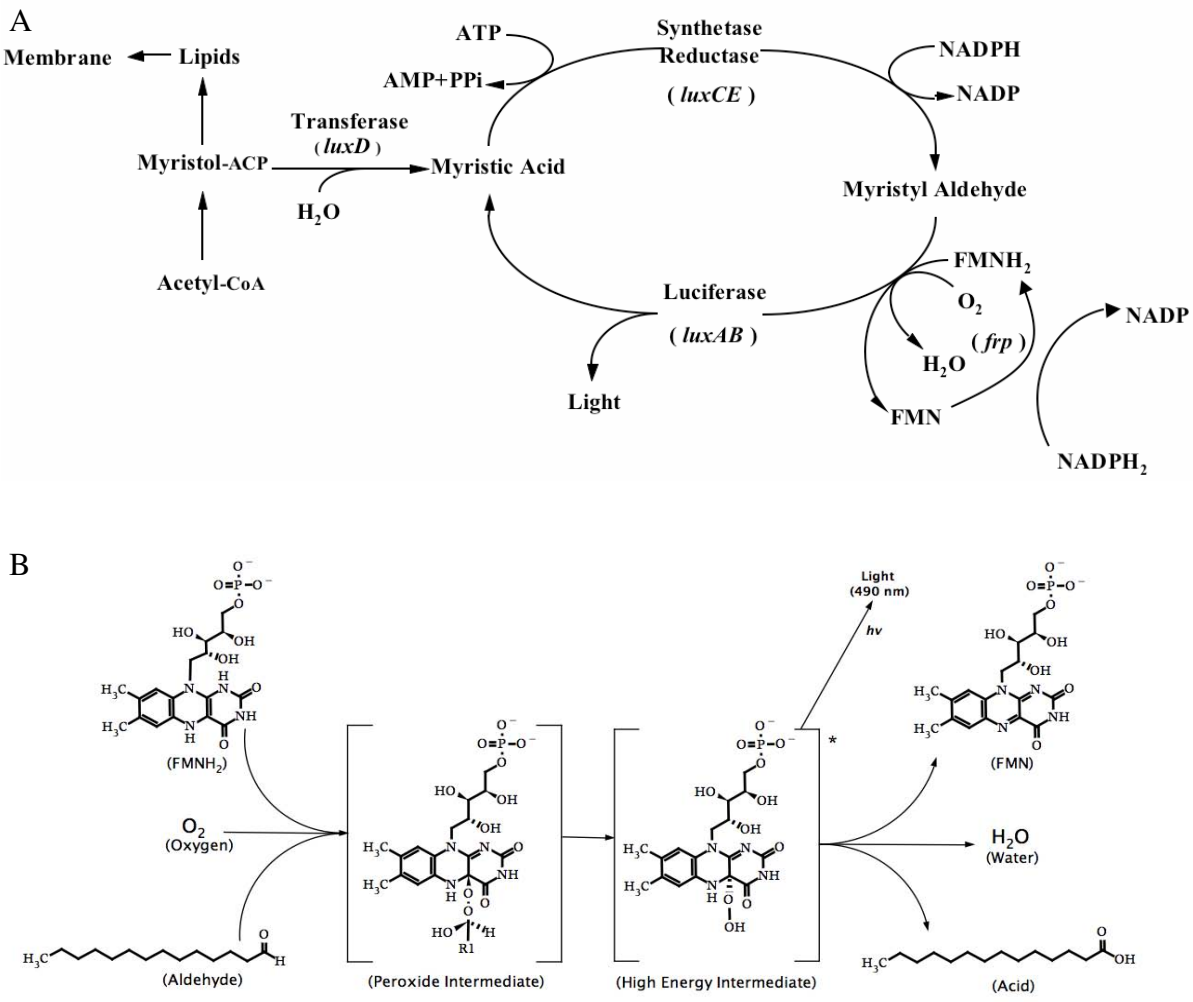

Figure 1. Bioluminescent reaction catalyzed by the bacterial luciferase genes.

A) The luciferase is formed from a heterodimer of the *luxA* and *luxB* gene products. The aliphatic aldehyde is supplied and regenerated by the products of the *luxC*, *luxD*, and *luxE* genes. The required oxygen and reduced riboflavin phosphate substrates are scavenged from endogenous metabolic processes, however, the flavin reductase gene (*frp*) aids in reduced flavin turnover rates in some species. B) The production of light, catalyzed by the products of the *luxA* and *luxB* genes, results from the decay of a high energy intermediate (R1 = $C_{13}H_{27}$). Originally published in (Close, Ripp et al. 2009), reprinted with permission.

were able to consistently produce light from autolysates of *Achromobacter fischeri* cultures upon addition of FMN. At this time they also reported the requirement for a luciferin compound of unknown structure. This was the first indication that FMN was required for bacterial bioluminescence. It was not until the next year that the structure of the luciferin was confirmed to be a long chain fatty aldehyde (Strehler, Harvey et al. 1954).

This completed the list of required substrates, and an understanding was established that bacterial luciferase catalyzes the production of light through oxidation of a long chain fatty aldehyde in the presence of oxygen and reduced riboflavin phosphate. The genes encoding the bacterial luciferase were first cloned and expressed in *E. coli* in 1982 (Belas, Mileham et al. 1982), while the full bacterial luciferase cassette was cloned and expressed the next year (Engebrecht, Nealson et al. 1983). In the mid 1990's the first crystal structure of the bacterial luciferase heterodimer was determined (Fisher, Raushel et al. 1995), providing the first glimpse at the proteins that had captured researchers imaginations for hundreds of years.

When the bacterial luciferase enzyme is supplied with oxygen, $FMNH_2$, and a long chain aliphatic aldehyde, it is able to produce light primarily at a wavelength of 490 nm. There is a secondary emission peak at 590 nm, however, this is only detectable using highly sensitive Raman scattering (Thouand, Daniel et al. 2003). The natural aldehyde for this reaction is believed to be tetradecanal, however, the enzyme is capable of functioning with alternative aldehydes as substrates (Meighen 1991). The first step in the generation of light from these substrates is

the binding of $FMNH_2$ by the luciferase enzyme, and until recently its active site on the enzyme was not known. It has recently been confirmed, however, that $FMNH_2$ binds on the α subunit in a large valley on the C-terminal end of the β-barrel structure (Campbell, Weichsel et al. 2009).

In order for the reaction to proceed, the luciferase must undergo a conformational change following $FMNH_2$ attachment. This movement is primarily expressed in a short section of residues known as the protease labile region—a section of 29 amino acids residing on a disordered region of the α subunit joining α-helix α7a to β-strand β7a. The majority of residues in this sequence are unique to the α subunit and have long been implicated in the bioluminescent mechanism (Baldwin, Christopher et al. 1995). Following attachment of $FMNH_2$, this region becomes more ordered and is stabilized by an intersubunit interaction between Phe272 of the α subunit and Tyr115 of the β subunit. This conformational change has been theorized to stabilize the α subunit in a conformation favorable for the luminescent reaction to occur (Campbell, Weichsel et al. 2009).

NMR studies have suggested that $FMNH_2$ binds to the enzyme in its anionic state ($FMNH^-$) (Vervoort, Muller et al. 1986). With the flavin bound to the enzyme, molecular oxygen then binds to the C4 atom to form an intermediate 4α-hydroperoxy-5-hydroflavin (Nemtseva and Kudryasheva 2007). It is important to note that this critical C4 atom was determined to be in close proximity to a reactive thiol from the side chain of Cys106 on the α subunit (Campbell, Weichsel et al. 2009), a residue that has long been hypothesized to play a role in the

bioluminescent reaction, but recently has been proven to be non-reactive through mutational analysis (Baldwin, Chen et al. 1987).

It has been shown, however, that C4 is the central atom for the luciferase reaction and, following establishment of the hydroperoxide there, it is capable of interaction with the aldehyde substrate via its oxygen molecule to form a peroxyhemiacetal group. This complex then undergoes a transformation (through an unknown intermediate or series of intermediates) to an excited state generally accepted to be a luciferase-bound 4α-hydroxy-5-hydroflavin mononucleotide. As this complex decays, it yields oxidized FMN, a corresponding aliphatic acid, and light (Figure 1B) (Nemtseva and Kudryasheva 2007). There have classically been many theories proposed to explain the exact process required for light emission (Hastings and Nealson 1977), and these continue to expand today as technology for detecting the intermediate complexes has improved. For a review of the proposed mechanism and their strengths and weaknesses, the reader is directed to Nemtseva and Kudryasheva (Nemtseva and Kudryasheva 2007).

While the bacterial luciferase protein is all that is required to generate light in the presence of its required substrates, it is often beneficial for investigators to express other genes from the operon in order to supply the luciferase with the substrates required for its autonomous function. To accomplish this, it is necessary to co-express the *luxC, luxD,* and *luxE* genes. The products of these genes assemble into a multi-enzyme complex and are responsible for biosynthesis of myristyl aldehyde using components already present in the cell, thus negating the requirement to supply an aldehyde substrate exogenously.

The *luxD* gene encodes a transferase protein and is the first to act in the aldehyde biosynthesis pathway. It is responsible for the transfer of an activated fatty acyl group to water, forming a fatty acid. During the course of this reaction the enzyme itself becomes acylated. The newly formed fatty acid is next passed off to the *luxC* gene product, which activates the acid by attaching AMP from a molecule of ATP, thereby creating a fatty acyl-AMP that remains tightly bound to the enzyme. The fatty acyl-AMP is then transferred to the *luxE* gene product via transfer of the acyl group. This protein acts as a reductase and catalyzes the reduction of the fatty acyl-AMP to aldehyde using NADPH to supply the required reducing power (Meighen 1991). This allows for the *in vivo* generation of the aldehyde substrate. Because the organism naturally supplies the remaining $FMNH_2$ and oxygen substrates, the co-expression of these genes represents the minimum requirement for allowing the *lux* system to operate in a fully autonomous fashion.

lux **biosensors and applications**

Prior to the demonstration of autonomous *lux* function in the mammalian cellular environment detailed here, the use of *lux* as a reporter has been limited solely to use in prokaryotic organisms and the lower eukaryote *Saccharomyces cerevisiae*. However, the experimental designs that have been employed are similar to those used when the system is expressed in a mammalian cellular host. The most basic bacterial luciferase associated reporter assays are those based on determining the presence or level of bioavailability of toxic compounds.

Taking advantage of the autonomous nature of the *lux* operon, bioreporters have been engineered to constitutively express light under environmental conditions. Upon exposure of the bioluminescent reporter to a toxic compound, it undergoes a metabolic slowdown or death, causing a decrease in the total bioluminescent signal (Kelly, Lajoie et al. 1999). These assays, such as the commonly used Microtox assay (Johnson 2005), can be used to indicate that a toxic compound is present but they do not necessarily identify what that compound is. To permit identification of the toxicant, multiple bioreporter types are engineered to specifically respond only to certain target compounds or analytes of interest. The ability of cells to regulate transcription in response to specific compounds is taken advantage of in these sensing strategies to create fusions of target specific gene sequences with the bioluminescent *lux* genes. Thus, when exposed to a target compound, these bioreporter cells will emit bioluminescent light signals that are either dependent on the addition of a decanal substrate (if only the *luxAB* genes are used) or fully autonomously (if the *luxCDABE* genes are used together) (Ripp, DiClaudio et al. 2009). A distinct advantage of the fully autonomous *luxCDABE*-based bioreporters is the ability to report target analyte presence continuously and in a real-time or near real-time format. Historically, one problem associated with real-time monitoring has been the slow turnover time of the bioluminescent reaction. Coupled with the long life of the luciferase heterodimer, this has made it difficult to resolve reporter function over short periods of time. In order to compensate for this, it has been demonstrated that inclusion of a protease tag can shorten the lifespan of the luciferase proteins and

increase the temporal resolution of *lux*-based reporters (Allen, Wilgus et al. 2007). In addition to the traditional chemical targets, *lux*-based reporter systems have also been designed to detect biological targets such as food and waterborne pathogens. In these systems, a bacteriophage, or bacterial virus, is used as a carrier of the *lux* genes and its ability to infect only certain bacterial hosts is exploited as a means towards delivering bioluminescence to a target bacterium (Ripp 2009).

An important advantage stemming from the autonomous nature of the bacterial luminescence cassette is that, since it does not require substrate addition for expression, it can be used remotely if coupled to a proper detection device. This allows for the monitoring of compounds of interest that may be inaccessible to the researcher under normal conditions because of logistical or safety concerns (Nivens, McKnight et al. 2004).

As a truly autonomous expression system, *lux* interfaces extremely well with signal transducers and has seen widespread use in biosensor applications. Fiber optic cables represent one of the easiest interfaces, with the bioreporters immobilized at one end of the cable and the other end terminating at a photomultiplier tube (PMT) or other luminometer-type device. The cable can then be inserted into liquid, solid, or gaseous samples to remotely monitor for target analytes such as heavy metals, polycyclic aromatic hydrocarbons (PAHs), or for a general assessment of sample toxicity (Heitzer, Malachowsky et al. 1994; Polyak, Bassis et al. 2001; Leth, Maltoni et al. 2002; Chang, Lee et al. 2004; Ivask, Green et al. 2007). Multi-fiber optical devices immobilized with differently target sensitive

bioreporters have also been developed and field tested for multiplexed monitoring (Hakkila, Green et al. 2004). In this same vein, but perhaps more user friendly, is the Lumisens 2 instrument developed by Horry (Horry, Charrier et al. 2007), a device where bacteria acting as *lux*-based reporters are immobilized on a disposable card rather than the fiber optic cable itself. A fiber optic cable then scans each individually immobilized bioreporter to monitor for bioluminescence output in a flow-through format. Similar flow-through samplers have been constructed using bioreactors containing growing cultures of the bioreporter into which bare fiber optic cables are inserted. Upon exposure to a target analyte or toxic intermediate, the bioreporter culture yields increased (or diminished) bioluminescence that is detectable via the integrated fiber optics. Continuous, on-line water toxicity monitoring has been demonstrated using small-scale (1–2 mL) bioreactors and larger commercially available systems such as the TOXcontrol sensor that can be plumbed into pre-existing water lines (Lee and Gu 2005). Fiber optics have also been used to monitor *lux*-expressing bacteria in their natural environment to non-invasively assess metabolic and physiological responses to ecosystem perturbations, for example, the addition of a contaminant (Dorn, Mahal et al. 2004).

Although functional, the requisite linkage of the fiber optic cable to a PMT or other light gathering device necessitates size and power constraints that are not conducive to miniaturization. To address this, several groups have developed different variations of chip-based microluminometers that can directly interface with the bioreporter organisms. This negates the need for a fiber optic cable to

channel the signal to a transducer and instead forms an all-inclusive bioreporter-on-a-chip biosensor. This technology was first demonstrated with the bioluminescent bioreporter integrated circuit (BBIC) that consisted of a small (1.5 × 1.5 mm), low-power (3 mW) CMOS microluminometer for light gathering and a transmitter for remote data transmission (Vijayaraghavan, Islam et al. 2007). Polymer encapsulants attach the bioreporters directly on to the BBIC surface or the BBIC can be interfaced with bioreporter inoculated flow-cells or bioreactors. For field monitoring, the BBIC has been incorporated into a handheld wand that operates off of an internal lithium watch battery (Figure 2) (Ripp, Daumer et al. 2003).

As a photodetector add on, MOEMS (Micro-Opto-Electro-Mechanical-System) can increase detection limits by minimizing system noise using an integrated heterodyne optical system (IHOS) technique that modulates bioreporter bioluminescence prior to photoconversion (Elman, Ben-Yoav et al. 2008). A MOEMS modulator/solid state photodetector interface has been tested with a *lux* bioreporter and a minimum detectable signal of 10^9 photons/sec/cm^2 was demonstrated. To accommodate multiplexed, multi-analyte sensing on a single chip, Eltoukhy *et al*. (Eltoukhy, Salama et al. 2006) designed a 128 channel array CMOS microluminometer capable of holding and individually sensing multiple bioreporters simultaneously, thus enabling high density fingerprinting of sample chemical makeup using any of the many differently analyte-specific bioreporters

Figure 2. Example of a CMOS microluminometer transducer in a hand-held biosensor format.

Bioreporter cells engineered to emit bioluminescent light signals are directly interfaced to the transducer element to form a compact and remotely operable biosensor. Originally published in (Close, Ripp et al. 2009), reprinted with permission.

available, all within a single lab-on-a-chip platform. Avalanche photodiodes (APDs) may also be of utility to bioreporter sensing as they can be designed for photon counting, much like a photomultiplier tube, but in a miniaturized standalone design (Yotter and Wilson 2003). APDs currently represent the most sensitive solid-state devices available and can achieve quantum efficiencies greater than 90%. However, they require higher operating voltages, generate excessive background noise that may mask low level signals generated from bioreporter cells, and their complex circuitry translates into high cost. Despite these disadvantages, Daniel *et al*. (Daniel, Almog et al. 2008) have preliminarily tested an APD in conjunction with a stress responsive *lux* bioluminescent bioreporter within a 10 µL sample chamber and demonstrated sufficient sensitivity at low part-per-million concentrations of a nalidixic acid inducer. This group has also recently developed an integrating sphere device capable of measuring absolute photon numbers emanating from bioluminescent cells, which, although too complex and fragile to serve as a biosensor, should find important utility in shaping factors fundamental to biosensor engineering such as quantum yield and minimum signal detection parameters (Daniel, Almog et al. 2009).

While many of these examples have utilized bacteria as the host for the *lux* system, they provide valuable insights into how human cells expressing mammalian-adapted *lux* genes can be employed to serve as biosensors under real-world conditions. There are, of course, logistical concerns surrounding the growth and maintenance of human cell lines as compared to bacterial cells, but

advances in cell culture techniques and cell encapsulation technology will one day allow for duplication of many of these experimental designs using human cells as the reporter organism. This would allow the determination of human bioavailability under environmental conditions and provide valuable information on metabolism and uptake of the above mentioned targets in way that has not previously been possible.

Firefly luciferase

Firefly luciferase (Luc) is the best studied of a large number of luminescent proteins to be discovered in insects. The insects represent a large related group of bioluminescent organisms, with over 2,500 species reported to be capable of generating light (Viviani 2002). While the vast majority of these luminescent reactions remain unstudied, the exception is in the order Coleoptera (beetles) where systems have been characterized for the chick beetles, railroad worms, and fireflies (predominantly *Photinus pyralis*) (Fraga 2008). Fireflies produce light in an organ called a lantern, using the rapid introduction of oxygen as a trigger for luminescence in order to attract mates as well as deter potential predators (Lewis and Cratsley 2008).

The first studies of the mechanism behind insect luminescence were carried out in the late 1800's by Raphael Dubois using ground up abdomens from the Elanteridae beetle. It was from these experiments that Dubois first proposed the existence of a system employing a luciferase and a luciferin for the production of light. The next advance came from Newton Harvey, who reported on the

specificity of luciferase/luciferin interactions and confirmed the requirement for molecular oxygen (Fraga 2008). In the mid 1900's William McElroy began what was to be a long and successful career working with firefly luciferase by discovering the requirement that ATP be involved in the luminescent reaction (McElroy 1947). Based in part on these findings, his group soon proposed that the bioluminescent reaction occurred via a two step process (Hastings, McElroy et al. 1953) and was the first to determine the structure of the firefly luciferin as 2-(4-hydroxybenzothiazol-2-yl)-2-thiazoline acid (White, Field et al. 1961) — commonly abbreviated as D-luciferin in the literature. In the late 1960's and 1970's the mechanism underlying the luminescent reaction was reported (White, Rapaport et al. 1969; McCapra 1976), as was the confirmation of the intermediate products of this proposed reaction (Fraga 2008). The mechanism was finally secured in 1980 when oxyluciferin was isolated as a purified product of the D-luciferin luminescence reaction (White, Steinmetz et al. 1980). The latest advance in the understanding of firefly luciferase came in 1996 when Conti (Conti, Franks et al. 1996) published the crystal structure of the luciferase at a resolution of 2.0 Å. This opened the door for targeted mutagenesis investigations and gave researchers the first look at the structure of this reporter protein.

The Luc protein catalyzes the oxidation of the reduced luciferin (D-luciferin) in the presence of ATP-Mg^{2+} and oxygen to generate CO_2, AMP, PP_i, oxyluciferin, and yellow-green light at a wavelength of 562 nm (Figure 3). It is important to note that D-luciferin is a chiral molecule, and while both the D and L forms can bind to Luc and participate in adenylation reactions, only the D form is capable of

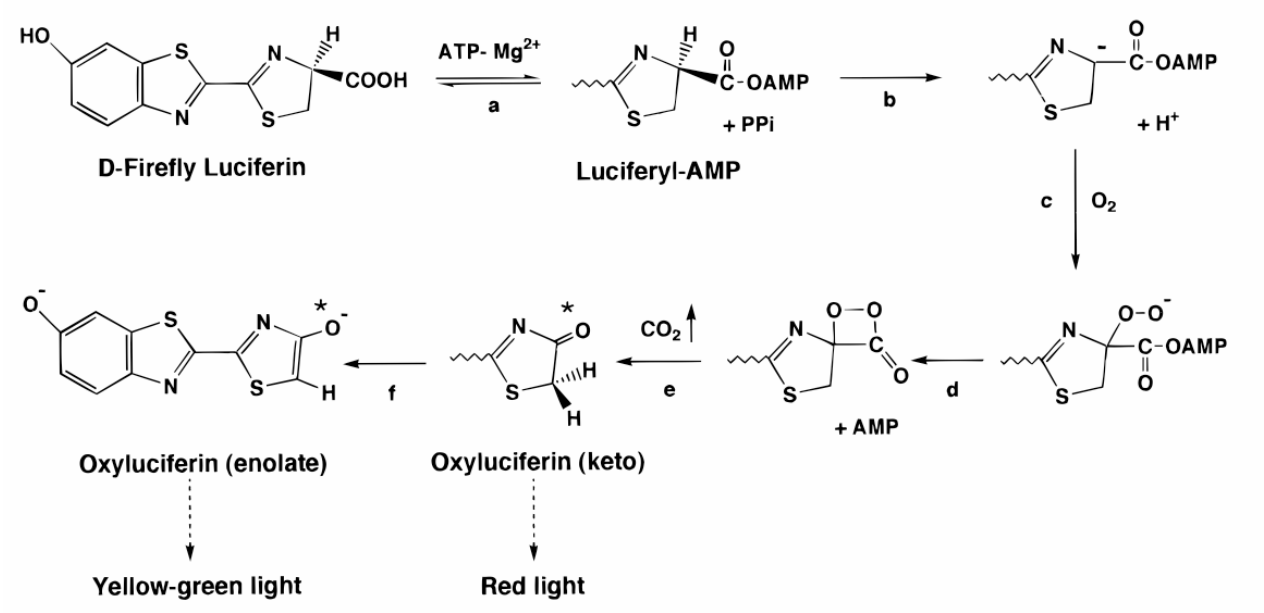

Figure 3. Bioluminescent reaction catalyzed by firefly luciferase.

The luciferase protein holds the reduced luciferin to allow for adenylation (a). This process is followed by a deprotonation reaction that leads to the formation of a carbanion (b) and attack by oxygen (c), driving the formation of a cyclic intermediate (d). As this intermediate decays, carbon dioxide is released, forming the excited state luciferin in either the keto (e) or enolate (f) form. Originally published in (Branchini, Magyar et al. 1998), reprinted with permission.

continuing on in the reaction to generate light (Fraga 2008). This reaction was originally reported to occur with a quantum yield of 0.88 (Seliger and McElroy 1960), but has since been shown to actually achieve a quantum yield closer to only 0.41 (Ando, Niwa et al. 2007). Because of the high quantum yield, the reaction is well suited to use as a reporter with as few as 10^{-19} mol of luciferase (2.4×10^5 molecules) able to produce a light signal capable of being detected (Gould and Subramani 1988).

It has been known since the early 1950's that the chemical reaction underlying firefly luminescence is a two-step process that first requires adenylation of D-luciferin followed by oxidation and the production of light (Hastings, McElroy et al. 1953). Prior to the initiation of the reaction, the Luc protein must first bind to D-luciferin. However, at this time it is not yet capable of undergoing oxidation or producing light. The first step in the generation of light is the adenylation of the bound D-luciferin with the release of pyrophosphate (Ugarova 1989). The function of this adenylation is to increase the acidity of the C4 proton of the thiazoline ring on D-luciferin. This allows for removal of a proton from C4 causing formation of a carbanion (McCapra, Chang et al. 1968). This carbanion is then attacked by oxygen, displacing AMP and driving the formation of a cyclic peroxide with an associated carbonyl group (a dioxetanone ring). As the bonds supporting this structure collapse, it becomes decarboxylated, releasing CO_2 and forming an electronically excited state of oxyluciferin in either the enol or keto form (Ugarova 1989).

The kinetics of this reaction can be altered by varying the concentration of the substrates, with low concentrations (in the nM range) showing steady light production and high concentrations (μM range) producing a bright flash followed by decay to 5 – 10% of the maximum (DeLuca, Wannlund et al. 1979). There are multiple possible inhibitory compounds that could be responsible for the kinetic profile generated under high substrate concentrations. It has previously been shown that, even though oxyluciferin is a natural product of the luciferase reaction, it is capable of remaining bound as an inhibitor to enzymatic turnover (Denburg, Lee et al. 1969). The same was found to be true of another potential byproduct, L-AMP, which can account for up to 16% of the product formed during the luminescent reaction (Fontes, Ortiz et al. 1998). This may, in part, explain how the addition of CoA to the luminescent reaction can result in improved performance. When CoA is added during the initial steps of the reaction, it prevents the fast signal decay normally observed, and when it is added following this decay it can promote re-initiation of the flash kinetics. This can be attributed to CoA's interaction with L-AMP to form L-CoA, resulting in turnover of the Luc enzyme and reoccurrence of the luminescent reaction (Airth, Rhodes et al. 1958).

Insects, and specifically beetles, that produce luminescence are quite diverse in the colors they are capable of producing. It was originally believed that the colors were the result of divergent luciferase structures, however, the sequences of four luciferase genes from *Pyrophorus plagiophthalamus* with four different emission spectra were sequenced and it was found that they shared up to 99%

amino acid identity (Wood, Lam et al. 1989). There are currently three mechanisms that have been proposed to explain the multiple bioluminescent colorations: the active site polarity hypothesis (DeLuca 1969), the tautomerization hypothesis (White and Branchini 1975), and the geometry hypothesis (McCapra, Gilfoyle et al. 1994).

The active site polarity hypothesis is based on the idea that the wavelength of light produced is related to the microenvironment surrounding the luminescent protein during the reaction. In non-polar solvents the spectrum is shifted towards blue and in polar solvents it is more red-shifted. It is questionable, however, if polarity fluctuations can account for large scale changes like those that have been observed in *P. plagiophthalamus*. The tautomerization hypothesis states that the wavelength of light produced is dependent on whether either the enol or keto form of the luciferin is formed during the course of the reaction. A recent study has reported that by altering the substrate of the reaction the keto form of the luciferin can produce either red or green light, making this hypothesis unlikely as well (Branchini, Murtiashaw et al. 2002). Finally, the geometry hypothesis suggests that the geometry of the excited state oxyluciferin is responsible for determining the emission wavelength. In a 90° conformation it would achieve its lowest energy state and red light would be produced, whereas in the planar conformation it would be in its highest energy state and green light would be produced. Intermediate colors would be the result of geometries between these two extremes (Viviani 2002).

Luc biosensors and applications

Firefly luciferase makes an excellent reporter for the reasons previously discussed, however, its major hurdle for use has always been the inability for detection in real-time due to the requirement for addition of a separate luciferin. Despite this drawback, Luc has become the most popular reporter protein for bioluminescent imaging because its bright signal allows for detection even at low reporter population sizes. For example, Kim and colleagues have demonstrated this advantage with the newest generation of these reporters designed for tumor detection. The investigators were able to inject codon-optimized Luc containing 4T1 mouse mammary tumor cells subcutaneously and then image single bioluminescent cells at a background ratio of 6:1 (Kim, Urban et al. 2010). This experiment effectively demonstrates how a Luc-based reporter can be used to continuously monitor cancer development from a single cell all the way to complete tumor formation.

Some researchers have also managed to take advantage of the dependence of the Luc system on the presence of its D-luciferin substrate to produce a detectable signal. Through bioluminescence resonance energy transfer (BRET) Angers et. al. was able to demonstrate the presence of G-protein coupled receptor dimers on the surface of living cells. By tagging a subset of β_2-adrenergic receptor proteins with Luc and a subset with the red-shifted variant of green fluorescent protein, YFP, it was possible to detect both a luminescent and fluorescent signal in cells expressing both variants, but no fluorescent signal in cells expressing only YFP since no fluorescent excitation signal was used

(Angers, Salahpour et al. 2000). This was made possible because the bioluminescent signal from Luc required to stimulate the fluorescent signal of YFP was not constantly produced, allowing the researchers to detect YFP independently from the Luc signal, and then subsequently visualizing where Luc was expressed either in tandem or independently of the associated YFP protein.

Due to its persistence as the most widely used bioluminescent protein in the optical imaging field, there have been myriad other uses of the Luc protein in both cell culture and small animal imaging applications. Multiple reviews have been published detailing the standard and novel implementations of this versatile protein, but suffice it to say that it is not without reason that Luc is consistently employed by a wide variety of researchers. The intense bioluminescent signal allows for facile detection using short integration times and simultaneously allows for detection under conditions of heave photo-scattering and absorption. The examples used here provide only brief highlights as to the functional sensitivity and range of use afforded by the Luc reporter system.

Green fluorescent protein

Green fluorescent protein (GFP) was first discovered during investigation into the related chemiluminescent protein aequorin from the jellyfish *Aequorea Victoria* (Shimomura, Johnson et al. 1962). Since that time it has been realized that the *Aequorea* derived GFP is just one of a larger family of homologous fluorescent proteins capable of producing light in a variety of colors due to alterations in the covalent structure of their chromophores or differences in the

surrounding non-covalent environment (Giepmans, Adams et al. 2006). Despite its early discovery, the use of GFP as a research tool did not begin until after it was successfully cloned almost thirty years later (Prasher, Eckenrode et al. 1992). However, soon after the cDNA was available, its function was validated in both prokaryotic and eukaryotic organisms by Chalfie (Chalfie, Tu et al. 1994), and since that time it has been used in numerous applications including localization studies, protein expression monitoring, as a reporter gene, as a viability marker, to detect the onset of apoptosis, and many others (reviewed in (Zimmer 2002)).

GFP has become a favored tool for molecular studies because it is autofluorescent and does not require the addition of any cofactors to properly function in exogenous systems (Naylor 1999), although it does require activation by an excitation light source before its signal can be measured. It has been shown to be resistant to heat, alkaline pH fluctuations, chaotropic salts, organic solvents, and many proteases (Ehrmann, Scheyhing et al. 2001), and its expression in exogenous environments is primarily non-toxic (Zimmer 2002) with a few proven exceptions (Hanazono, Yu et al. 1997; Liu, Jan et al. 1999) that may be due to production of hydrogen peroxide as a by-product of synthesis (Tsien 1998). However, the slow posttranslational chromophore formation and oxygen requirement of GFP, along with potential difficulty in distinguishing its signature from background fluorescence (Zimmer 2002), can be problematic, especially in aerobic organisms. Because of this, alternate fluorescent proteins such as those based on flavin mononucleotide are often used when developing reporters for

anaerobic organisms (Drepper, Eggert et al. 2007). Time, though, has proven that the benefits outweigh the challenges for most investigators, and GFP has taken its place as one of the most popular tools currently available for cellular and molecular signaling research.

Wild-type GFP protein is able to absorb light at two different wavelengths. A minor peak occurs at 475 nm with the major peak at 397 nm (Figure 4). Regardless of which excitation wavelength is used, emission occurs only at 504 nm (Patterson, Knobel et al. 1997). The different absorption peaks have been attributed to varying protonation states of the fluorophore, with the neutral state corresponding to the major absorption peak at 397 nm and the anionic form contributing to the minor peak at 475 nm (Niwa, Inouye et al. 1996). The large shift between the major absorption peak at 397 nm and the emission at 504 nm can be attributed to an excited state proton transfer from the side chain of the Tyr66 residue of the fluorophore (Chattoraj, King et al. 1996) to the carboxylate oxygen of Glu222 (Zimmer 2002).

Based on this interconversion of the fluorophore, a three state model of photoisomerization has been put forward to explain the chemical basis for shifts in absorption. This model states that excitation of the neutral state fluorophore can cause conversion to the anionic form via an intermediate (Chattoraj, King et al. 1996). The intermediate is structurally similar to the neutral form of the fluorophore, but has become deprotonated at the phenol group of Tyr66 (Zimmer 2002). Excitation of the anionic form is capable of directly emitting fluorescence,

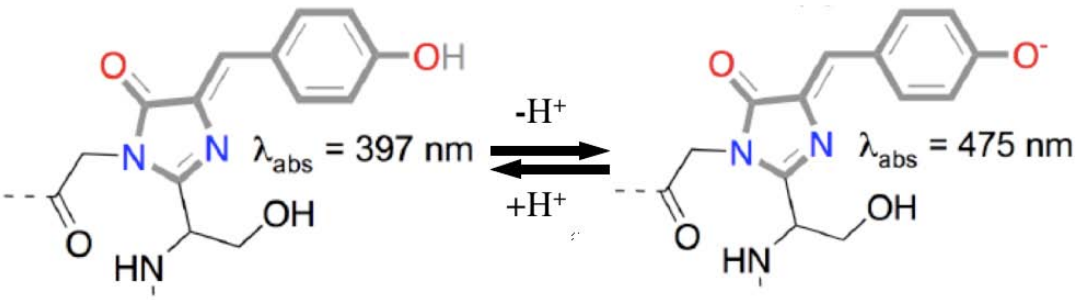

Figure 4. The dual absorption peaks in the GFP spectra are the result of different charge states in the GFP chromophore.

The neutral state (left) is responsible for the major peak at 397 nm while the anionic form (right) is responsible for the minor peak at 475 nm. Regardless of the chromophore charge state, emission occurs at 504 nm. Adapted from Scholarpedia.org.

while the neutral state must necessarily convert into an excited form of this intermediate prior to emission (Jung, Wiehler et al. 2005). While it is possible for the neutral form to convert to the anionic form following excitation, this is not the most favorable reaction. The majority of excited, neutral fluorophores will convert briefly to the intermediate state, where fluorescence will occur, followed by reversion back to the neutral state (Chattoraj, King et al. 1996). Interconversion between the neutral and anionic states is possible, but requires both proton transfer and conformational change to occur (Zimmer 2002). Similarly, the majority of anionic fluorophores will revert to the ground state following fluorescent emission, but could instead undergo a conformational change to the intermediate state and then continue on to adopt a neutral charge state (Chattoraj, King et al. 1996).

In a wild-type population, GFP contains a 6:1 ratio of neutral to anionic fluorophores (Tsien 1998), explaining why the major absorption peak is found at 397 nm. However, upon extended ultraviolet (UV) illumination this peak will begin to decrease and the minor peak will increase (Cubitt, Heim et al. 1995). This behavior corresponds to the photoisomerization of the neutral fluorophore form responsible for the major absorption peak being converted into the anionic form as discussed above. While the photoisomerization characteristics of GFP can prove problematic for quantification, they do allow for the study of protein movement by excitation with intense UV light at 397 nm followed by excitation at

475 nm in order to track the movement of the photoisomerized fluorophores (Yokoe and Meyer 1996).

Following the discovery of GFP, it was quickly proven that amino acid substitutions were capable of altering its fluorescent characteristics. Since that time, versions of GFP have been developed that fold more efficiently at higher temperatures (Crameri, Whitehorn et al. 1996), avoid dimerization at high concentration (Zacharias, Violin et al. 2002), or fluoresce in the blue (Heim, Prasher et al. 1994), cyan (Heim and Tsien 1996), or yellow (Ormo, Cubitt et al. 1996) wavelengths. Homologs have since been discovered that fluoresce in the red range as well (Matz, Fradkov et al. 1999). The history and development of these variants is outside the scope of this review, but an excellent classification has been made by Tsien (Tsien 1998) and abridged by Zimmer (Zimmer 2002) dividing the known variants into seven classes based on spectral characteristics. When applied in concert, these variants of the GFP protein have given researchers the ability to use multiple GFP-based reporters in the same environment at the same time, improving the usefulness and range of this already dynamic protein.

GFP biosensors and applications

Since it was first demonstrated that GFP could be expressed in *E. coli* (Chalfie, Tu et al. 1994), it has been used in countless experiments in organisms ranging from bacteria to cultured human cells and even commercialized for sale in designer pets. Aside from basic localization assays, the two main uses of GFP

as a reporter focus on either the induction or suppression of GFP expression to indicate interaction with an analyte of interest. One of the more popular assays focusing on the suppressed expression of GFP is the determination of cell viability. In these assays, cells expressing GFP are exposed to compounds of interest and the severity of toxicity is determined by monitoring the decrease in fluorescent expression (Choi, Deng et al. 2008). This allows researchers to process a large number of samples very quickly in an automated fashion. As the cells are killed or their metabolism is slowed by interaction with toxic substances, the overall amount of fluorescence will decrease. This type of assay has the added advantage of determining the amount of a given compound that will be bioavailable to the organism being tested.

The inverse of this type of experiment is to induce the expression of GFP as a positive result. In this case the gene encoding for GFP is placed under the control of a genetic promoter that responds specifically to the analyte of interest. This allows for visual detection when the cell is exposed to the target analyte. An advantage of this type of experimental design is that the amount of fluorescence produced can be correlated to the concentration of analyte, allowing for an approximate quantification (Gvakharia, Bottomley et al. 2009). It is also possible to use the fluorescence of GFP as a marker to isolate those members of the community showing a response by using fluorescence activated cell sorting (FACS) (Bumann and Valdivia 2007). Using GFP to confirm interaction with a compound of interest, quantify the amount of exposure, and isolating exposed

cells simultaneously illustrates its dynamic functionality in modern bioreporter research.

Biosensor integration of GFP-based bioreporters, however, remains fairly limited due to signal output by GFP being contingent upon an excitation light source. Thus, these set-ups require one energy source to excite GFP and another to measure GFP, and the associated complexity and bulkiness are often not suitable for biosensor applications. There has been some application success using fiber optic cables where one cable is used for excitation and another for emission measurement. Shetty (Shetty, Ramanathan et al. 1999), for example, constructed a GFP-based bioreporter sensitive to the monosaccharide L-arabinose and entrapped it within a dialysis membrane tied to the tip of a fiber optic bundle. Fibers terminating at a tungsten lamp served as the excitation source while separate fibers terminating at a PMT served as the detector. Immersing the reporter-entrapped sensor end of the fiber bundle in liquid was then shown capable of detecting L-arabinose at varying concentrations. To improve sensitivity, Knight (Knight, Goddard et al. 1999) bypassed fiber optics by interfacing a PMT directly with a flow-cell containing a eukaryotic-based GFP bioreporter sensitive to DNA damaging genotoxic compounds using an argon laser to provide the excitation source. Realizing the necessity for miniaturization and less complexity, new fluorescence detection techniques based on small footprint biosensor compliant platforms are becoming somewhat available. Complementary–metal–oxide–semiconductor (CMOS) photodetectors better tuned to the green light signature provide enhanced detection (Yotter, Warren et

al. 2004), as do avalanche photodiodes, while tightly focused laser beams provide excitation down to the single cell level (Wells 2006). However, incorporating all necessary components into a true biosensor format remains challenging. Recently a 12 cm diameter microfluidics-based lab-on-a-compact disk (CD) device that microcentrifugally moved and mixed microliter volumes of water test samples with a GFP bioreporter sensitive to arsenic have been created (Rothert, Deo et al. 2005) (Figure 5). Although sensing was accomplished with a fiber optic probe positioned above the CD, the device could likely be easily reconfigured to accommodate a chip-based sensor to promote further miniaturization.

***in vivo* bioluminescent imaging (BLI)**

Whole animal bioluminescent imaging (BLI) is progressively becoming more widely applied by investigators from diverse backgrounds because of its low cost, high throughput, and relative ease of operation in visualizing a wide variety of *in vivo* cellular events (Baker 2010). The ability to visualize cellular processes or other biological interactions without the requirement for animal subject sacrifice allows for repeated imaging and releases investigators from the constraints of considering their process of interest on a “frame-by-frame” basis using labeled slides. In addition, the ability to continually monitor a single individual reduces the amount of inter-animal variation and can reduce error, leading to higher resolution and less data loss. With continuing advances in the hardware and software required for performing these experiments, it is also becoming easier for

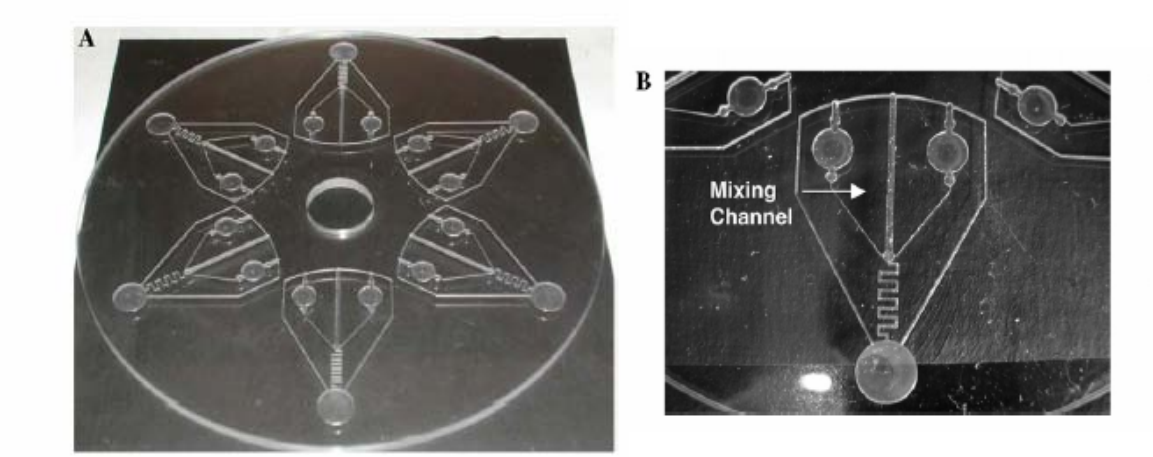

Figure 5. Miniaturization of detection technologies allows for increased ease of use.

A) A lab-on-a-CD microfluidic device used in conjunction with GFP bioreporters sensitive towards arsenic. B) A close-up view of the microfluidic channeling that permits sample and bioreporter mixing. Originally published in (Rothert, Deo et al. 2005), reprinted with permission.

researchers with little background in molecular imaging to obtain useful and detailed publication-ready images.

The mainstays of BLI are the light generating luciferase enzymes such as firefly luciferase, *Renilla* luciferase, *Gaussia* luciferase, *Metridia* luciferase, *Vargula* luciferase, or bacterial luciferase (Thompson, Nagata et al. 1989; Wood, Lam et al. 1989; Lorenz, McCann et al. 1991; Meighen 1991; Verhaegen and Christopoulos 2002; Markova, Golz et al. 2004). Of these however, the firefly and *Renilla* luciferases are the most popular for optical imaging. These bioluminescent proteins are preferred over their fluorescent counterparts because the lack of endogenous bioluminescent reactions in mammalian tissue allows for near background-free imaging conditions whereas the prevalence of fluorescently active compounds in these tissues can interfere with target resolution upon exposure to the fluorescent excitation wavelengths required for the generation of signal output.

Firefly luciferase (Luc), *Renilla* luciferase (RLuc), and bacterial luciferase (*lux*) all exhibit distinct imaging characteristics ranging for the substrate required (if any) to the wavelength at which their bioluminescent signal is produced. It is this diversity that has lead to their popularity for *in vitro* BLI. While none of them individually is suited to every experimental design, they can be interchanged and sometimes used in combination to function in a wide variety of imaging applications. The advantages and disadvantages of these reporter proteins as they relate to their use in BLI are listed in Table 1.

Table 1. Comparison of BLI reporter proteins.

Reporter	Advantages	Disadvantages
Firefly and click beetle luciferase • D-luciferin substrate	• High sensitivity and low signal-to-noise ratio • Quantitative correlation between signal strength and cell numbers • Low background in animal tissues • Variations of firefly luciferase (stabilized and red-shifted) and click beetle luciferases (red and green) are available • Different colors allow multi-component monitoring	• Requires exogenous luciferin addition • Fast consumption of luciferin can lead to unstable signal • ATP and oxygen dependent • Currently not practical for large animal models
Renilla and *Gaussia* luciferase • Coelenterazine substrate	• High sensitivity • Quantitative correlation between signal strength and cell numbers • Stabilized and red-shifted *Renilla* luciferase are available • Secretion of *Gaussia* luciferase allows for subject-independent bioluminescence measurement	• Requires exogenous coelenterazine addition • Low anatomic resolution • Increased background due to oxidation of coelenterazine by serum • Oxygen dependent • Fast consumption of coelenterazine can lead to unstable signal • Currently not practical for large animal models
Bacterial luciferase	• High sensitivity and low signal-to-noise ratio • Quantitative correlation between signal strength and cell numbers • Fully autonomous system, no requirement for addition of exogenous substrate • Noninvasive • Stable signal • Rapid detection permitting real-time monitoring	• Bioluminescence at 490 nm prone absorption in animal tissues • Low anatomic resolution • NADPH and oxygen dependent • Not as bright as other luciferases • Currently not practical for large animal models

Optical properties of biological tissues

The unique constraints of performing data collection from within a living medium must be considered in relation to any choice of reporter system. The detection of a luminescent signal from within a tissue sample is dependent on several factors, including the flux of photons from the reporter, the total number of functional reporter cells in the sample, and the location of the reporter cells within the tissue sample itself (Troy, Jekic-McMullen et al. 2004). In addition, the visualization of the bioluminescent signal is dependent on the absorption and scattering of that signal prior to detection. The scattering of a bioluminescent signal cannot be controlled, however, changing its wavelength can alter the absorption characteristics of the signal significantly. This is due to the fact that the majority of luminescent absorption is the result of interaction of the signal with endogenous chromophoric material. By moving to a more red-shifted emission wavelength, where the levels of absorption within tissue are lower, it becomes possible to measure a greater amount of signal intensity than would be possible from an identical reporter with a lower, more blue-shifted emission wavelength (Chance, Cope et al. 1998). For this reason, it is important to consider the emission wavelength of a given reporter system, along with the other desired attributes of that reporter, prior to its introduction into any experimental design. For example, the bioluminescent signal from the *lux* reaction is produced at 490 nm. This is relatively blue-shifted as compared to the Luc-based bioluminescent probes that display their peak luminescent signal at 560 nm. The shorter wavelength of the *lux*-based signal has a greater chance of becoming attenuated

within the tissue and therefore may not be as easily detected if it is used in deeper tissue applications (such as intraperitoneal or intraorganeller injections), and may require longer integration times to achieve the same level of detection as a longer wavelength reporter would when injected subcutaneously. Therefore, if short measurement times and low population level cell detections are the goals of a particular experiment, a Luc-based reporter would be beneficial compared to a *lux*-based reporter despite potential problems introduced through substrate administration in the Luc system. However, if a near surface detection of large cell populations (such as a subcutaneous tumor) was the end goal, the effects of absorption and scattering could be overcome by the depth and position of the reporter, thus allowing for selection of the more blue-shifted *lux* reporter system.

Imaging equipment

The challenge of detecting and locating bioluminescent light emissions from within living subjects has been met by several commercial suppliers of *in vivo* imaging equipment (Table 2). A basic imaging system consists of a light-tight imaging chamber into which the subject is placed and a high quantum efficiency charged coupled device (CCD) camera, usually supercooled to less than -80°C to reduce thermal noise, that collects emitted light. The camera typically first takes a photographic image of the subject followed by a bioluminescent image. When superimposed, regions of bioluminescence become mapped to the

Table 2. Commercial manufacturers of *in vivo* imaging systems.

Company	URL
Caliper Life Sciences	http://www.caliperls.com/tech/optical-imaging/
Berthold Technologies	http://www.berthold.com/ww/en/pub/home.cfm
Carestream	http://www.carestreamhealth.com/in-vivo-imaging-systems.html
Photometrics	http://www.photometrics.com/
Li-Cor Biosciences	http://www.licor.com/index.jsp
Cambridge Research & Instrumentation	http://www.cri-inc.com/index.asp
UVP	http://www.uvp.com/

subject's anatomy for pinpoint identification of source emissions. Acquisition times can range from a few seconds to several minutes depending on signal strength. Software displays the image in a pseudocolored format and provides the tools needed to quantify, adjust, calibrate, and background correct the resulting image. Integrated gas anesthesia systems, heated stages, and isolation chambers are typically available to accommodate animal handling.

The technology incorporated into *in vivo* imaging systems is rapidly advancing to meet user needs in a greater diversity of application backgrounds. CCD cameras are being replaced by more sensitive intensified CCD (ICCD) and electron multiplying CCD (EMCCD) cameras that can manage acquisition times of millisecond durations. These fast processing times along with powerful software now permit real-time tracking of conscious, moving subjects (see, for example, the IVIS Kinetic system from Caliper Life Sciences). Anesthesia can have dramatic, unknown, and interfering effects on animals, and the ability to image in its absence is a major step forward in *in vivo* imaging technology. In addition, imaging systems are becoming better integrated with existing medical technologies for multi-parameter analyses. For example, electrocardiogram (ECG) or X-ray procedures can operate in parallel with imaging acquisition. The ability of software to overlay and map these data to the bioluminescent image, often as a 3D representation, offers unique opportunities to visualize physiological status and kinetics.

The major drawback of *in vivo* imaging systems is their inability to detect signal at tissue depths beyond a few centimeters. Without major advances in

imaging sensitivity, either with the camera systems, the internal signal, or almost certainly both in tandem, *in vivo* imaging applications may become limited solely to small animals and the translational leap to humans will never occur. Rather than relying on a camera to visualize the signal externally, it may be feasible and potentially more practical to monitor the signal internally using implantable sensors. Although not yet a viable technology, proof-of-concept microluminometer integrated circuits of only a few square millimeters in size have been developed and validated for bioluminescent signal acquisition (Vijayaraghavan, Islam et al. 2007). These so-called bioluminescent bioreporter integrated circuits, or BBICs, were specifically designed for capturing the 490 nm bioluminescent light signal emitted by the bacterial *lux* system, and accommodated on-chip transmitters for wireless data transmission. However, effectively interfacing the microluminometers with the luciferase reporter systems maintaining reporter viability, and implanting the chips remains challenging.

Common in vivo bioluminescent imaging modalities

Steady-state bioluminescent imaging

The classical hallmark of BLI is steady state imaging, a process whereby bioluminescently tagged cells are imaged over time to determine if light output is increasing or decreasing compared to the initial state. In this type of imaging, either a gain or loss of signal can be the desired result depending on the experimental design. Commonly, bioluminescent cells are injected into an animal model to determine the kinetics of tumorigenesis and growth. The use of

BLI as a substitute for mechanical or histological measurement of tumors has increased rapidly in recent years as it does not entail high levels of animal subject sacrifice nor tedious histological analysis, and can overcome the loss of accuracy associated with physical analysis due to the contribution of edema and necrotic centers to overall tumor size (Vaupel, Kallinowski et al. 1989). In addition, by monitoring tumor growth using BLI, an investigator can track changes within individual animals over time without requiring the subject to be sacrificed. This reduces the amount of intra-animal variability and can improve the detection of significant results.

In the opposite direction, decreases in bioluminescent expression can be used to quickly and efficiently perform drug efficacy screening. The same logistical concerns that have propelled BLI forward as the tool for choice for tumor monitoring are also making it the preferred choice for the screening of new compounds directed at tumor suppression or infection control. In addition, the use of mixed culture or whole animal models can more closely mimic the target microenvironmental conditions that may alter the compound's activity. As one example, McMillin et al. (McMillin, Delmore et al. 2010) illustrated that high throughput scalable mixed cell cultures with Luc tagged cancer cells can identify anti-cancer drugs that are specifically effective in the tumor microenvironment early in the discovery pipeline, thereby aiding in their prioritization for further study in ways not previously possible.

Multi-reporter bioluminescent imaging

In a basic experimental design, multi-reporter BLI is performed by simultaneously monitoring for expression of two or more divergent luciferase proteins. This is made possible because all of the characterized luciferase proteins have divergent bioluminescent emission wavelengths. This type of experimental design is especially useful when used to monitor potentially co-dependent, or inter-dependent protein expression such as that expressed during the maintenance of circadian rhythm. Here, the expression of multiple genes can be monitored in real time, without the need to expose cells to potentially influential doses of excitation light wavelengths as would be required for imaging using fluorescent targets (Honma, Yoshikawa et al.). Even when expression of the individual genes of interest is static, sequential imaging of multiple luciferase proteins provides a convenient method for localizing expression profiles of each gene *in vivo* (Heikkila, Vaha-Koskela et al. 2010).

The work of Audigier and colleagues (Audigier, Guiramand et al. 2008) demonstrates how imaging multiple bioluminescent reporters can be an opportune way to monitor translational dynamics using the function of the fibroblast growth factor two internal ribosomal entry site on neural development as a model. To determine the associated ratios of cap-dependent to cap-independent translation, they cloned the RLuc gene upstream of the site and the Luc gene downstream. By doing so, they were able to quantify and compare the levels of expression of each reporter protein independently from the same sample, helping to reduce sampling error.

Multi-component bioluminescent imaging

Similar to multi-reporter BLI, multi-component BLI relies on the co-expression of an alternate imaging construct, however, in this case the secondary construct is not itself bioluminescent. Classically, the luminescent emission signal of a substrate amended luciferase protein can be harnessed to act as the excitation signal for an associated fluorescent reporter protein, negating the requirement for treatment with a background stimulating exogenous light source. This process, known as bioluminescence resonance energy transfer (BRET) occurs naturally in the sea pansy *Renilla reniformis* and other marine animals (Ward and Cormier 1978), but can be used in research settings to boost the luminescent signal of a bioluminescent reporter, or, more popularly, to determine the interaction of two components of interest within a given system.

In some cases, the secondary component is not a fluorescent compound but rather a non-independently functional domain of the luciferase protein itself. These types of constructs are easily created using reporters such as Luc that have distinct N (N-Luc) and C (C-Luc) terminal domains joined by a linker region. These types of protein structures lend themselves nicely to separation into distinct components that, when brought together, can form a functional luciferase protein.

First described by Paulmurugan et al. (Paulmurugan, Umezawa et al. 2002), this process takes advantage of the lack of a bioluminescent signal in small animal tissue samples. The individual N and C terminal components of the Luc protein are not capable of producing light independently of one another, however,

when they were independently tethered to two proteins known to interact strongly, the researchers were able to demonstrate that bioluminescence could be restored upon substrate amendment. The complementation of a single luciferase protein as opposed to the adjoinment of a luciferase with a fluorescent partner does not require the pair matching of a luciferase/fluorescent reporter with overlapping emission/excitation wavelengths, and can permit co-visualization with other reporters in a single subject to permit multi-localization of groups of proteins.

Bioluminescence as a supplementary imaging technique

As the technology for small animal imaging continues to increase in power and availability, there is an increasing movement towards combining multiple imaging techniques to improve the amount of detail that can be obtained from a single subject. While no single imaging technique can provide an investigator with a comprehensive picture of the system as a whole, the combination of multiple techniques such as computed tomography (CT), positron emission tomography (PET), and BLI can help to “fill in the gaps” left by each approach in a rapid, sequential manner. The development of trimodal fusion proteins that are capable of simultaneously acting as a signal for fluorescence, bioluminescence, and PET, and the introduction of combined clinical PET/CT scanners has made it possible to obtain more information from a single animal subject than was previously believed possible (Deroose, De et al. 2007).

CHAPTER II

Demonstration Of Autonomous Bioluminescent Production In The Mammalian Cellular Background

Introduction

In vivo optical imaging is becoming increasingly utilized as a method for modern biomedical research. This process, which involves the non-invasive interrogation of animal subjects using light emitted either naturally from a luciferase protein or following excitation of a fluorescent protein or dye, has been applied to the study of a wide range of biological processes such as gene function, drug discovery and development, cellular trafficking, protein-protein interactions, and especially tumorigenesis and cancer treatment (Contag and Bachmann 2002) . While the detection limits and resolution of charge coupled devices (CCDs) has increased greatly in recent years (Oshiro 1998), there have been relatively few introductions of improved imaging compounds that function as light production centers within an animal subject *in vivo*.

Generally, the currently available imaging compounds can be divided into two classes: those containing luciferase proteins (capable of producing bioluminescent light without exogenous excitation) and those containing fluorescent compounds (dyes or proteins that require an initial excitation followed

by emission at a given wavelength). For mammalian-based whole animal imaging, fluorescent compounds are limited due to high levels of background fluorescence from endogenous biological structures upon excitation (Tsien 1998). Although dyes have been developed and employed that fluoresce in the near infrared wavelengths (Bloch, Lesage et al. 2005; Kalchenko, Shivtiel et al. 2006) where light absorption is lowest in mammalian tissues, they can become increasingly diffuse during the process of cellular division, negating their usefulness in long term monitoring studies (Contag and Bachmann 2002) . In contrast, luciferase proteins are highly amenable towards *in vivo* optical imaging (referred to as bioluminescent imaging or BLI) because they produce a controllable light signal in cells with little to no background bioluminescence, thus allowing for remarkably sensitive detection (Zhao, Doyle et al. 2005). While historically the luciferase proteins used have been based on beetle luciferases (i.e., firefly or click beetle luciferase) or marine aequorin-like proteins (those that utilize coelenterazine), these each possess disadvantages when applied to whole animal BLI. For example, the popular firefly luciferase protein is heat labile when incubated under whole animal BLI imaging conditions, and can display a half life as short as 3 min in its native state at 37°C (Baggett, Roy et al. 2004). Coelenterazine-stimulated luciferases are similarly handicapped in regards to long-term monitoring, as it has been reported that their rapid uptake of coelenterazine necessitates prompt imaging following substrate injection (Bhaumik and Gambhir 2002). Applications of both these luciferase systems also suffer from the drawback that they require addition of an exogenous

substrate to produce a detectable light signal. This current work reports for the first time that a modified bacterial luciferase gene cassette can be expressed in mammalian cells in culture or in whole animal BLI without the use of exogenous substrates or coincident infection with a bacterial host, thus overcoming the limitations imposed by currently available luciferase-based BLI assays.

Setting the bacterial bioluminescence system apart from other bioluminescent systems such as firefly luciferase and aequorin is its ability to self-synthesize all of the substrates required for the production of light. While the luciferase component is a heterodimer formed from the products of the *luxA* and *luxB* genes, its only required substrates are molecular oxygen, reduced riboflavin phosphate ($FMNH_2$), and a long chain aliphatic aldehyde. Oxygen and $FMNH_2$ are naturally occurring products within the cell while the *luxCDE* gene products produce and regenerate the aldehyde substrate using endogenous aliphatic compounds initially targeted to lipid biogenesis. To produce light, the luciferase protein first binds $FMNH_2$, followed by O_2, and then the synthesized aldehyde. This allows the *lux* cassette to utilize only endogenous materials to form an intermediate complex that then slowly oxidizes to generate light at a wavelength of 490 nm as a byproduct (Meighen 1991). The overall reaction can be summarized as:

$$FMNH_2 + RCHO + O_2 \rightarrow FMN + H_2O + RCOOH + hv_{490nm}$$

Realizing the distinct advantages bacterial luciferase would afford as a eukaryotic reporter, many groups have attempted to express the luciferase (*luxAB*) component of the *lux* system using either fusion proteins (Escher, Okane et al. 1989; Kirchner, Roberts et al. 1989; Almashanu, Musafia et al. 1990; Pazzagli, Devine et al. 1992) or multiple plasmids (Koncz, Olsson et al. 1987; Olsson, Escher et al. 1989), but with minimal success over the last twenty years. Although the use of *lux* in the study of bacterial infection of a mammalian host has been demonstrated using whole animal BLI (Contag, Contag et al. 1995), its functionality has not been demonstrated outside of a bacterial host until now. Recently, successful expression of a mammalian optimized luciferase dimer in an HEK293 cell line has provided for the limited use of *lux* as a mammalian bioluminescent reporter system, although the addition of luciferin in a manner similar to firefly luciferase is still required (Patterson, Dionisi et al. 2005). To fully exploit the advantages of bacterial luciferase, all five genes (*luxCDABE*) of the *lux* operon must be expressed simultaneously. Here it is demonstrated that codon-optimized, poly-bicistronic expression of the full *lux* cassette produces all of the products required for autonomous bioluminescent production in a mammalian background. It is further demonstrated that cells expressing the full *lux* cassette can be applied towards whole animal BLI without the need for substrate addition, thus overcoming the limitations imposed by currently available luciferase-based whole animal BLI probes.

Materials And Methods

Strain maintenance and growth

Escherichia coli cells were routinely grown in Luria Bertani (LB) broth with continuous shaking (200 rpm) at 37°C. When required, kanamycin or ampicillin was used at final concentrations of 40 and 100 μg/ml, respectfully, for selection of plasmid containing cells. Mammalian cell lines were propagated in Eagle's modified essential medium (EMEM) supplemented with 10% fetal bovine serum, 0.01 mM non-essential amino acids, and 0.01 mM sodium pyruvate. Cell growth was carried out at 37°C in a 5% CO_2 environment and cells were passaged every 3 - 4 d upon reaching 80% confluence. Neomycin and/or zeocin were used for selection of transfected cells at concentrations of 500 μg/ml and 200 μg/ml, respectfully, as determined by kill curve analysis, for each antibiotic.

Codon optimization of the bacterial bioluminescence genes

Codon usage patterns in the *luxCDE* genes for *P. luminescens* and the flavin reductase gene (*frp*) from *V. harveyi* were compared to the highest 10% of expressed genes as represented in GenBank. Silent mutations at the DNA level that would alter native codon usage were plotted to more closely mimic the preferred mammalian codons while maintaining 100% amino acid identity with the bacterial protein sequences. When multiple codons were preferred in equal or near equal frequencies by mammalian genes, the codon for the optimized sequence was randomly selected from the available options. These optimized

sequences were submitted and synthesized *de novo* by GeneArt and returned as synthetic DNA constructs inserted into unique *Kpn*I and *Sac*I restriction sites in pPCR-Script vectors (GeneArt). Codon-optimized versions of each gene were compared to their wild-type counterpart for predicted translational efficiency using the freely available GENSCAN software at http://genes.mit.edu. All sequences were deposited to GenBank under the following accession numbers GQ850533 (codon-optimized *luxC*), GQ850534 (codon-optimized *luxD*), GQ850535 (codon-optimized *luxE*), and GQ850536 (codon-optimized *frp*).

Vector construction

Previously described (Patterson, Dionisi et al. 2005) *P. luminescens luxA* and *luxB* genes partially codon-optimized for expression in human cell lines were obtained as a bicistronic operon in a pIRES vector (Clontech) and designated $pLux_{AB}$. This vector includes an internal ribosomal entry site (IRES) for increased translation of downstream gene insert. The remaining *P. luminescens* genes (*luxC*, *luxD*, *luxE*) and the flavin reductase gene (*frp*) were used in either their wild-type (wt) or codon optimized (co) states. co*luxC* was cloned into multiple cloning site (MCS) A of the pIRES vector using the unique *Nhe*I and *EcoR*I restriction sites (Figure 1 A-C). The co*luxE* gene was then inserted into MCS B using the unique *Sal*I and *Not*I restriction sites. This entire co*luxC*-IRES-co*luxE* sequence was then removed and ligated into pBudCE4.1 (Invitrogen) behind the human elongation factor 1α (EF-1α) promoter using unique *Xho*I and *Sfi*I restriction sites. A second pIRES vector was constructed by adding the co*luxD*

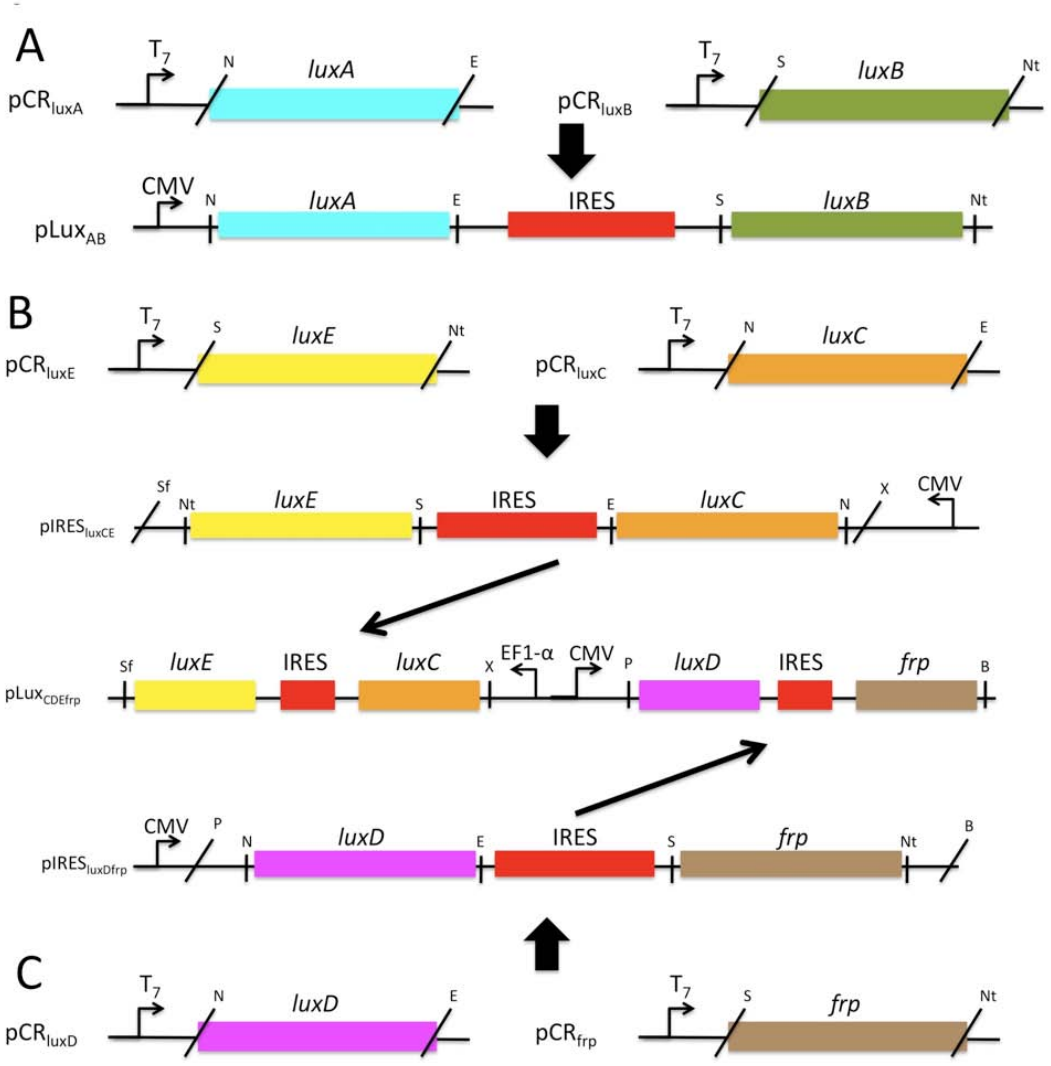

Figure 6. Schematic showing construction and expression of the full *lux* cassette using a two-plasmid system.

The two-plasmid system takes advantage of IRES-based bicistronic expression to drive transcription/translation of all the genes required for autonomous bioluminescent production. (A) The $pLux_{AB}$ plasmid contains the genes responsible for production of the luciferase protein. Individual *luxA* and *luxB* genes were removed from their respective vectors and ligated into the pIRES vector using the unique *Nhe*I (N) and *EcoR*I (E) or *Sal*I (S) and *Not*I (Nt) restriction sites. (B) The $pLux_{CDEfrp}$ plasmid expresses the genes required for production and regeneration of the aldehyde and $FMNH_2$ substrates. The individual *luxE* and *luxC* genes were cloned into a pIRES vector using the unique *Not*I (Nt) and *Sal*I (S) or *Nhe*I (N) and *EcoR*I (E) restriction sites. (C) A second pIRES vector was created that contained the *luxD* and *frp* genes inserted at the same sites. The entire *luxC*-IRES-*luxE* fragment was then inserted under the control of the EF1-α promoter in pBudCE4.1 using the unique *Xho*I (X) and *Sfi*I (Sf) restriction sites, while the *luxD*-IRES-*frp* fragment was inserted under the control of the CMV promoter using the unique *Pst*I (P) and *BamH*I (B) restriction sites. Originally published in (Close, Patterson et al. 2010).

gene to MCS A via the unique *Nhe*I and *EcoR*I restriction sites and the addition of co*frp* to MCS B using the unique *Sal*I and *Not*I restriction sites. This entire co*luxD*-IRES-co*frp* sequence was then inserted behind the pBudCE4.1 human cytomegalovirus immediate early promoter (CMV) using the unique *Pst*I and *BamH*I restriction sites to create $pLux_{CDEfrp}$:CO. This process was repeated using wild-type codon usage versions of each of the genes to generate an identically oriented, but non-codon-optimized, vector referred to as $pLux_{CDEfrp}$:WT.

Mammalian cell transfection

Transfection was carried out in six-well Falcon tissue culture plates (Thermo-Fisher). HEK293 cells stably expressing the $pLux_{AB}$ vector were passaged into each well at a concentration of approximately 1×10^5 cells/well and grown to 90 – 95% confluence in complete medium as described above. $pLux_{CDEfrp}$:CO and $pLux_{CDEfrp}$:WT plasmid vectors were purified from 100 ml overnight cultures of *E. coli* using the Wizard Purefection plasmid purification system (Promega). On the day of transfection, cell medium was removed and replaced and vector DNA was introduced using Lipofectamine 2000 (Invitrogen).

Selection of stable bioluminescent cell lines

Twenty-four h post-transfection, the medium was removed and replaced with complete medium supplemented with the appropriate antibiotic. Selection of successfully transfected clones was performed by refreshing selective medium every 4 – 5 d until all untransfected cells had died. At this time, colonies of

transfected cells were removed by scraping, transferred to individual 25 cm^2 cell culture flasks, and grown in complete medium supplemented with the appropriate antibiotics.

Benchtop luminescent detection

Protein extraction

Total protein was extracted from co-transfected $pLux_{CDEfrp}$:CO/$pLux_{AB}$ and $pLux_{CDEfrp}$:WT/$pLux_{AB}$ cell lines using a freeze/thaw procedure. Cells were first grown to confluence in 75 cm^2 tissue culture flasks, then mechanically detached and resuspended in 10 ml of PBS. Following collection, cells were washed twice in 10 ml volumes of PBS, pelleted and resuspended in 1 ml PBS. These 1 ml aliquots of cells were subjected to three rounds of freezing in liquid nitrogen for 30 sec, followed by thawing in a 37°C water bath for 3 min. The resulting cell debris was pelleted by centrifugation at 14,000g for 10 min and the supernatant containing the soluble protein fraction was retained for analysis.

Bioluminescent detection

Bioluminescence was measured using an FB14 luminometer (Zylux) with a 1 sec integration time. To prepare the sample for *in vitro* bioluminescent measurement, 400 μl of the isolated protein extract was combined with 500 μl of either oxidoreductase supplemented light assay solution containing 0.1 mM NAD(P)H, 4 μM FMN, 0.2% (w/v) BSA and 1 U of oxidoreductase protein isolated from *V. fischeri* (Roche), or oxidoreductase deficient light assay solution (distilled

water substituted for the 1 U of oxidoreductase protein). Following the initial bioluminescent reading, samples were amended with 0.002% (w/v) n-decanal and the readings were continued to determine if additional aldehyde could increase light output. All bioluminescent signals were normalized to total protein concentration as determined by BCA protein assay (Pierce) and reported as relative light units (RLU)/mg total protein. All sample runs included processing of cell extracts from HEK293 cells stably transfected with $pLux_{AB}$ as a control for light expression upon amendment. To prepare cells for *in vivo* bioluminescent measurement, the total cell contents of a 75 cm^2 tissue culture flask were resuspended in 1 ml of Dulbecco's Modified Eagle Medium (DMEM) without phenol red supplemented with 10% fetal bovine serum, 0.01 mM non-essential amino acids, and 0.01 mM sodium pyruvate. A 15 μl aliquot of cells was removed and counted using a hemocytometer to allow all values to be normalized to viable cell counts. The remainder was used directly for bioluminescent measurement using the FB14 luminometer with a 1 sec integration time.

Growth curve analysis

Cells were harvested during exponential growth from a 75 cm^2 tissue culture flask and split into four 25 cm^2 tissue culture flasks at ~5×10^4 cells/cm^2. At 24 h intervals, the cells were detached from the flasks by mechanical agitation and resuspended in 3 ml phosphate buffered saline (PBS). A 15 μl aliquot was removed and diluted into an equal volume of trypan blue. Cells were counted

using a hemocytometer and the average of 4 counts was used to determine the total viable cell number.

Bioluminescent detection from cell culture

Determination of minimum detectable cell number in culture

Actively growing HEK293 cells expressing $pLux_{CDEfrp}$:CO/$pLux_{AB}$ were trypsinized and harvested from 75 cm^2 tissue culture flasks and counted using a hemocytometer. Using a 24-well tissue culture plate, groups of approximately either 500,000, 250,000, 100,000, 50,000, 40,000, 30,000, 20,000, 10,000, 5,000, 2,000, or 1,000 cells were plated in each of three wells in 1 ml of DMEM without phenol red supplemented with 10% fetal bovine serum, 0.01 mM non-essential amino acids, and 0.01 mM sodium pyruvate. As a negative control, three wells were supplemented with 1 ml of media without cells to observe background. Average radiance in photons/sec/cm^2/sr was determined in the IVIS Lumina using a 10 min integration time 15 h after plating.

Correlation of cell population size and bioluminescent output

To establish the relationship of cell number to bioluminescent flux, the average radiance values from cells producing a visible light signal under the conditions above were correlated to cell number.

Bioluminescent detection as a target for small animal imaging

Ethics statement

All animal work was performed in adherence to the institutional guidelines put forth by the animal care and use committee of the University of Tennessee. All animal research procedures were approved by the University of Tennessee Animal Care and Use Committee (protocol number 1411) and were in accordance with National Institutes of Health guidelines.

Cellular harvesting and preparation for injection

Actively growing HEK293 cells expressing pLuxCDEfrp:CO/pLuxAB were trypsinized and harvested from 225 cm^2 tissue culture flasks and counted using a hemocytometer. Using the average of two counts with the hemocytometer, cells were resuspended at approximately 5×10^6 cells / 100 µl PBS in a 1.5 ml tube (Eppendorf). Cells were maintained at 37℃ in a water bath until required for injection.

Whole animal bioluminescent imaging

Five week old nu/nu (nude) mice were anesthetized via isoflurane inhalation until unconscious. Subjects were then subcutaneously injected with ~5 $\times 10^6$ HEK293 cells co-transfected with $pLux_{CDEfrp}$:CO/$pLux_{AB}$ in a 100 µl volume of PBS. An equal number of HEK293 cells (~5×10^6) containing only $pLux_{AB}$ were injected as a negative control in the same volume. The subject was imaged immediately following the injections and average radiance was determined over integration times of 1 to 10 min at intervals over a 30 min period.

Determination of minimum detectable cell number following subcutaneous injection

Six week old nude mice were anesthetized via isoflurane inhalation until unconscious and then injected with decreasing numbers of HEK293 cells expressing $pLux_{CDEfrp}$:CO/$pLux_{AB}$. In a preliminary experiment, animals were subcutaneously injected at 4 separate locations with 5 million, 2.5 million, 1 million, and 500,000 cells, each in a volume of 100 µl PBS. The subject was imaged for 10 min following injection of the final group of cells. Minimum detectable cell numbers were further delineated in a second round of injections in a fresh mouse model using cell concentrations of 500,000, 250,000, 50,000, and 25,000 cells in 100 µl PBS and identically imaged.

Results

Benchtop bioluminescent detection from stably transfected HEK293 cells

To determine and compare the bioluminescent output kinetics of HEK293 cells containing the *luxCDEfrp* genes in either their wild-type ($pLux_{CDEfrp}$:WT) or codon-optimized ($pLux_{CDEfrp}$:CO) form, cells were propagated under identical conditions, harvested, and resuspended directly in a cuvette for measurement of bioluminescence against a standard photomultiplier tube interface. Cells containing $pLux_{CDEfrp}$:CO/$pLux_{AB}$ showed an average bioluminescent production 12-fold greater than background in the presence of untransfected control cells and 9-fold greater than the bioluminescent production of their wild-type counterparts (Table 3). The superior bioluminescent production by cells

Table 3. Bioluminescent production from unsupplemented HEK293 cells expressing *P. luminescens lux* genes.

Cell Line	Bioluminescent Detection (RLU/sec)
Cell Free Media	745 (± 63)
Untransfected HEK293 Cells	655 (± 44)
HEK293 + $pLux_{AB}$ + $pLux_{CDEfrp}$:WT	884 (± 44)
HEK293 + $pLux_{AB}$ + $pLux_{CDEfrp}$:CO	7600 (± 1241)

containing $pLux_{CDEfrp}$:CO/$pLux_{AB}$ validates our dual plasmid, bicistronic, codon-optimized expression strategy and substantiates our hypothesis that the full bacterial *lux* cassette can be designed for functional autonomous expression in a mammalian cell line.

Growth curve analysis

To determine if the maintenance and expression of full complements of *lux* genes was detrimental to cellular growth rates in HEK293 cells, the rates of growth among wild-type, $pLux_{CDEfrp}$:CO, and $pLux_{CDEfrp}$:WT containing cells was monitored over the course of a normal passage cycle. It was hypothesized that any adverse effects from production of aldehyde or increased presence of $FMNH_2$ resulting from the expression of the $pLux_{CDEfrp}$ plasmid would result in a slowed growth rate relative to the wild-type HEK293 cell line. No significant difference in the rates of growth was observed among any of the cell lines tested (Figure 7), suggesting that any adverse effects resulting from expression of the *luxCDEfrp* genes are minimal in regards to cellular growth and metabolism.

Bioluminescent detection from cell culture

For a *lux*-based system to function as a reporter in whole animal BLI, the resulting signal must be detectable using commercially available equipment designed for this purpose and be easily distinguishable from background light emissions. To determine if this was the case in HEK293 cells expressing full *lux* cassettes, approximately equal numbers of cells containing either codon-optimized or wild-type *lux* genes were plated in 24-well tissue culture plates and

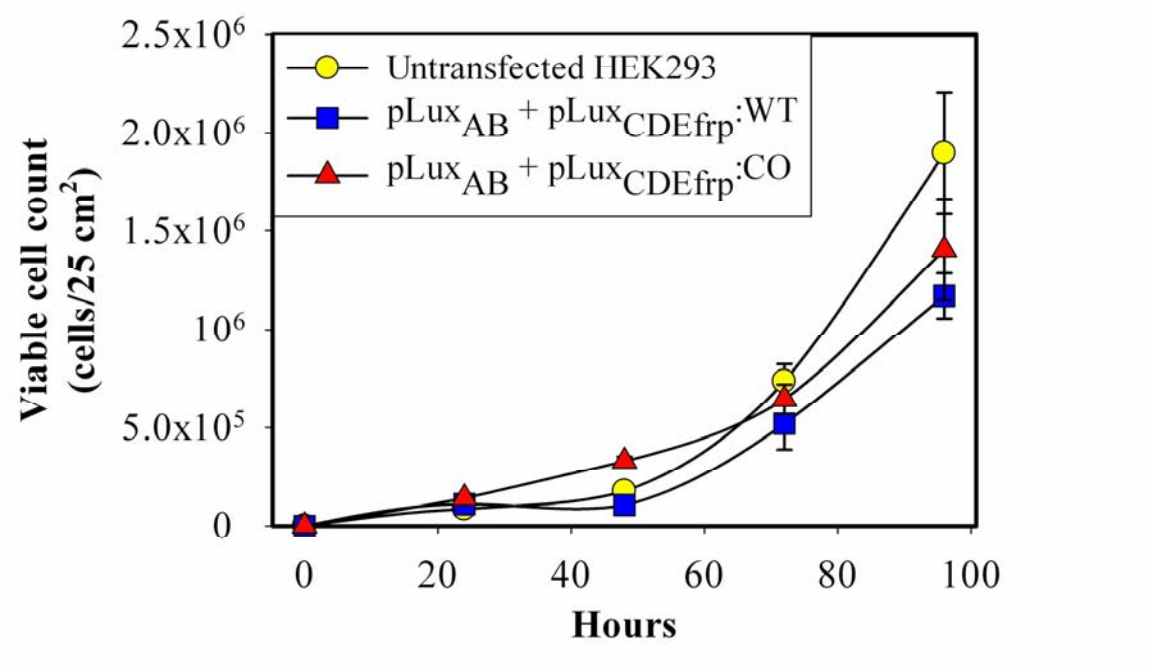

Figure 7. Growth rates of *lux*-containing HEK293 cells.

Growth curve analysis of cells containing no plasmids (negative control, untransfected HEK293) or cells containing $pLux_{AB}$ co-transfected with either $pLux_{CDEfrp}$:WT or $pLux_{CDEfrp}$:CO. Cells were grown over a 96 h period until 80% confluent, representing normal passage conditions. Values are the average of three trials and are reported with the standard error of the mean. Originally published in (Close, Patterson et al. 2010).

compared with untransfected cells as a negative control for background. The bioluminescent signal from cells co-transfected with codon-optimized *luxCDEfrp* was differentially detectable from background using a 10 sec integration time (Figure 8A) and increased in magnitude with no appreciable increase in background up to integration times of 30 min (Figure 8 B-F). To determine the maximal duration of the bioluminescent signal during constitutive expression under experimental conditions, approximately equal numbers of HEK293 cells in either their untransfected state or containing $pLux_{AB}$ co-transfected with either $pLux_{CDEfrp}$:WT or $pLux_{CDEfrp}$:CO were continually monitored for bioluminescence production (Figure 8G) in an IVIS Lumina imaging system using a stage temperature of 37°C to mimic as closely as possible their normal growth conditions. Cells containing the *lux* cassette genes demonstrated bioluminescent output over an approximate three-day period without any exogenous input. Peak bioluminescent output was achieved between 12 and 13 h for both the codon-optimized and wild-type containing cell lines, however, following peak bioluminescent output a slow decrease in bioluminescent production over time was observed. This decrease is presumably due to a combination of the inability to reliably regulate the air temperature, CO_2 levels, and humidity in the imaging system, and the continued depletion of nutrients from the media during the normal process of cellular growth and metabolism. While the bioluminescent output of cells containing $pLux_{CDEfrp}$:WT/$pLux_{AB}$ was of a lesser magnitude than that of their codon-optimized counterparts over this time period, their bioluminescent expression profiles were similar under the same conditions,

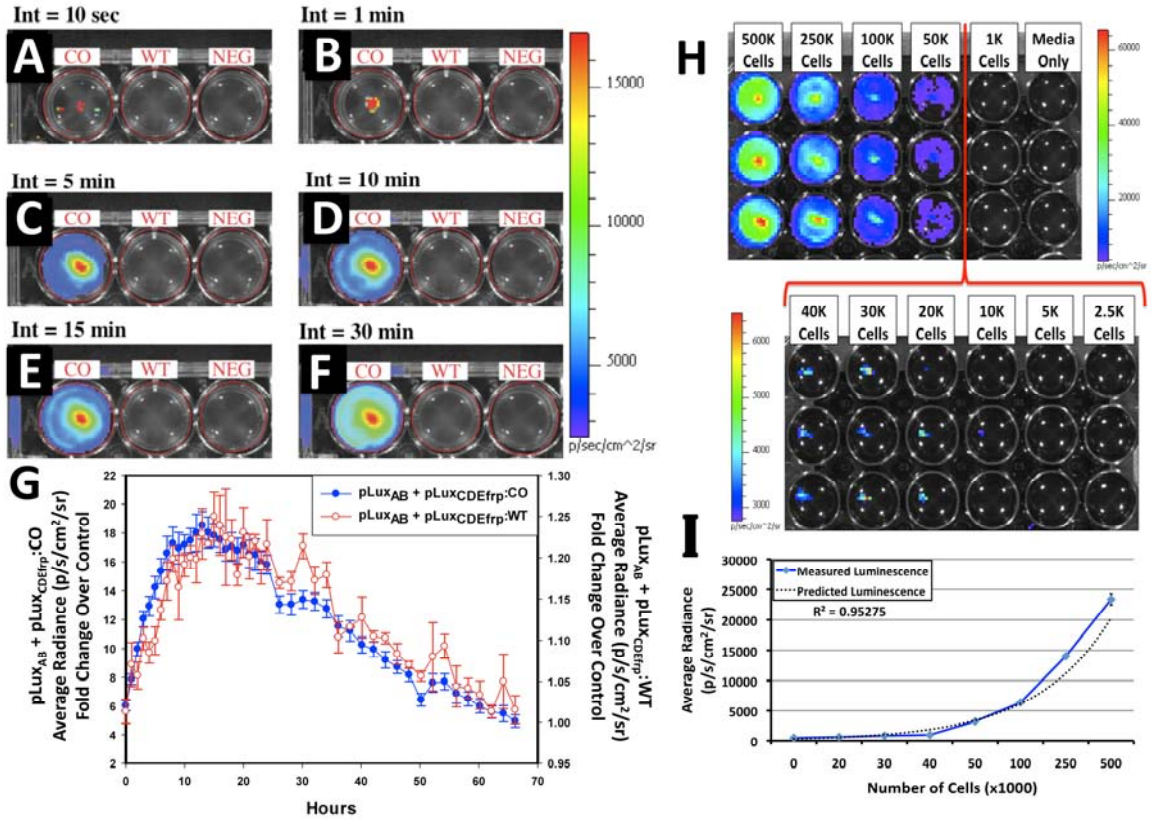

Figure 8. *in vitro* bioluminescent imaging of *lux* cassette containing cells.

$pLux_{CDEfrp}$:CO/$pLux_{AB}$ containing (CO), $pLux_{CDEfrp}$:WT/$pLux_{AB}$ containing (WT), and untransfected negative control (NEG) HEK293 cells were plated in 24-well tissue culture plates and integrated for (A) 10 sec, (B) 1 min, (C) 5 min, (D) 10 min, (E) 15 min, and (F) 30 min. Bioluminescence from cells co-transfected with $pLux_{CDEfrp}$:CO/$pLux_{AB}$ was distinguishable from background in the presence of untransfected cells after 10 sec and showed no increase in background detection even after a 30 min integration time. Long term *in vitro* expression (G) demonstrates the temporal longevity of the signal without exogenous amendment. The minimum detectable number of bioluminescent cells was determined (H) by plating a range of cell concentrations in equal volumes of media in triplicate (downward columns) in an opaque 24-well tissue culture plate. The minimum number of cells that could be consistently detected was approximately 20,000. Average radiance was shown to correlate with plated cell numbers (I), yielding an R^2 value of 0.95275. Originally published in (Close, Patterson et al. 2010).

suggesting that the codon-optimization process had not significantly altered the function of the *lux* proteins *in vivo*.

To be useful as an optical reporter, cells expressing bioluminescence must be detectable over a dynamic population range. To determine the minimum detectable cell number, HEK293 cells containing $pLux_{CDEfrp}$:CO/$pLux_{AB}$ at concentrations ranging from 1,000 to 500,000 cells were plated in triplicate in equal volumes of media over a constant surface area and imaged over a 10 min integration time. The minimum number of cells reliably detected above background was approximately 20,000 although some visible signal was detected at approximately 10,000 cells in at least one case (Figure 8H).

A major advantage imparted by the use of bioluminescent or fluorescent-tagged reporter cells is that they allow an investigator to approximately quantify the population size of those cells noninvasively in a living host. For this approximation to be made using a *lux*-based system, it must be demonstrated that the bioluminescent flux of the cell population correlates tightly with the overall population size. To determine if this is the case in HEK293 cells constitutively expressing codon-optimized bacterial luciferase genes, the average radiance of cells producing a visibly detectable bioluminescent signal was determined over cell concentrations ranging from 500,000 to 1,000 cells. The average radiance closely correlated with the number of cells present (R^2 = 0.95275) over all visibly detectable cell numbers tested (Figure 8I).

Bioluminescent detection from a small animal model system

Although *lux* has been previously used in whole animal BLI (Contag, Contag et al. 1995), this is the first demonstration of its functionality outside of a bacterial host. Bacteria-free expression of this genetic system assures that the results seen are directly related to the object of study, and are not artifacts of a host-pathogen interaction stemming from the previously required bacterial infection. To demonstrate this functionality, 5 week old nude mice were subcutaneously injected with HEK293 cells co-transfected with $pLux_{CDEfrp}$:CO/$pLux_{AB}$ or $pLux_{AB}$ alone and imaged. Cells containing only $pLux_{AB}$ were injected as a negative control to determine if the substrates supplied by the *luxCDEfrp* genes in the $pLux_{CDEfrp}$ plasmid were capable of being scavenged from endogenously available stocks within the host in the presence of the luciferase dimer formed by the products of the *luxAB* genes on the $pLux_{AB}$ plasmid. Bioluminescent signal emission from injected $pLux_{CDEfrp}$:CO/$pLux_{AB}$ HEK293 cell lines was detectable immediately (< 10 sec) following injection (Figure 9A), mirroring the results of subcutaneous tumor mimic bioluminescence from firefly luciferase (FLuc)-tagged (Inoue, Kiryu et al. 2009) and Renilla luciferase (RLuc)-tagged (Bhaumik and Gambhir 2002) cells following intravenous (IV) injection of their D-luciferin or coelenterazine substrates, respectfully. Following injection, the *lux* signal increased slowly in intensity over the full 60 min course of the assay (Figure 9B). This is in contrast to FLuc-based bioluminescent signals that exhibit a steady decline over the same period following IV injection of D-luciferin to a level ~20% of their initial intensity (Inoue, Kiryu et al. 2009). RLuc bioluminescence is even

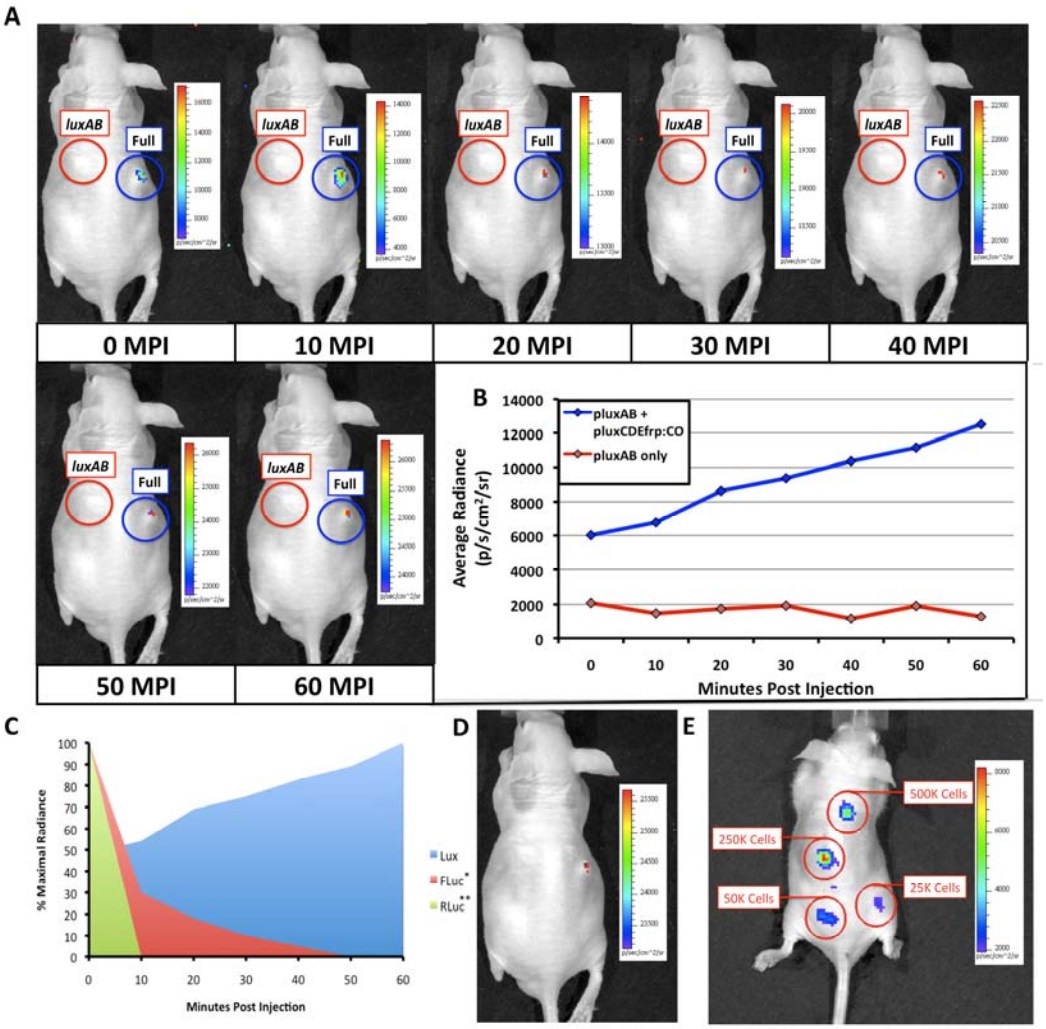

Figure 9. *in vivo* bioluminescent imaging using HEK293 cell expression of mammalian-adapted *lux*.

(A) HEK293 cells containing the mammalian adapted $pLux_{CDEfrp}$:CO/$pLux_{AB}$ cassette (Full) were subcutaneously injected into nude mice and imaged. Detection occurred nearly immediately (< 10 sec) post-injection and remained visible up to the 60 min time point of the imaging assay. HEK293 cells containing only the $pLux_{AB}$ plasmid (*luxAB*) were subcutaneously injected into the same mouse as a negative control. Note that the automatic scaling of signal intensity differs among images, therefore creating the false appearance that image intensity is decreasing after the 10 min post-injection time point when in fact it continually increases as shown in panel (B). (C) Comparison of mammalian-adapted *lux*-based bioluminescence from HEK293 cells versus published data on the expression of FLuc (*(Inoue, Kiryu et al. 2009)) and RLuc (**(Bhaumik and Gambhir 2002)) tagged cells over the 60 min course of the assay. (D) Upon termination of the assay 60 min post injection, the bioluminescent signal from HEK293 cells expressing the full complement of *lux* genes was detectable using an integration time as low as 30 sec. (E) Subcutaneous injection of HEK293 cells containing $pLux_{CDEfrp}$:CO/$pLux_{AB}$ at concentrations ranging from 500,000 to 25,000 cells in 100 µl volumes of PBS demonstrated a tested lower limit of detection of 25,000 cells using a 10 min integration time. MPI, minutes post injection. Originally published in (Close, Patterson et al. 2010).

more temporally limited and subsides within 5 min following IV injection of coelenterazine (Bhaumik and Gambhir 2002) (Figure 9C). In contrast, the *lux* bioluminescent signal remained detectable 60 min after injection using integration times as low as 30 sec (Figure 9D). Conversely, FLuc signals are asymptotically approaching their minimum (Inoue, Kiryu et al. 2009) and RLuc signals have become fully attenuated (Bhaumik and Gambhir 2002) by 30 min, thus making imaging at all but the shortest post-injection incubation times impossible (Figure 9C). It is important to note that the duration of the bioluminescent signal in FLuc containing systems can be extended by using a subcutaneous or intraperitoneal injection of luciferin, however, each injection route also produces a different bioluminescent emission profile over time (Inoue, Kiryu et al. 2009). Because they forgo the addition of exogenous substrates to trigger bioluminescence, *lux*-based systems are not subject to these effects. The lack of a signal after injection of cells expressing only $pLux_{AB}$ at any of the time points sampled (Figure 9) confirms that the luciferase dimer alone is not capable of producing unintended bioluminescence above the background levels of light detection by scavenging endogenously available substrates. These results demonstrate the utility of the *lux* system in providing bioluminescent data on relatively prolonged time scales without the potentially error-inducing requirement of disturbing the experimental environment to invasively inject additional luciferin substrate.

Having illustrated the ability to reliably detect at least 20,000 cells in a tissue culture setting (Figure 8H), the minimum detectable number of cells in

small animal models remained to be determined. The detection of bioluminescent cells following subcutaneous injection is more difficult than detection in a culture setting due to the increased presence of chromophoric material leading to higher absorption of emitted photons as they must travel through more tissue to reach the detector. Subcutaneous injections of decreasing numbers of cells into a nude mouse model revealed that the introduction of at least 25,000 cells was capable of producing a detectable signal (Figure 9E). As predicted from the correlation of cell number to bioluminescent flux, injection of higher cell concentrations produced larger bioluminescent signals over identical integration times.

Discussion

Development of the *lux* cassette into a functional and autonomous mammalian bioluminescent system provides researchers a unique new tool that allows for real-time monitoring of bioluminescence from whole animals or cell cultures without exogenous substrate addition or cell lysis. The first step in the creation of this reporter was the functional demonstration of the luciferase heterodimer formed by the *luxAB* genes (Patterson, Dionisi et al. 2005). This set the stage for the use of *lux* in eukaryotic cells as a non-autonomous reporter system via the addition of aldehyde. Since that time, the production of aldehyde has been demonstrated in *S. cerevisiae* (Gupta, Patterson et al. 2003), leading to the development of the first eukaryotic *lux*-based autonomous reporter system.

Here it has been demonstrated for the first time that expression of codon-optimized forms of the *luxCDE* genes from *P. luminescens* and the *frp* gene from *V. harveyi* are capable of producing sufficient levels of the aldehyde and $FMNH_2$ substrates required to drive light production autonomously in mammalian cells. It is further demonstrated that these bioluminescent cells can be applied in whole animal BLI without the need for substrate addition.

While the addition of *luxCDEfrp* to cells containing *luxAB* demonstrates light emission at a level 12-fold greater than background (Table 3), it remained to be determined if the associated increase in aldehyde production would be cytotoxic, as had been demonstrated in *luxAB* containing *S. cerevisiae* and *Caenorhabditis elegans* cells (Hollis, Lagido et al. 2001). If this scenario was determined to be true, the increased presence of aldehyde may therefore cause those cells capable of most efficiently producing aldehyde to inhibit their own growth, mimicking the effects of antibiotic selection and causing them to be out-competed in culture by cells expressing lower levels of aldehyde production. This investigation revealed no significant variation among the growth rates of untransfected HEK293 cells or those expressing either $pLux_{CDEfrp}$:WT/$pLux_{AB}$ or $pLux_{CDEfrp}$:CO/$pLux_{AB}$ at levels capable of supporting continuous bioluminescent production (Figure 7). These cells are necessarily producing the required aldehyde substrate as demonstrated by their constitutive bioluminescent production, but do not show a detectable difference in their rate of growth when compared to cells that are grown under identical conditions but without the

luxCDE genes required for the production and maintenance of the aldehyde substrate.

When these codon-optimized *lux* containing HEK293 cells were used in cell culture, concentrations of approximately 20,000 cells were reliably detected in 1 ml of media immediately using a 10 min integration time (Figure 8H). Increasing cell numbers in the same volume and area correlated with measured levels of bioluminescence emission, allowing one to predict the total cell number in a given sample from the measured average radiance (Figure 8I) and permitting non-invasive estimation of target size based on bioluminescent measurements.

When the same bioluminescent cell lines were applied in whole animal BLI, the low levels of detectable background signal and deficit of endogenous bioluminescent production associated with mammalian cells enabled *lux*-based bioluminescence to remain detectable. This sensitivity was demonstrated both in cell culture and under subcutaneous whole animal BLI conditions where very little light is produced due to attenuation of the bioluminescent signal by absorption from endogenous chromophores (Vo-Dinh 2003). It has been demonstrated here that cells co-transfected with the codon-optimized *luxCDEfrp* genes can produce a lasting signal that can be amplified over integration times as long as 30 min with little to no background to interfere with signal acquisition (Figure 8F) in a cell culture setting. However, it is important to note that the bioluminescent signal from this reaction is produced at 490 nm. This is relatively blue-shifted as compared to the Luc-based bioluminescent probes that display their peak luminescent signal at 560 nm. The shorter wavelength of the *lux*-based signal

has a greater chance of becoming attenuated within the tissue and therefore may not be as easily detected if it is used in deeper tissue applications (such as intraperitoneal or intraorganeller injections), and may require longer integration times to achieve the same level of detection as a longer wavelength reporter would when injected subcutaneously. For instance, it has been reported that a single cell expressing Luc can be detected following subcutaneous injection (Kim, Urban et al. 2010), whereas it is now demonstrated that the approximate lower level of detection for *lux*-tagged cells is closer to 25,000 cells, most likely due to the lower quantum efficiency of the *lux* bioluminescent system coupled with the higher rates of attenuation due to absorption at the emission wavelength of 490 nm. Therefore, the goals of a particular experiment should be carefully weighed before applying a *lux*-based bioluminescent reporter. While a *lux*-based system can produce a continuous bioluminescent signal over prolonged time periods without being subjected to the dynamic effects of repeated luciferin injections, it may not be appropriate for situations with high levels of signal attenuation due to its lower emission wavelength.

Despite such drawbacks, the use of cells expressing bacterial luciferase genes as a probe for whole animal BLI solves many of the problems associated with the currently available luciferase-based imaging systems. Previous work with *lux* genes isolated from *P. luminescens* has demonstrated that the luciferase is thermostable at the 37°C temperature required for mammalian imaging experiments (Colepicolo, Cho et al. 1989). This prevents the associated loss of signal associated with the short half-life of the firefly luciferase, which has been

shown to be thermolabile at 37°C in its native state (Baggett, Roy et al. 2004). In addition, the autonomous nature of bioluminescent production associated with the *lux* system circumvents continuous re-injection of the test animal with an exogenous luciferin substrate. This simultaneously reduces the amount of invasive injections required for imaging experiments, eliminates the detection of artificial results stemming from any non-specific biological reactions with the luciferin compound being administered, and negates the inability to compare otherwise similar experiments due to differential bioluminescent production kinetics based on dissimilar routes of substrate injection. Thus, the bacterial luciferase offers a more specific, longer lasting, and more humane luciferase-based reporter system than the currently available alternatives.

While mammalian-adapted bacterial luciferase gene expression has some notable disadvantages such as requisite introduction of multiple gene sequences and bioluminescent production at a wavelength that is relatively highly absorbed in mammalian tissues, it remains easily detectable using currently available imaging technology and offers several important advantages over the currently available reporter systems for prolonged expression without the cost or disturbance to the system associated with substrate administration. It is shown here that expression of the *luxCDEfrp* genes in mammalian cells can produce the requisite co-substrates for bioluminescent production and that codon optimization of these genes improves their performance - leading to an overall increase in light production as compared to their wild-type counterparts. When co-expressed with the *luxAB* genes responsible for formation of the luciferase heterodimer,

aldehyde production occurs at a level capable of inducing autonomous light production, but not of high enough concentration to be adversely cytotoxic. When cells containing full complements of *lux* genes are enlisted as probes in whole animal BLI, they are easily detectable when introduced at levels comparable to cells expressing other currently employed target luciferase genes and allow for facile differentiation from background over prolonged integration times at 37°C, making them ideal reporter systems for cell culture, subcutaneous, or other low absorption environments that require prolonged, real-time monitoring without disruption.

CHAPTER III

Comparison Of Mammalian-Adapted Bacterial Bioluminescence With Firefly Luciferase Bioluminescence And Fluorescence From The Green Fluorescent Protein

Introduction

Previously it has been demonstrated that autonomous bioluminescent production from a mammalian cell line expressing human-optimized (ho) bacterial luciferase (*lux*) cassette genes can be used as a target for cell culture and small animal bioluminescent imaging (BLI) (Close, Patterson et al. 2010). Here the bioluminescent expression of a mammalian HEK293 cell line transfected with the ho*lux* genes is compared with the bioluminescent expression of the same cell line expressing a commercially available, ho-firefly luciferase gene (*luc*) and the fluorescent expression of a commercially available, improved green fluorescent protein (GFP). The *luc* and *gfp* genes are two of the most widely known and used reporter genes for optical imaging (Choy, O Connor et al. 2003) and therefore provide excellent points of comparison for determining if ho*lux* expression would be beneficial in a given experiment.

The three systems are intrinsically different, and as such, have the potential to fulfill alternative niches within the needs of the bioimaging community. The

ho*lux* system is unique among bioluminescent systems because of its ability to self-synthesize and/or scavenge all required substrates from the host cell in order to produce bioluminescence in a fully autonomous fashion. The system itself is composed of five genes with the *luxA* and *luxB* gene products forming the heterodimeric luciferase enzyme, and the *luxD*, *luxC* and *luxE* gene products forming a transferase, a synthase, and a reductase respectfully, that work together to produce and regenerate the required myristyl aldehyde co-substrate from endogenous myristyl groups. A sixth gene, *frp*, encodes an NAD(P)H:flavin reductase that helps to cycle endogenous FMN into the required $FMNH_2$ co-substrate. Along with molecular oxygen, these components supply the enzyme with all the required substrates to produce a bioluminescent signal at 490 nm (Meighen 1991).

The Luc system catalyzes the oxidation of reduced luciferin in the presence of ATP-Mg^{2+} and oxygen to generate CO_2, AMP, PP_i, oxyluciferin, and yellow-green light at a wavelength of 562 nm. This reaction was originally reported to occur with a quantum yield of 0.88 (Seliger and McElroy 1960), but has since been shown to actually achieve a quantum yield closer to only 0.41 (Ando, Niwa et al. 2007). The Luc system used in these experiments utilizes a commercially available ho*luc* gene from the Promega Corporation (*luc2*). This gene encodes for an altered protein that improves translational efficiency in the mammalian cellular background and has also been destabilized to promote lower background and increased induction levels (Promega 2009).

The GFP system is perhaps one of the most well characterized and longest studied of any reporter system available (Wang, John et al. 2008). It differs from the ho*lux* and Luc systems in that it is a fluorescent reporter. Upon excitation at 395 or 478 nm it produces a fluorescent emission signal at 507 nm, allowing for detection. These experiments use an improved *gfp* gene that is commercially available from Invitrogen. This version of *gfp* has been optimized for higher levels of solubility and greater than 40-fold increase in fluorescent yield over the wild-type GFP protein (Crameri, Whitehorn et al. 1996). Despite these engineered improvements, the requisite excitation signal for this, like the majority of GFP-variants, elicits high levels of background fluorescence under small animal imaging conditions (Choy, O Connor et al. 2003; Troy, Jekic-McMullen et al. 2004). As such, its use in small animal imaging is becoming increasingly supplanted by proteins or dyes that emit light in the near infrared range where autofluorescence and absorption levels are lower (Hilderbrand and Weissleder 2009), although its use in the literature is still common and its classical dominance in the optical imaging field makes it an excellent benchmark for comparison.

The Luc and GFP imaging targets are representative of the types of reporter systems commonly employed in the optical imaging community (Burdette 2008), and provide well known benchmarks against which to compare the bioluminescent expression of the new ho*lux* system. Here the luminescent profile and intensity of ho*lux* expressing HEK293 cells is compared with the luminescent and fluorescent profiles and intensities of HEK293 cells expressing

the human optimized Luc and improved GFP systems in cell culture and small animal imaging conditions. The shape and duration of the resulting light signals over time are compared, as are respective signal intensities and minimum detectable reporter cell numbers to establish which type of reporter system may be most appropriate under a given set of imaging conditions.

Materials And Methods

Strain maintenance and growth

Escherichia coli cells were routinely grown in Luria Bertani (LB) broth with continuous shaking (200 rpm) at 37°C. When required, kanamycin or ampicillin was used at final concentrations of 40 and 100 μg/ml, respectfully, for selection of plasmid containing cells. Mammalian cell lines were propagated in Eagle's modified essential medium (EMEM) supplemented with 10% fetal bovine serum, 0.01 mM non-essential amino acids, and 0.01 mM sodium pyruvate. Cell growth was carried out at 37°C in a 5% CO_2 environment and cells were passaged every 3 - 4 d upon reaching 80% confluence. Neomycin and/or zeocin were used for selection of transfected cells at concentrations of 500 μg/ml and 200 μg/ml, respectfully, as determined by kill curve analysis, for each antibiotic.

Development of constitutively active stable cell lines

Transfection

Transfection was carried out in six-well Falcon tissue culture plates (Thermo-Fisher). HEK293 cells were passaged into each well at a concentration of ~4 × 10^5 cells/well in complete medium the day before transfection. Plasmid vectors were purified from 100 ml overnight cultures of *E. coli* using the Wizard Purefection plasmid purification system (Promega). On the day of transfection, cell medium was removed and replaced and vector DNA was introduced using Lipofectamine 2000 (Invitrogen).

Selection of stable cell lines

Twenty-four h post-transfection, the medium was removed and replaced with complete medium supplemented with the appropriate antibiotic. Selection of successfully transfected clones was performed by refreshing selective medium every 4 – 5 d until all untransfected cells had died. At this time, colonies of transfected cells were removed by scraping, transferred to individual 25 cm^2 cell culture flasks, and grown in complete medium supplemented with the appropriate antibiotics.

Screening of firefly luciferase containing HEK293 cell lines

Following stable selection with antibiotics, cells containing the *luc2* gene were tested to preferentially isolate lines producing the greatest luminescent signal following addition of D-luciferin. Cells were passaged from individual 25 cm^2 culture flasks (Corning) to individual wells of an optically clear 24-well culture

plate (Costar) and grown until confluence (1 – 2 d). Upon reaching confluence cells were lysed by application of 1X lysis buffer (Stratagene). Plates were then transferred to a Synergy 2 microplate reader (BioTek) and luminescence was measured following addition of 100 µl substrate-assay buffer (Stratagene) using an 8 sec delay and 10 sec integration time. The cell line producing the greatest luminescent output during testing was selected and maintained for experimental use.

Screening of GFP containing HEK293 cell lines

Following stable selection with antibiotics, cells containing the *gfp* gene were tested to preferentially isolate the line producing the greatest fluorescent output signal upon excitation. Cells were passaged from individual 25 cm^2 culture flasks (Corning) into black 24-well culture flasks (Costar) in a 2 ml volume of PBS. Immediately following passage cells were assayed for fluorescent production in a Wallac 1420 Multilabel counter (Perkin Elmer) using an excitation wavelength of 485 nm and a 510 nm emission filter. Cells lines producing the highest levels of fluorescence under these conditions were then subjected to a second round of testing. In the second stage, cells stably expressing GFP were grown to confluence in 25 cm^2 culture flasks (Corning) and harvested by trypination. Cell counts were obtained as the average of two counts using a hemocytometer and cells were plated into black 24-well culture plates (Costar) at a concentration of ~1×10^6 cells/well in a 1 ml volume of PBS. Cells were then assayed for fluoresce in an IVIS Lumina *in vivo* imaging system (Caliper Life

Sciences) using the GFP filter set and a 1 sec integration time. The cell line displaying the highest fluorescent emission signal under these conditions was selected and maintained for experimental use.

Bioluminescent measurement of bacterial luciferase expressing HEK293 cells in culture

Dynamics of bioluminescent production over time

Actively growing HEK293 cells expressing $pLux_{CDEfrp}$:CO/$pLux_{AB}$ (ho*lux*) were trypsinized and harvested from 75 cm^2 tissue culture flasks (Corning) and viable cell counts were determined as the average of two counts using a hemocytometer. Approximately 1×10^6 cells per well were plated in each of three wells in opaque 24-well tissue culture plates (Costar) in DMEM without phenol red and supplemented with 10% fetal bovine serum, 0.01 mM non-essential amino acids, and 0.01 mM sodium pyruvate. Along with the transfected cells, an equal number of untransfected HEK293 cells were plated to determine background luminescent detection levels. Photon counts were recorded using an IVIS Lumina *in vivo* imaging system and analyzed with Living Image 3.0 software (Caliper Life Sciences). The change in light output over time was determined in photons (p)/sec/cm^2/steridian (sr) for each well using integration times of 10 min and reported as the average of three runs with the standard error of the mean.

Minimum detectable population size

To determine the minimum detectable population size, serial dilutions of cells ranging from ~1 $\times$ 10^6 cells per well to ~100 cells per well were plated in each of three wells in opaque 24-well tissue culture plates in DMEM without phenol red and supplemented with 10% fetal bovine serum, 0.01 mM non-essential amino acids, and 0.01 mM sodium pyruvate. Along with the transfected cells, an equal number of untransfected HEK293 cells were plated to determine background luminescent detection levels. Photon counts were recorded using an IVIS Lumina *in vivo* imaging system and analyzed with Living Image 3.0 software (Caliper Life Sciences). Average radiance for all population sizes was determined in photons (p)/sec/cm^2/steridian (sr) for each well using an integration time of 10 min 17 h post-plating, as this was shown to be the period of maximum bioluminescent production as determined by tracking the dynamics of bioluminescent output as described above. Following initial analysis, a more specific minimum detectable population size was determined by performing a second assay using cell concentrations ranging between the lowest detectable number of the initial assay and the highest undetectable number of cells plated and comparing the average radiance of each population to the level of background light detected over cell-free medium. For all measurements, statistical differences were determined by using Student's *t* tests with a *p* value cutoff of $p = 0.05$.

Bioluminescent measurement of firefly luciferase expressing HEK293 cells in culture

Dynamics of bioluminescent production over time

Actively growing HEK293 cells expressing pGL4.50[*luc2*/CMV/Hygro] (Luc) were trypsinized and harvested from 75 cm^2 tissue culture flasks (Corning) and viable cell counts were determined as the average of two counts using a hemocytometer. Approximately 1×10^6 cells per well were plated in each of three wells in opaque 24-well tissue culture plates (Costar) in DMEM without phenol red and supplemented with 10% fetal bovine serum, 0.01 mM non-essential amino acids, and 0.01 mM sodium pyruvate. Along with the transfected cells, an equal number of untransfected HEK293 cells were plated to determine background luminescent detection levels. Immediately prior to imaging, all wells were spiked with 0.07 mg D-luciferin/ml (Caliper Life Sciences). Photon counts were then recorded using an IVIS Lumina *in vivo* imaging system and analyzed with Living Image 3.0 software (Caliper Life Sciences). The change in light output over time was determined in photons (p)/sec/cm^2/steridian (sr) for each well using integration times of 10 sec and reported as the average of three runs with the standard error of the mean.

Minimum detectable population size

To determine the minimum detectable population size, serial dilutions of cells ranging from ~1×10^6 cells per well to ~100 cells per well were plated in each of three wells in opaque 24-well tissue culture plates in DMEM without

phenol red and supplemented with 10% fetal bovine serum, 0.01 mM non-essential amino acids, and 0.01 mM sodium pyruvate. Along with the transfected cells, an equal number of untransfected HEK293 cells were plated to determine background luminescent detection levels. Immediately prior to imaging, all wells were spiked with 0.07 mg D-luciferin/ml (Caliper Life Sciences). Photon counts were then recorded using an IVIS Lumina *in vivo* imaging system and analyzed with Living Image 3.0 software (Caliper Life Sciences). Average radiance for all population sizes was determined in photons (p)/sec/cm^2/steridian (sr) for each well using an integration time of 10 sec immediately following the addition of luciferin, as this was shown to be the point of maximal bioluminescent output as determined by tracking the change in bioluminescent production dynamics as described above. Following initial analysis, a more specific minimum detectable population size was determined by performing a second assay using cell concentrations ranging between the lowest detectable number of the initial assay and the highest undetectable number of cells plated and comparing the average radiance of each population to the level of background light detected over cell-free medium. For all measurements, statistical differences were determined by using Student's *t* tests with a *p* value cutoff of $p = 0.05$.

Fluorescent measurement of GFP expressing HEK293 cells in culture

Dynamics of bioluminescent production over time

Actively growing HEK293 cells expressing pCDNA3.1-CT-GFP (GFP) were trypsinized and harvested from 75 cm^2 tissue culture flasks (Corning) and

viable cell counts were determined as the average of two counts using a hemocytometer. Approximately 1×10^6 cells per well were plated in each of three wells in opaque 24-well tissue culture plates (Costar) in either DMEM without phenol red and supplemented with 10% fetal bovine serum, 0.01 mM non-essential amino acids, and 0.01 mM sodium pyruvate or in PBS. Regardless of the assay medium, an equal number of untransfected HEK293 cells were plated to determine background fluorescent production levels upon addition of the excitation signal. Cells were stimulated in an IVIS Lumina *in vivo* imaging system using the supplied GFP excitation filter and photon counts were recorded using the supplied GFP emission filter. The resulting photon counts were analyzed with Living Image 3.0 software (Caliper Life Sciences). The change in fluorescent output over time was determined in photons (p)/sec/cm^2/steridian (sr) for each well using integration times of 1 sec and reported as the average of three runs with the standard error of the mean.

Minimum detectable population size

To determine the minimum detectable population size, serial dilutions of cells ranging from ~1×10^6 cells per well to ~100 cells per well were plated in each of three wells in opaque 24-well tissue culture plates in either DMEM without phenol red and supplemented with 10% fetal bovine serum, 0.01 mM non-essential amino acids, and 0.01 mM sodium pyruvate or in PBS. Regardless of the assay medium, an equal number of untransfected HEK293 cells were plated to determine background luminescent detection levels. Twenty-four h post

plating, cells were stimulated in an IVIS Lumina *in vivo* imaging system using the supplied GFP excitation filter and photon counts were recorded using a 1 sec integration time with the supplied GFP emission filter. Twenty-four h post plating was chosen as this was determined to be the point of highest fluorescent radiance as determined by tracking the change in fluorescent production over time as described above. The resulting photon counts were analyzed with Living Image 3.0 software (Caliper Life Sciences) and recorded as photons (p)/sec/cm^2/steridian (sr) for each well. All reported values represent the average of three runs with the standard error of the mean. For all measurements, statistical differences were determined by using Student's *t* tests with a *p* value cutoff of $p = 0.05$.

Bioluminescent measurement of bacterial luciferase expressing HEK293 cells in a small animal model system

Ethics statement

All animal work was performed in adherence to the institutional guidelines put forth by the animal care and use committee of the University of Tennessee. All animal research procedures were approved by the University of Tennessee Animal Care and Use Committee (protocol number 1411) and were in accordance with National Institutes of Health guidelines.

Preparation of cells for injection

Actively growing HEK293 cells expressing pLuxCDEfrp:CO/pLuxAB (*lux*) were trypsinized and harvested from 225 cm^2 tissue culture flasks and counted

using a hemocytometer. Using the average of two counts with the hemocytometer, cells were resuspended at approximately 5×10^6 cells / 100 µl PBS in a 1.5 ml tube (Eppendorf) for subcutaneous injection or at approximately 1×10^7 cells / 100 µl PBS in a 1.5 ml tube (Eppendorf) for intraperitoneal injection. Following resuspension, cells were maintained at 37°C in a water bath until required for injection.

Subcutaneous injection

Five week old nu/nu (nude) mice (NCRNU-M, Taconic Farms Inc.) were anesthetized via isoflurane inhalation until unconscious. Subcutaneous injections of ~5×10^6 HEK293 cells expressing pLuxCDEfrp:CO/pLuxAB (*lux*) in 100 µl volumes of PBS were performed in both the shoulder and hip of each subject (n = 3) for a total of n = 6 subcutaneous injections. Due to the of the lack of endogenous bioluminescent processes in mammalian tissue, and to control for changes in overall animal size and dispersion of reporter-tagged cells following injection, readings were gathered as total flux values and presented in photons (p)/second (s). All subjects were imaged immediately following the injections using 1 min integration times. Total flux from each injection site was determined by drawing regions of interest (ROI) of identical size over each location. Readings were recorded once every 10 min over a 60 min period to determine the change in flux over time.

To determine the minimal detectable number of cells *in vivo*, a subject was subcutaneously injected at three locations - the scruff of the neck, the mid back,

and hip – with the relevant range of cells as determined by the previously described minimum detectable cell number assays under culture conditions. All cell concentrations were injected in a 100 μl volume of PBS. The subject was then imaged using integration times of up to 10 min to determine if a luminescent signal could be detected above background at the injected concentrations of cells. For all measurements, statistical differences were determined by using Student's *t* tests with a *p* value cutoff of $p = 0.05$.

Intraperitoneal injection

To measure bioluminescent flux following intraperitoneal injection of the *lux* cell line, five week old nu/nu (nude) mice (NCRNU-M, Taconic Farms Inc.) were anesthetized via isoflurane inhalation until unconscious and each subject (n = 2) then received a single injection of ~1×10^7 HEK293 cells expressing pLuxCDEfrp:CO/pLuxAB (*lux*) in a 100 μ1 volume of PBS. All subjects were imaged immediately following the injections using 1 min integration times. Total flux from each injection site, measured as p/s, was determined by drawing regions of interest (ROI) of identical size over each location. Readings were recorded once every 10 min over a 60 min period in order to determine the change in flux over time.

Bioluminescent measurement of firefly luciferase expressing HEK293 cells in a small animal model system

Preparation of cells for injection

Actively growing HEK293 cells expressing *luc2* (Luc) were trypsinized and harvested from 225 cm^2 tissue culture flasks and counted using a hemocytometer. Using the average of two counts with the hemocytometer, cells were resuspended at approximately 5×10^5 cells / 100 µl PBS in a 1.5 ml tube (Eppendorf) for subcutaneous injection or at approximately 1×10^6 cells / 100 µl PBS in a 1.5 ml tube (Eppendorf) for intraperitoneal injection. Following resuspension, cells were maintained at 37°C in a water bath until required for injection.

Subcutaneous injection

Five week old nu/nu (nude) mice (NCRNU-M, Taconic Farms Inc.) were anesthetized via isoflurane inhalation until unconscious. Subcutaneous injections of ~5×10^5 HEK293 cells expressing *luc2* (Luc) in 100 µl volumes of PBS were performed in both the shoulder and hip of each subject (n = 3) for a total of n = 6 subcutaneous injections. Due to the of the lack of endogenous bioluminescent processes in mammalian tissue, and to control for changes in overall animal size and dispersion of reporter-tagged cells following injection, readings were gathered as total flux values and presented in photons (p)/second (s). Following subcutaneous injection of the reporter cells, each subject was subjected to intraperitoneal injection of 150 mg D-luciferin/kg and then imaged immediately

using 1 sec integration times. Total flux from each injection site was determined by drawing regions of interest (ROI) of identical size over each location. Readings were recorded once every 10 min over a 60 min period to determine the change in flux over time.

To determine the minimal detectable number of cells *in vivo*, a subject was subcutaneously injected at three locations - the scruff of the neck, the mid back, and hip – with the relevant range of cells as determined by the previously described minimum detectable cell number assays under culture conditions. All cell concentrations were injected in a 100 μl volume of PBS. Prior to imaging, the subject was intraperitoneally injected with 150 mg D-luciferin/kg. The subject was then imaged using integration times of up to 10 min to determine if a luminescent signal could be detected above background at the injected concentrations of cells. For all measurements, statistical differences were determined by using Student's *t* tests with a *p* value cutoff of $p = 0.05$.

Intraperitoneal injection

To measure bioluminescent flux following intraperitoneal injection of the Luc cell line, five week old nu/nu (nude) mice (NCRNU-M, Taconic Farms Inc.) were anesthetized via isoflurane inhalation until unconscious and each subject (n = 2) then received a single injection of ~1×10^7 HEK293 cells expressing *luc2* (Luc) in a 100 μl volume of PBS. Following injection of the reporter cell line, all subjects were injected at the same location with 150 mg D-luciferin/kg and then imaged immediately following the injections using 10 sec integration times. Total

flux from each injection site, measured as p/s, was determined by drawing regions of interest (ROI) of identical size over each location. Readings were recorded once every 10 min over a 60 min period in order to determine the change in flux over time.

Fluorescent measurement of GFP expressing HEK293 cells in a small animal model system

Preparation of cells for injection

Actively growing HEK293 cells expressing *gfp* (GFP) were trypsinized and harvested from 225 cm^2 tissue culture flasks and counted using a hemocytometer. Using the average of two counts with the hemocytometer, cells were resuspended at approximately 5×10^6 cells / 100 µl PBS in a 1.5 ml tube (Eppendorf) for subcutaneous injection or at approximately 1×10^7 cells / 100 µl PBS in a 1.5 ml tube (Eppendorf) for intraperitoneal injection. Following resuspension, cells were maintained at 37°C in a water bath until required for injection.

Subcutaneous injection

Five week old nu/nu (nude) mice (NCRNU-M, Taconic Farms Inc.) were anesthetized via isoflurane inhalation until unconscious. Subcutaneous injections of ~5×10^6 HEK293 cells expressing *gfp* (GFP) in 100 µl volumes of PBS were performed in both the shoulder and hip of each subject (n = 3) for a total of n = 6 subcutaneous injections. Subjects were imaged immediately following injection

with the reporter cell line using GFP excitation and emission filter with an integration time of 1 sec. Total flux from each injection site was determined by drawing regions of interest (ROI) of identical size over each location. Readings were recorded once every 10 min over a 60 min period to determine the change in flux over time.

To determine the minimal detectable number of cells *in vivo*, a subject was subcutaneously injected at three locations - the scruff of the neck, the mid back, and hip – with the relevant range of cells as determined by the previously described minimum detectable cell number assays under culture conditions. All cell concentrations were injected in a 100 μl volume of PBS. The subject was then imaged using integration times ranging from 0.5 sec to 3 min to determine if a fluorescent signal could be detected above background at the injected concentrations of cells. For all measurements, statistical differences were determined by using Student's *t* tests with a *p* value cutoff of $p = 0.05$.

Intraperitoneal injection

To measure fluorescent flux following intraperitoneal injection of the Luc cell line, five week old nu/nu (nude) mice (NCRNU-M, Taconic Farms Inc.) were anesthetized via isoflurane inhalation until unconscious and each subject (n = 2) then received a single injection of ~1×10^7 HEK293 cells expressing *gfp* (GFP) in a 100 μl volume of PBS. Total flux from each injection site, measured as p/s, was determined by drawing regions of interest (ROI) of identical size over each location following a 1 sec integration under GFP excitation and emission filters in

the IVIS Lumina *in vivo* imaging system (Caliper Life Sciences). Readings were recorded once every 10 min over a 60 min period in order to determine the change in flux over time.

Results

Bioluminescent measurement of bacterial luciferase expressing HEK293 cells in culture

Minimum detectable population size

Cells expressing the ho*lux* cassette genes produced a visible light signal over a range from approximately 1×10^6 cells/well to 1.5×10^4 cells/well using a 10 min integration time (Figure 10A). A detectable light signal was inconsistently observed at a concentration of ~1×10^4 cells/well, however this was determined not to be significantly distinguishable from background ($p = 0.72$) (Figure 11). In general, detection of lower cell populations as significantly different than background was more feasible at time points further from the initial plating (Table 4).

Dynamics of bioluminescent production over time

The luminescent profile of ho*lux* expression demonstrated a consistent increase in average radiance from an initial post-plating value of 1,800 p/s/cm^2/sr to a peak of 6,400 p/s/cm^2/sr 16 h post-plating (Figure 10B). Following peak bioluminescence, the cells expressed a slow decrease in average radiance over

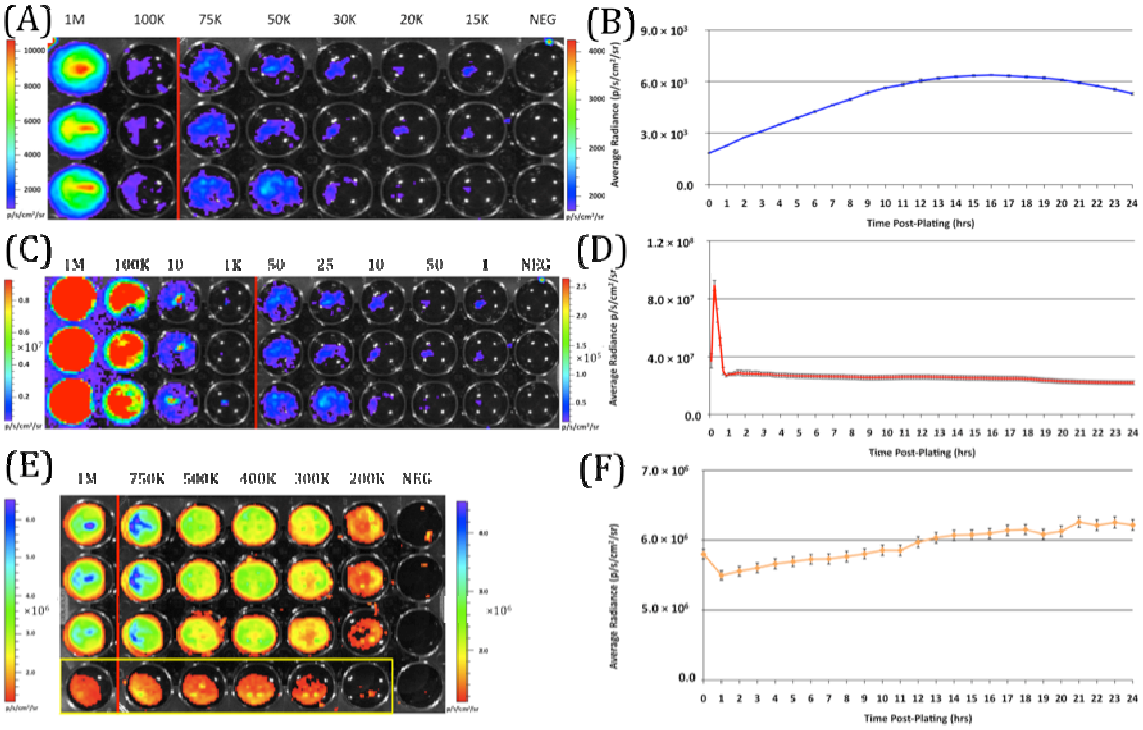

Figure 10. Comparison of *in vitro* imaging results.

Pseudocolor representation of the bioluminescent or fluorescent flux from cell concentrations ranging from 1 million (1M) to several thousand (K) to approximately single cell levels (NEG = negative control wells) stably transfected with (A) ho*lux*, (C) Luc, or (E) GFP. Red lines indicate the combination of two separate runs, each represented by the corresponding color scale on the right or left side of the figure. The yellow box in (E) indicates wells containing equal numbers of untransfected HEK293 cells to determine levels of background autofluorescence. Note that autoscaling of the pseudocolor image assigns brighter colors and larger areas to the larger population sizes of low level detection experiments although their scale indicates overall lower levels of flux compared to larger population sizes. Average bioluminescent or fluorescent flux dynamics for the (B) ho*lux*, (D) Luc, and (F) GFP containing cell populations of ~1 $\times$ 10^6 cells over a 24 h period demonstrate the differences in signal intensity over time.

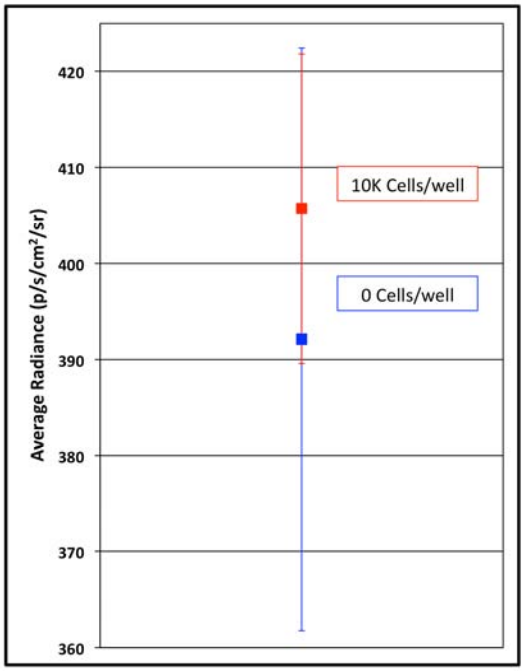

Figure 11. Detection of 10,000 *lux*-tagged HEK293 cells was not possible at statistically significant levels.

Despite presenting an intermittently detectable pseudocolor image, a population of ~10,000 ho*lux* expressing cells could not be statistically differentiated from background light detection. Boxes represent the mean values of three trials, reported with overlapping standard error of the means.

Table 4. Detection of *lux*-expressing HEK293 cells over time.

Larger population sizes of *lux*-expressing cells were visible sooner following plating. Green boxes represent time points where the indicated cell population was significantly distinguishabe from background. Red hatched boxes represent time points where the indicated cell population was not significantly distinguishable from background light detection.

Lux																									
	Time Post Plating (h)																								
Cell Population Size	0	1	2	3	4	5	6	7	8	9	10	11	12	13	14	15	16	17	18	19	20	21	22	23	24
15K Cells/well																									
20K Cells/well																									
30K Cells/well																									
50K Cells/well																									
75K Cells/well																									
100K Cells/well																									
1M Cells/well																									

the remainder of the 24 hr assay, averaging a reduction of 135 (± 16) p/s/cm^2/sr per hr. Expression was consistent over the course of the assay with the standard error of the mean averaging 58 (± 4) p/s/cm^2/sr at each time point surveyed.

Bioluminescent measurement of firefly luciferase expressing HEK293 cells in culture

Dynamics of bioluminescent production over time

The luminescent profile of the Luc expressing cells displayed a large initial intensity, with a peak average radiance of 8.9 (± 0.4) $\times$ 10^7 p/s/cm^2/sr 10 min following addition of 0.07 mg D-luciferin/ml. This level of radiance was not maintained, however, and had decreased to 3.0 (± 0.3) $\times$ 10^7 p/s/cm^2/sr by 40 min post addition. The decrease in radiance occurred during the period 10 to 30 min post substrate addition, after which the signal remained steady (± 9.3 $\times$ 10^5 p/s/cm^2/sr) for the remainder of the assay. Concurrent with the higher bioluminescent output of the Luc expressing cells compared to ho*lux* was a larger standard error. The average error over the course of the Luc luminescence assay was 2.9 (± 0.6) $\times$ 10^6 p/s/cm^2/sr (Figure 10D).

Minimum detectable population size

Cells expressing the human-optimized *luc2* gene displayed a significantly greater average radiance ($p < 0.01$) than those expressing the human-optimized *lux* genes and as a result were visible at lower concentrations. Luc expressing cells produced a visible signal over a range from ~1 $\times$ 10^6 cells/well down to 250

cells/well at an integration time of 1 sec (Figure 10C and Figure 12A). Although concentrations as low as 50 cells/well could be differentiated from background if the integration time was extended to 10 sec (Figure 12B), this concentration of cells was not determined to be statistically greater than background light detection ($p = 0.65$) while using the 1 sec integration time required to prevent saturation of the camera at the higher cell concentrations (Figure 12A). Detection of the Luc-tagged cell populations showed the opposite trend of those expressing the ho*lux* genes and was generally easier to differentiate from background at time points closer to luciferin addition (Table 5).

Fluorescent measurement of GFP expressing HEK293 cells in culture in cell culture medium

When HEK293 cells expressing GFP were tested in DMEM without phenol red it was not possible to detect the fluorescent signal of the cells above the background level of fluorescent detection at any of the population sizes surveyed. In order to better differentiate the target signal from background, the integration time was lowered down to a minimum of 0.5 sec, however this had no effect on the ability to distinguish signal from noise. Based on these results it was concluded that the assay would be preformed in PBS, as this media did not contain any serum proteins or compounds to contribute to the production of non-specific background signal in the presence of the GFP excitation signal.

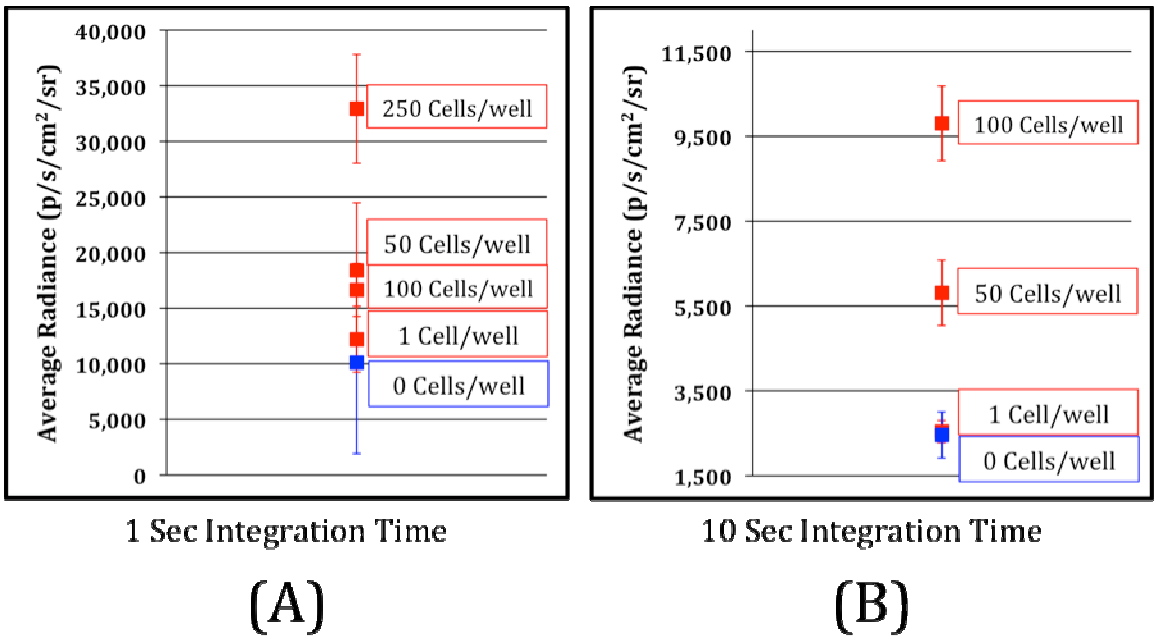

Figure 12. Minimum population size detection of Luc-tagged HEK293 cells.

Short integration times (~1 sec) are required to prevent saturation of the CCD camera when using a Luc-based reporter system due to its high levels of bioluminescent flux following D-luciferin amendment. However, at integration times of 1 sec (A) it is not possible to differentiate Luc-expressing cell populations below ~250 cells from background light detection. Increasing the integration time to ~10 sec (B) in the absence of larger population sizes to prevent camera saturation allows for detection down to ~50 cells. Boxes represent the mean values of three trials, reported with the standard error of the mean.

Table 5. Detection of Luc-expressing HEK293 cells over time.

Larger populations of Luc-expressing cells were visible over longer periods of time following the addition of D-luciferin. Due to the highly dynamic nature of Luc expression, readings are reported at 10 min intervals. Green boxes represent time points where the indicated cell population was significantly distinguishable from background. Red hatched boxes represent time points where the indicated cell population was not significantly distinguishable from background light detection.

In phosphate buffered saline

Dynamics of bioluminescent production over time

Average radiance of HEK293 cells stably expressing GFP in a PBS as a medium increased slightly but not significantly ($p = 0.08$) over the course of the assay from an initial value of 6.0 (± 0.06) × 10^6 p/s/cm^2/sr to a peak of 6.6 (± 0.07) × 10^6 p/s/cm^2/sr by 22 h after the initial plating. Over the full course of the assay the average radiance remained relatively steady at 6.2 (± 0.05) × 10^6 p/s/cm^2/sr with an average error of 7.3 (± 0.3) × 10^4 p/s/cm^2/sr (Figure 10F).

Minimum detectable population size

Fluorescent detection from GFP emission presented the least sensitive lower limits of detection for any of the three reporter systems tested when PBS was used as the assay medium. Under these conditions detection ranged from ~1 × 10^6 cells/well down to 5 × 10^5 cells/well (Figure 10E). Although wells of less than ~5 × 10^5 cells/well clearly show fluorescent signals, they were not significantly different from background following subtraction of background tissue autofluorescence (Figure 13). Similar to the ho*lux*-expressing cells, detection ability increased for the smaller population sizes over the course of the assay (Table 6). A full comparison of the pertinent expression data for all three reporter systems is detailed in Table 7.

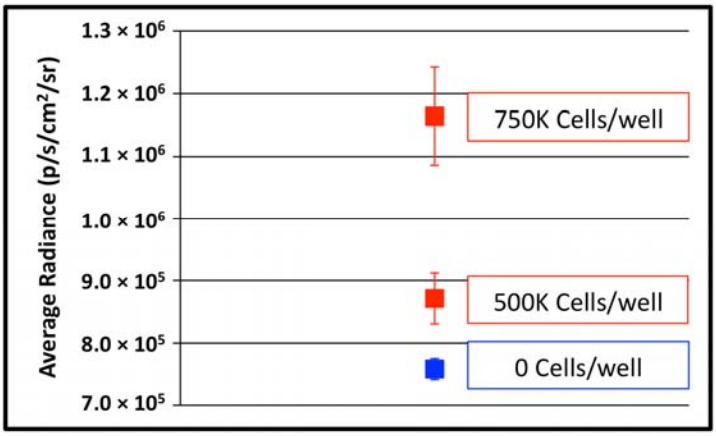

Figure 13. Minimum population size detection of GFP-tagged HEK293 cells.

Cells expressing GFP were visible down to population sizes of ~5×10^5 cells. Boxes represent the mean values of three trials, reported with the standard error of the mean.

Table 6. Detection of GFP-expressing HEK293 cells over time.

GFP-expressing cells could be significantly differentiated from background fluorescence detection at all time points following plating when greater than ~5 × 10^5 cells were present. Detection of ~5 × 10^5 cells became possible 9 hr after plating, while detection of less than ~5 × 10^5 cells was not possible at any of the time points surveyed. Green boxes represent time points where the indicated cell population was able to be significantly distinguishable from background. Red hatched boxes represent time points where the indicated cell population was not significantly distinguishable from background light detection.

GFP																								
	Time Post Plating (hr)																							
Cell Population Size	0	1	2	3	4	5	6	7	8	9	10	11	12	13	14	15	16	17	18	19	20	21	22	23	24
100 Cells/well																									
1K Cells/well																									
10K Cells/well																									
100K Cells/well																									
500K Cells/well																									
750K Cells/well																									
1M Cells/well																									

Table 7. Summary of comparisons between the ho*lux*, Luc, and GFP reporter systems under *in vitro* and *in vivo* imaging conditions.

in vitro

	Maximum Average Radiance (p/s/cm^2/sr)	Time To Peak Average Radiance (h)	Range Of Average Radiance (p/s/cm^2/sr)	Average Error (p/s/cm^2/sr)	Minimum Detectable Cell Number Across All Time Points
ho*lux*	6.4 (± 0.1) × 10^3	16	4.6 × 10^3	58 (± 4)	1 × 10^5
Luc	8.8 (± 0.4) × 10^7	0.17	8.9 × 10^7	2.9 (± 0.6) × 10^6	250
GFP	6.6 (± 0.1) × 10^6	22	6.0 × 10^5	7.3 (± 0.3) × 10^4	7.5 × 10^5

in vivo

Subcutaneous

	Maximum Total Flux (p/s)	Average Error (p/s)	Number Of Cells Injected	Integration Time (sec)	Minimum Detectable Cell Number
ho*lux*	1.5 (± 0.2) × 10^5	1.6 (± 0.3) × 10^4	5 × 10^6	60	2.5 × 10^4
Luc	2.0 (± 0.2) × 10^8	4.0 (± 0.5) × 10^7	5 × 10^5	1	2.5 × 10^3

Intraperitoneal

	Maximum Total Flux (p/s)	Average Error (p/s)	Number Of Cells Injected	Integration Time (sec)
ho*lux*	3.6 (± 0.2) × 10^5	7.0 (± 2.2) × 10^3	1 × 10^7	60
Luc	1.6 (± 0.3) × 10^9	5.8 (± 2.1) × 10^7	1 × 10^6	10

Bioluminescent measurement of bacterial luciferase expressing HEK293 cells in a small animal model system

Subcutaneous injection

Average flux from subcutaneous injection of ~5 $\times$ 10^6 ho*lux* expressing cells was 1.5 ($\pm$ 0.2) $\times$ 10^5 p/s and remained relatively constant over the full course of the 60 min assay, displaying a minimum flux of 1.3 ($\pm$ 0.1) $\times$ 10^5 p/s and a maximum of 1.5 ($\pm$ 0.2) $\times$ 10^5 p/s. The standard errors of the readings were relatively low, averaging 1.6 ($\pm$ 0.3) $\times$ 10^4 p/s and therefore provide readings with increased resolution compared to the Luc reporter system. Over the full course of the assay, the bioluminescent profile remained relatively flat, displaying a range of 2.8 $\times$ 10^4 p/s between the lowest and highest recorded values (Figure 14A). To obtain a representative pseudocolor image during acquisition, integration times of 1 min were used, however, it was previously demonstrated that detection following subcutaneous injection of ~5 $\times$ 10^6 ho*lux*-expressing cells is possible using ~30 sec integration times (Close, Patterson et al. 2010). It was also demonstrated that following subcutaneous injection the lower level for detection was 25,000 cells when using increased integration times (~10 min) (Figure 14B).

Intraperitoneal injection

Intraperitoneal injections of ~1 $\times$ 10^7 ho*lux* expressing cells yielded a disparate bioluminescent profile from that of the subcutaneous injections. The largest total flux was measured immediately following injection at a rate of

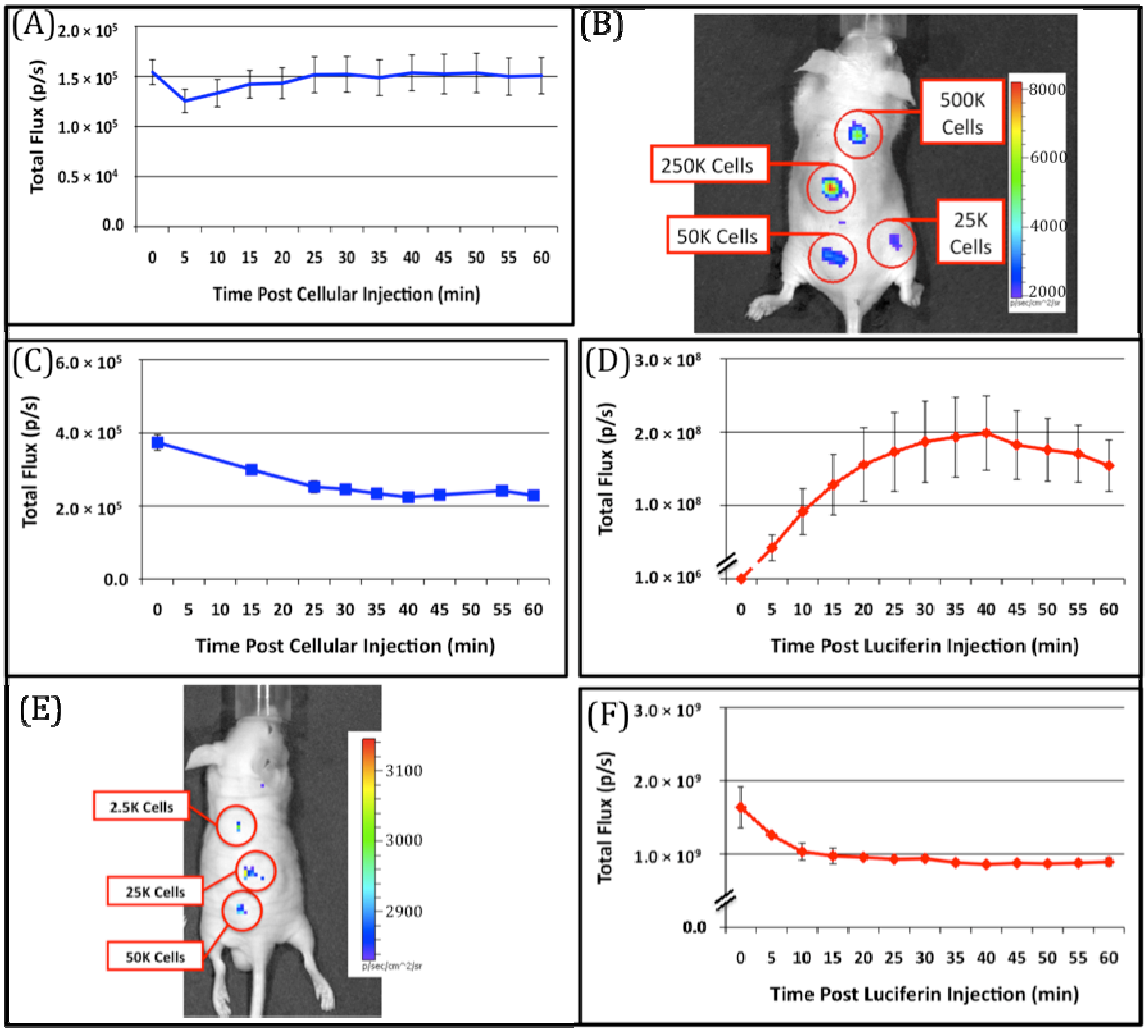

Figure 14. Comparison of *in vivo* bioluminescence for ho*lux* and Luc cells.

The bioluminescent signal following subcutaneous injection of ho*lux*-expressing cells (A) remains relatively stable following injection and is detectable (B) down to a minimum of ~25,000 cells. Signal dynamics are significantly altered (C), but of approximately the same strength following intraperitoneal injection. Total flux from subcutaneous injection of Luc-expressing cells (D) is significantly higher, and as such is detectable (E) down to ~2,500 cells. Bioluminescent output from intraperitoneal injected Luc-expressing cells (F) expressed peak flux immediately following D-luciferin injection, but then quickly diminished over the remainder of the assay.

3.6 (± 0.2) × 10^5 p/s. Following this initial light output, the total flux continued to trend downward over the remainder of the assay (Figure 14C). The greatest decrease, presumably from dispersion of the cells following injection, occurred during the first 15 min, during which the total flux decreased from the maxima to 2.4 (± 0.2) × 10^5 p/s. After this time, the rate of bioluminescent production remained relatively flat, decreasing ~67,000 p/s by the final time point of the 60 min assay. Due to the diffusion of cells within the intraperitoneal cavity following injection and the increased amount of scattering and absorption associated with intraperitoneal imaging, pseudocolor images obtained using a 60 sec integration time were not as well defined as those from the subcutaneous injections despite the injection of a higher number of cells (Figure 15 A and C). The expression value differences (in p/s) that lead to these changes in pseudocolor representation are presented in Table 7.

Bioluminescent measurement of firefly luciferase expressing HEK293 cells in a small animal model system

Subcutaneous injection

Subcutaneous injection of ~5 × 10^5 Luc containing cells produced a bell curve of bioluminescent production. Immediately following intraperitoneal injection of 150 mg D-luciferin/kg the average total flux from each injection site was 1.0 (± 0.2) × 10^6 p/s. Total flux then increased rapidly over the next 40 min to a maximum of 2.0 (± 0.5) × 10^8 p/s before declining for the remainder of the 60 min assay. Along with the increased flux values were increased error ranges at each time point as compared to the ho*lux*-expressing cell line. Standard error of

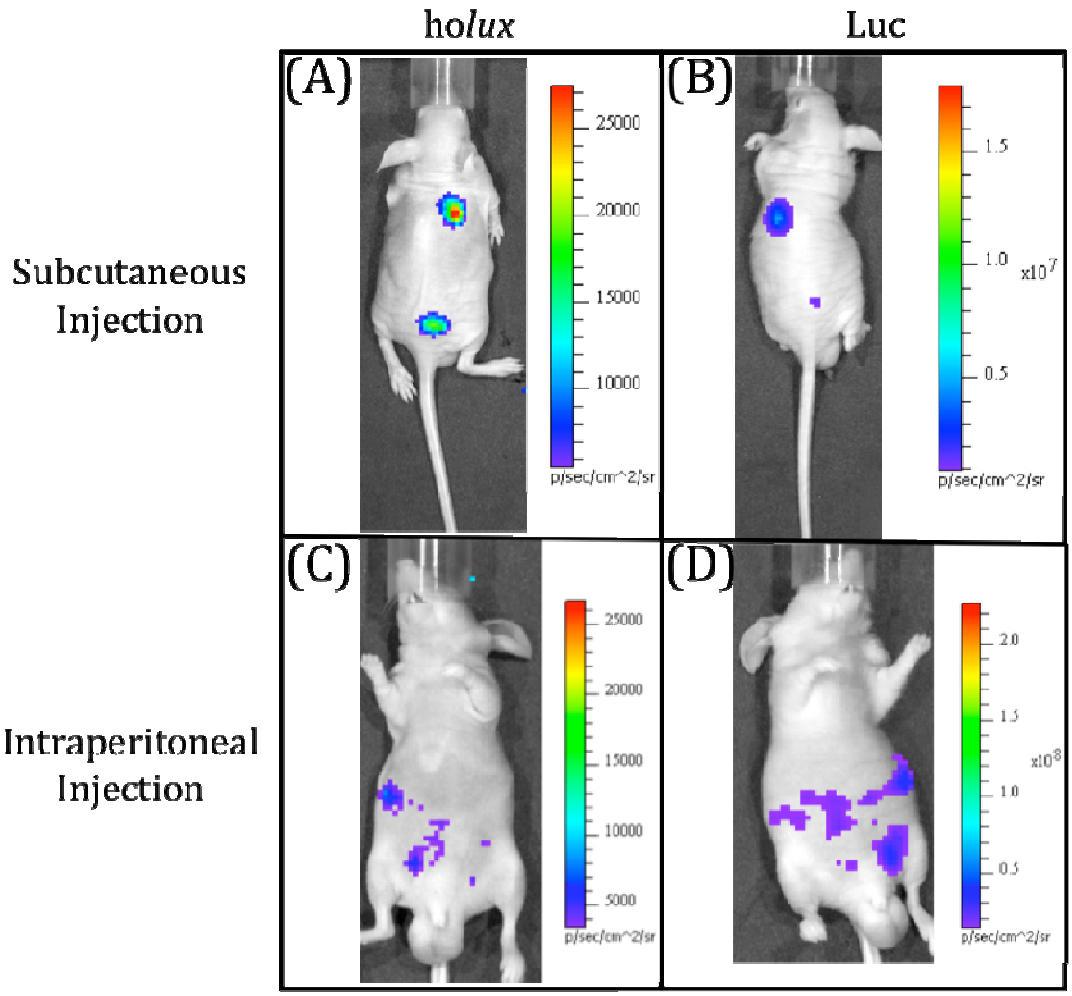

Figure 15. Comparison of pseudocolor images of subcutaneously and intraperitonealy injected ho*lux* and Luc Cells.

Subcutaneously injected (A) ho*lux* or (B) Luc expressing cells are capable of presenting relatively similar images despite the large differences in total flux from each reporter system if the integration time is increased from 1 sec (Luc) to 60 sec (ho*lux*). Similar increases must be made to maintain uniform representative detection following intraperitoneal injection of the (C) ho*lux* and (D) Luc cells as well, with the ho*lux* system requiring a 60 sec integration time to achieve similar peudocolor patterning as a 10 sec integration of the Luc system.

each reading averaged 4.0 (± 0.5) × 10^7 p/s (Figure 14D). Visual detection of signal was never problematic, with a 1 sec integration providing ample exposure for facile visual representation of the subcutaneous injection site (Figure 15B). With the system under the control of the CMV promoter, the minimum detectable cell number was determined to be 2,500 under subcutaneous imaging conditions (Figure 14E).

Intraperitoneal injection

Intraperitoneal injections of ~1 × 10^6 Luc expressing cells produced a much different time dependent bioluminescent expression profile than that obtained following subcutaneous injections (compare Figure 14F to Figure 14D). The magnitude of bioluminescent flux notwithstanding, the time dependent bioluminescent profile following intraperitoneal injection of Luc expressing cells yielded a profile similar to that obtained following intraperitoneal injections of ho*lux* expressing cells (compare Figure 14F to Figure 14C). The highest total flux occurred immediately after intraperitoneal injection of 150 mg D-luciferin/kg at 1.6 (± 0.3) × 10^9 p/s. The bioluminescent flux then quickly decreased to 1.0 (± 0.1) x 10^9 p/s by 10 min post luciferin injection. For the remaining 50 min of the assay the total flux remained relatively constant, averaging 9.2 (± 0.2) × 10^8 p/s. As with the ho*lux*-expressing cells, integration time had to be extended to obtain a representative visual image of the intraperitoneal injection site. Intraperitoneal injection of ~1 × 10^6 Luc-expressing cells, followed by immediate imaging post D-luciferin injection using a 10 sec integration time, produced a pseudocolor visual

representation similar to the pseudocolor images obtained using a 60 sec integration time following injection of ~1 × 10^7 ho*lux*-expressing cells, but did not produce images that were as well defined as those following subcutaneous injection (Figure 15 B and D). This is presumably due to the increases in absorbance and scattering associated with injection into the intraperitoneal cavity. A summary of the differences between Luc expression *in vivo* or *in vitro* following either a subcutaneous or intraperitoneal injection can be found in Table 7.

Fluorescent measurement of GFP expressing HEK293 cells in a small animal model system

Subcutaneous injection

Subcutaneous injections ranging from ~1 × 10^4 to ~1 × 10^7 GFP expressing cells failed to produce a detectable fluorescent signal when expressed in a nude mouse model. When regions of interest were drawn over the injection site of ~1 × 10^7 cells in a 100 µl volume of PBS, these locations did not produce significantly more fluorescent flux then was measured over background from a region of identical size distal from the injection site (p = 0.739). The location of the injection did not have a statistically detectable effect on the strength of the resulting fluorescent signal, with injection into the shoulder or the rump resulting in similar levels of detection for equal numbers of injected cells (p = 0.050).

Intraperitoneal injection

Similar to the results obtained following subcutaneous injection, intraperitoneal injection of GFP expressing cells at population sizes up to ~1 $\times$ 10^7 were not able to be detected at any time point during the 60 min course of the assay. Regions of interest of identical size drawn either over the injection site, or distal from the injection site at an area not expected to display fluorescent signal displayed similar levels of fluorescent flux across all surveyed time points (p = 0.100).

Discussion

There have been myriad demonstrations of the bioluminescent and fluorescent profiles obtained in culture or small animal imaging when employing the Luc or GFP proteins as targets. The variety and scope of published literature utilizing these, or versions of these, reporters is testament to their usefulness, as well as the expression strategies to which they can be adapted within the confines of a particular experimental design. To aid in the comparison of the three different systems under conditions that are as uniform and comparable as could be achieved, each was expressed in the same cellular background (HEK293) and placed under the control of identical cytomegalovirus (CMV) promoters. The use of identical promoters should encourage similar levels of expression when each construct is expressed in the HEK293 cell line (Qin, Zhang et al. 2010). However, in the ho*lux* cell line, although *luxAB* is driven by

the CMV promoter, the *luxC* and *luxE* genes are instead under the control of the human elongation factor 1α (EF-1α) promoter. Because the previously published demonstration of ho*lux* function was designed in this manner (Close, Patterson et al. 2010) it was not subjected to any modification prior to expression in order to allow for consistent comparison with the previously published results.

As expected, bioluminescence from the Luc system was detectable at lower cell concentrations and displayed a significantly larger total flux than ho*lux*-containing cells in the mouse imaging experiments and its detection level was lower than both the *lux* and GFP reporters in the cell culture imaging scenarios. Under conditions where only small populations of Luc-expressing cells were assayed in cell culture as few as 50 Luc cells/well were visible (Figure 10C and Figure 12B) compared with a minimum of 15,000 cells/well for the ho*lux* system (Figure 10A) and 500,000 cells/well in the GFP system when cells were imaged in PBS (Figure 10E and Figure 13). The need to use PBS as a liquid medium to detect lower GFP-expressing cell numbers due to the autofluorescence from the cell culture medium represents a crucial problem with using fluorescent systems for prolonged cell culture imaging. The lack of medium components such as serum and nutrients required for low-level fluorescent detection does not promote continued cellular growth, thereby preventing potential autonomous fluorescent monitoring without regular medium changes. The inclusion of these compounds can prevent this, but increases the minimum detectable cell number beyond 1 million cells/well, and therefore could not be detected under our imaging conditions.

Another approach to overcome the poor sensitivity of GFP in culture is to use an alternate cell line capable of more efficiently expressing the reporter. It has previously been demonstrated that GFP expression under the control of the CMV promoter in the MCF-7 breast cancer cell line is capable of being detected at lower numbers of GFP expressing cells/well (Caceres, Zhu et al. 2003), however, these experiments were conducted in wells of significantly smaller surface area (0.32 cm^2 as compared to 1.9 cm^2) than used in these experiments. When the results from both experiments are normalized to media volume, this corresponds to a lower detection level of ~250 cells/µl using MCF-7 cells compared to ~500 cells/µl when expressed in HEK293 cells.

Our results demonstrate, however, that the use of bioluminescence rather than fluorescence overcomes this problem completely; however, there is a large difference in the bioluminescent output levels and imaging strategies between the ho*lux* and Luc systems. The ho*lux* system has the advantage of not requiring addition of a substrate to elicit bioluminescent production, therefore allowing for completely autonomous bioluminescent readings that should routinely correlate with cell number, regardless of time. The disadvantage of the ho*lux* system is that it is significantly less efficient than the Luc system. While the average radiance of ~1×10^6 ho*lux* cells had a peak value of 6,400 p/s/cm^2/sr, this is comparable to the peak average radiance of only ~100 HEK-Luc cells/well (although this number of cells/well cannot be reliably detected following the initial bioluminescent burst following substrate amendment as shown in Table 5). Therefore, detection of small numbers of cells in culture is best suited to a Luc-

based reporter system, especially if the production of light is only to be monitored over short time periods. However, if working with larger cell populations, the use of a ho*lux*-based reporter system gives the benefit of continuous bioluminescent output, and is not dependent on the addition of luciferin to the cell culture medium. Regardless of which reporter system is employed, the use of a bioluminescent system (either ho*lux* or Luc) has the advantage of low background detection when compared with the use of a fluorescent system such as GFP in a medium-based cell culture setting.

When applied to small animal imaging, the same general benefits for each reporter system are reiterated. The major disadvantage of working with GFP or alternate fluorescent reporter systems in an animal model is the relatively high level of background fluorescence resulting from excitation of endogenous chromophoric material within the subject tissue. The use of a bioluminescent reporter helps to overcome this disadvantage due to the low levels of background autoluminescence in mammalian tissues (Welsh and Kay 2005). While Luc-based systems have most often been utilized for small animal imaging, the ho*lux* system provides a distinct advantage for near-surface target visualization. Although not as bright as the Luc system (total flux averaged 1.5 ($\pm$ 0.2) $\times$ 10^5 p/s for a subcutaneous injection of ~5 $\times$ 10^6 HEK293 ho*lux* cells vs. an overall average total flux of 1.4 ($\pm$ 0.2) $\times$ 10^8 p/s for a subcutaneous injection of ~5 $\times$ 10^5 Luc cells) the bioluminescent profile of the ho*lux*-containing cells was relatively flat over the full course of the assay, while the bioluminescent profile of the Luc-containing cells varied greatly following substrate injection. In addition, the act of

luciferin supplementation encompasses its own set of concerns. It has been well documented that the bioluminescent profile can be altered depending on the route of substrate administration for Luc-based systems (Inoue, Kiryu et al. 2009), with each route having different uptake rates throughout the body (Lee, Byun et al. 2003). Also of concern, the process of substrate injection allows for the introduction of error due to differences in the efficiency of each injection and/or the possibility of potential injection failure (i.e. injection into the bowel during intraperitoneal administration) (Inoue, Kiryu et al. 2009). Any changes in the quality of the luciferin over time during multiple injections (Mohler 2010) as well as the possible introduction of tissue damage that can prohibit further injections are also of concern (O'Neill, Lyons et al. 2010). For large-scale experiments, the cost of luciferin must also be taken into consideration, as it is an expensive substrate. Therefore, the use of a ho*lux*-based reporter is more simplistic and economical and may provide more reliable results if relatively large numbers of cells are being imaged close to the surface of the subject.

The inability to detect injections of GFP-expressing HEK293 cells at concentrations up to ~1×10^7 is in line with what has been previously reported in the literature. It has been previously demonstrated that HEK293 cells expressing GFP were not detectable until 7 d post injection when population sizes of 1×10^6 cells were used for injection (Choy, O Connor et al. 2003). With the doubling time of HEK293 cells reported to be 34 h, these cells should have reached a population size of ~1×10^7 by ~5 days, two full days prior to when they were first reported to be detectable. When GFP is expressed in other cell lines, however,

the time until detection can change. It has been reported that injection of ~1 $\times$ 10^7 GFP expressing MCF-7 cells was possible 1 d following injection (Caceres, Zhu et al. 2003), however, no information was given as to the detection ability immediately following injection. Although it may have been possible to elicit a detectable fluorescent signal by injection a higher concentration of GFP expressing cells, injection size was limited to ~1 $\times$ 10^7 cells because this was the largest injection size commonly reported in the literature.

While previous reports have suggested that detection of a single cell expressing the *luc* reporter gene is possible in the 4T1 mouse mammary tumor line (Kim, Urban et al. 2010), it is shown here that a minimum of 2,500 cells are required when the Luc system is expressed in HEK293 cells under the control of a CMV promoter (Figure 14E). Despite the increase in cells required for detection under our expression conditions, this number was still well below that required for detection of the ho*lux*-expressing cells (Figure 14B). The diminished performance of the ho*lux* cells compared to Luc-containing cells during both minimal detection level testing and intraperitoneal injection demonstrates that the associated benefits of the ho*lux* system are of little value if they cannot be easily detected under experimentally relevant imaging conditions. In cases where deep tissue imaging is required, the use of a Luc-based system can be advantageous despite the concerns associated with substrate addition, especially since its use in these types of experiments is widespread and well documented. Whether subcutaneous or intraperitoneal injection is chosen as the route of administration, it is important to realize that the decreased efficiency of the ho*lux* system as

compared to the Luc system necessitates an increase in integration time to obtain similar detection levels (Figure 15). The amount of time required for signal detection must therefore be considered in the context of a given experiment to determine if detection of the ho*lux* signal at a level similar to what a researcher may be accustomed to using a Luc-based system is acceptable.

The greatest advantages of the new ho*lux* system, however, are the ability for researchers to integrate its use alongside other established fluorescent and bioluminescent systems and the ability to exploit the unique autonomous nature of *lux* bioluminescent expression with novel detection methods. Because the presence of fluorescently labeled cells would not be detected under bioluminescent imaging conditions (i.e. in the absence of an excitation signal), the location and size of bioluminescent signals could be determined and then differentiated from any fluorescent signals detected following administration of the excitation signal. In addition, the ho*lux* signal could be determined prior to substrate injection in conjunction with alternative bioluminescent reporter systems to sequentially determine the location and size of differentially labeled cell populations within a living host. Alternatively, the autonomous nature of *lux* bioluminescent expression could allow it to be paired with miniaturized integrated circuit microluminometers (Islam, Vijayaraghavan et al. 2007) that could one day be implanted under the skin of an animal subject, allowing for real-time detection of signal without the need for external imaging equipment. This possibility opens the door for development of integrated biofeedback circuits that can autonomously monitor and subsequently react to numerous *in vivo* disease

conditions. So while the introduction of a ho*lux* imaging target certainly does not displace the use of currently available fluorescent and bioluminescent imaging targets, it can overcome some of the shortcomings of these systems and integrates well with them as an additional tool for noninvasive imaging.

CHAPTER IV

Use Of Mammalian-Adapted Bacterial Luciferase Genes As A Reporter System For Use In The Mammalian Cellular Background

Introduction

For many years researchers have been using bacteria and simple eukaryotes such as yeast to serve as proxies for measuring the bioavailability of exposed chemicals to human cells. These simple models have distinct advantages of being easy to manipulate in the laboratory, inexpensive to maintain, and highly amenable to high throughput experimental design. However, as attractive as they might be, they are not completely representative of human derived cells. As such, there is always some amount of caution that must be taken when interpreting the data obtained using these models and relating it to human bioavailability. Oftentimes human derived cells cannot be used for bioavailability screening because of the lack of reporter systems allowing for real-time, autonomous reporting of the associated effects. Fluorescent reporter systems can be employed that do not require addition of potentially influential substrates for signal generation, however, these systems have high levels of background and can require expensive equipment to properly

filter their excitation and emission signals (Tsien 1998). The use of currently available bioluminescent systems can overcome some of these technical hurdles and allow for inexpensive bench top monitoring, but does so at the cost of potentially error inducing substrate addition.

The simplest solution to this problem is to work in a less complex model system such as *Escherichia coli* or various other traditional prokaryotic organisms. This is most often done to partially alleviate the cost, scalability, and narrowed reporter availability issues that have traditionally restricted direct testing in mammalian cell lines. However, these logistical considerations come at a cost. Oftentimes the use of a prokaryotic or lower eukaryotic organism dictates that there will be significant differences in the metabolic pathways and extracellular receptor profiles as compared to those present when directly testing in mammalian cells. This has traditionally been a problem when studying the effects of compounds such as estrogen, which cannot be metabolically processed by prokaryotic organisms, or attempting to elucidate the intricacies of organelle formation, which again is not feasible using a bacterium lacking in these cellular components (Campbell, Reece et al. 2007).

In some cases, such as screening for estrogenic compounds, a lower eukaryotic host such as *Saccharomyces cerevisiae* is therefore employed that is capable of reacting to the presence of the target compound (Sanseverino, Gupta et al. 2005). However, even when using another eukaryotic organism as a proxy, there is no way to directly relate the ensuing findings to human bioavailability. Ultimately, the only way to draw direct comparisons to how a given compound

will affect a human cell is to directly test it on the tissue of interest. The use of mammalian cells that can react to the presence of a compound of interest either through the production or reduction of a bioluminescent signal in a near real-time fashion would provide a novel method for the detection and evaluation of biomedically relevant compounds in an efficient and high throughput manner, filling the niche left by the currently available mammalian-compatible reporter systems.

These concerns are clearly illustrated in the toxicology field, where it is estimated that ~$2.7 billion is spent on toxic chemical screening alone, with much of that sum being directed to animal testing (Hartung 2009). Despite this expenditure, the use of animal subjects has proven to be a poor substitute for human exposure. In one classic example, testing using rodents was shown to be able to correctly identify toxic effects in humans at a rate of only 43% (Olson, Betton et al. 2000). The use of a high throughput mammalian cell line that can be used as a screen for compound toxicity could greatly improve upon the current detection methods, as well as provide a low cost method to determine which compounds should be studied in greater detail (Ekwall, Silano et al. 1990).

Here the use of human derived HEK293 cells stably transfected with the *luxCDABEfrp* genes of the bacterial bioluminescence cassette (*lux*) is investigated as a means of overcoming the limitations imposed by currently available mammalian cell based bioavailability detection methods. To investigate the utility of these cells to act as biosensors for the presence of a specific target chemical, a version of the *lux* gene cassette was created that regulated the

expression of the *luxC* and *luxE* genes in response to doxycycline using the commercially available TET-On system (Clontech). The TET-On system represents a common method for evaluating the effectiveness of a reporter system as it has previously been shown to be effective for expression of a wide array of reporter genes across multiple mammalian cell lines (Freundlieb 2007) and therefore allows for the facile comparison of reporter function with previously published models.

It has previously been demonstrated that bioluminescence can be detected from small numbers of human cells expressing the *lux* genes, and that the bioluminescent flux can be correlated to overall cell population size (Close, Patterson et al. 2010). This makes the substrate-free, real-time bioluminescent response of a *lux*-expressing cell line an excellent platform for development into a mammalian-based reporter system designed to signal target compound detection, as well as allowing for it to be developed into a first-of-its-kind biosentinel for toxic chemical exposure. The latter is made possible because the persistence of the bioluminescent signal without excitation or addition of substrate makes it possible to measure changes in overall bioluminescent production as an indicator for changes in cellular growth and metabolism.

These types of measurements would not be possible using other reporter systems due to the economic and logistical concerns related to constantly simulating the reporter protein in order to generate the continuous signal required for real-time monitoring. The ability to autonomously produce a bioluminescent signal in response to a specific compound of interest without the requirement of

investigator intervention allows for the possibility of high throughput, on-line, remote detection systems that could significantly improve on the cost and efficiency of current detection methods. In addition, the ability to efficiently screen multiple compounds in parallel in order to evaluate their potential cytotoxic effects directly on human cells gives the *lux* reporter system an advantage over other fluorescent or bioluminescent reporter systems in the field of toxicology.

Materials And Methods

Strain maintenance and growth

Escherichia coli cells were routinely grown in Luria Bertani (LB) broth with continuous shaking (200 rpm) at 37°C. When required, kanamycin or ampicillin was used at final concentrations of 40 and 100 μg/ml, respectfully, for selection of plasmid containing cells. Mammalian cell lines were propagated in Eagle's modified essential medium (EMEM) supplemented with 10% fetal bovine serum, 0.01 mM non-essential amino acids, and 0.01 mM sodium pyruvate. Cell growth was carried out at 37°C in a 5% CO_2 environment and cells were passaged every 3 - 4 d upon reaching 80% confluence. Neomycin, hygromycin, and/or zeocin were used for selection of transfected cells at concentrations of 500 μg/ml, 100 μg/ml, or 50 μg/ml, respectfully, as determined by kill curve analysis, for each antibiotic.

Cloning of the tetracycline response element

PCR amplification

Primers were designed (TET-forward 5'-GCTAGCAGGTGGCGTGTACGGTGGGA-3', TET-reverse 5'-GCGGCCGCTCCAGGCGATCTGACGGTTC-3') to amplify a 349 bp region of the pTRE-Tight-BI plasmid (Clontech) containing both the tetracycline response element and its associated CMV promoter sequence. The TET forward primer was engineered to contain an NheI restriction site, while the TET reverse primer was engineered with an associated NotI restriction site. This allowed for the attainment of an altered PCR product that contained a 5' NheI restriction site, followed by the tetracycline response element and CMV promoter, then a 3' NotI restriction site. The resulting PCR product was then immediately TOPO cloned into the pCR4-TOPO vector (Invitrogen) to create pCR4-TET. This plasmid was used as the basis for allowing propagation and maintenance of the receptor fragment.

Introduction of the tetracycline response element into $pLux_{CDEfrp}$

The tetracycline response element and its associated CMV promoter were removed from pCR4-TET using the NheI and NotI restriction sites. In parallel with this reaction, the EF1-α promoter was removed from $pLux_{CDEfrp}$ using the same restriction sites. Following restriction digest, both reactions were purified by gel electrophoresis. The ~350 bp band representing the tetracycline response element and the CMV promoter were extracted from the lane containing the

pCR4-TET digestion and the ~8.9 kb band representing the $pLux_{CDEfrp}$ plasmid with the EF1-α promoter removed was extracted from the lane containing the $pLux_{CDEfrp}$ digestion. Both isolated fragments were purified using QIAquick Gel Extraction kits (Qiagen). The purified fragments were ligated together for 5 min at room temperature using T4 DNA polymerase (Promega) in LigaFast buffer (Promega) to create the plasmid $pLux_{CDEfrp}$-TET. The ligated plasmid DNA was then used directly for transformation. Chemically competent *E. coli* were inoculated with 2 µl of the $pLux_{CDEfrp}$-TET ligation product and selected by growth on LB medium containing 100 µg Ampicillin/ml. Successful uptake the $pLux_{CDEfrp}$-TET plasmid was confirmed by restriction digest and the success of the ligation reaction was confirmed by sequencing.

Transfection of $pLux_{AB}$ and $pLux_{CDEfrp}$ in HEK293 cells

Transfection was carried out in six-well Falcon tissue culture plates (Thermo-Fisher). The day prior to transfection, HEK293 cells were passaged into each well at a concentration of approximately 1×10^5 cells/well and grown to 90 – 95% confluence in complete medium. $pLux_{AB}$ and $pLux_{CDEfrp}$-TET plasmid vectors were purified from 100 ml overnight cultures of *E. coli* using the Wizard Purefection plasmid purification system (Promega). On the day of transfection, cell medium was removed and replaced and vector DNA mixed in a 1:1 ratio was introduced using Lipofectamine 2000 (Invitrogen).

Screening of stably transfected reporter cell lines

Twenty-four h post-transfection, the medium was removed and replaced with complete medium supplemented with the appropriate antibiotic. Selection of successfully transfected clones was performed by refreshing selective medium every 4 – 5 d until all untransfected cells had died. At this time, colonies of transfected cells were removed by scraping, transferred to individual 25 cm^2 cell culture flasks, and grown in complete medium supplemented with the appropriate antibiotics.

To screen the resulting cell lines for the ability to regulate *luxC* transcription in response to doxycycline, relative reverse transcription PCR (rt-PCR) was used to determine the level of *luxC* mRNA present 24 h following the addition of 0, 10, or 100 ng doxycycline/ml to the complete growth medium. To this end, each isolated cell line was split into 4 25 cm^2 cell culture flasks upon reaching 80% confluence. Cells were then grown at 37°C and 5% CO_2 until again reaching ~80% confluence. At this point, one of the flasks was routinely passaged to maintain a stock of cells for future use. The remaining 3 flasks were spiked with 0, 10, or 100 ng doxycycline/ml and returned to the incubator. Twenty-four h post doxycycline addition, cells were harvested and total RNA was isolated using an RNeasy isolation kit (Qiagen). Isolated RNA was used directly for rt-PCR analysis, and cell lines displaying the greatest range in *luxC* transcription between 0 ng Doxycycline/ml treatment and either 10 ng or 100 ng doxycycline/ml treatment were selected for bioluminescent screening.

Bioluminescent measurement in response to doxycycline

Cell lines displaying the greatest upregulation of *luxC* gene transcription following treatment with 10 ng and 100 ng Doxycycline/ml were passaged into 75 cm^2 tissue culture flasks (Corning) and grown at 37°C and 5% CO_2 until they reached 90% confluence. Cells were then harvested by trypsinization and cell number was determined as the average of two counts using a hemocytometer. Approximately 1×10^6 cells per well were plated in triplicate in opaque 24-well tissue culture plates (Costar) in DMEM without phenol red and supplemented with 10% fetal bovine serum, 0.01 mM non-essential amino acids, and 0.01 mM sodium pyruvate. Immediately post plating, wells were spiked with either 0, 10, 100, or 500 ng Doxycycline/ml. Photon counts were then recorded using an IVIS Lumina *in vivo* imaging system and analyzed with Living Image 3.0 software (Caliper Life Sciences). The change in light output over time was determined in photons (p)/sec (s) for each well by averaging the photon output over integration times of 10 min and reported with the standard error of the mean.

Bioluminescent measurement in response to toxic chemical exposure

To determine the ability of constitutively bioluminescent HEK293 cells to function as a bioreporter for toxic chemical exposure, cells stably expressing $pLux_{CDEfrp}/pLux_{AB}$ were exposed to increasing concentrations of the cytotoxic aldehyde n-decanal. HEK293 cells previously determined to be capable of continuous bioluminescent output from the expression of the $pLux_{CDEfrp}/pLux_{AB}$ plasmids were passaged into 75 cm^2 tissue culture flasks (Corning) and grown at

37℃ and 5% CO_2 until they reached 90% confluence. Cells were then harvested by trypsinization and cell number was determined as the average of two counts using a hemocytometer. Approximately 1×10^6 cells per well were plated in all wells in opaque 24-well tissue culture plates (Costar) in DMEM without phenol red and supplemented with 10% fetal bovine serum, 0.01 mM non-essential amino acids, and 0.01 mM sodium pyruvate. Triplicate wells were treated with serial dilutions of n-decanal ranging from 0.1% to 1×10^{-5}%, with a control set receiving no n-decanal amendment to determine maximal bioluminescent expression. Photon counts were then recorded using an IVIS Lumina *in vivo* imaging system and analyzed with Living Image 3.0 software (Caliper Life Sciences). The change in light output over time was determined in photons (p)/sec/cm^2/steridian (sr) for each well using integration times of 10 min once every hour for 24 h and reported as the average of three runs with the standard error of the mean.

Results

Regulation of luxC transcription in response to doxycycline dose

Following antibiotic selection of HEK293 cells co-transfected with $pLux_{AB}$/$pLux_{CDEfrp}$-TET, 11 cell lines were established that were capable of growing efficiently under selective media conditions. Each of these lines was interrogated for the ability to up regulate *luxC* gene transcription following

doxycycline amendment. The average C_T value for *luxC* detection in negative control cells containing no doxycycline was 13.6 (± 0.7) cycles. Following amendment with 10 ng doxycycline/ml, the average C_T value dropped to 11.9 (± 0.7), and following amendment with 100ng doxycycline/ml the average dropped to 11.5 (± 0.6). Of the eleven cell lines tested, only three showed significant ($p < 0.05$) reductions in C_T value at both 10 and 100 ng treatment levels as compared to the negative control, and also between the 10 and 100 ng treatment levels themselves (Table 8). The best performing cell line displayed a reduction of 3.5 cycles to reach C_T upon amendment with 10 ng doxycycline/ml, which corresponds to approximately 11-fold increase in *luxC* transcription. Upon induction with 100 ng doxycycline/ml, this cell line displayed a reduction of 4.3 cycles to reach C_T, an ~20-fold increase in transcription, although this was a difference of less than one cycle to reach C_T as compared to induction with 10 ng doxycycline/ml, it was determined to be a statistically significant increase in transcriptional level ($p = 0.027$). This cell line was chosen for determination of bioluminescent output in response to doxycycline addition.

Bioluminescent production in response to doxycycline dose

Using the cell line previously determined to have the most dynamic response to doxycycline treatment, cells were monitored to determine the magnitude and dynamics of bioluminescent production over a 24 h period following exposure to either 10 or 100 ng doxycycline/ml. Average background

Table 8. Regulation of *luxC* gene transcription in response to doxycycline treatment.

Cell lines demonstrating a significant ($p < 0.05$) reduction in C_T value between both negative control and 10 ng/ml doxycycline treatment and negative control and 100 ng/ml doxycycline treatment are indicated with the * symbol. The cell line selected for further testing is designated by the ** symbol.

Time	Negative Control (0 ng Doxycycline/ml)	10 ng Doxycycline/ml Treatment		100 ng Doxycycline/ml Treatment			
Cell Line	C_T Value	Δ C_T From Negative	*p* Value vs. Negative Control	Δ C_T From Negative	*p* Value vs. Negative Control	Δ C_T From 10 ng/ml Treatment	*p* Value vs. 10 ng/ml Treatment
# 1**	13.8 (± 0.2)	-3.5 (± 0.1)	< 0.01	-4.3 (± 0.2)	< 0.01	-0.8 (± 0.2)	0.03
# 2	19.5 (± 0.1)	-1.5 (± 0.4)	0.05	-3.2 (± 0.1)	< 0.01	-1.7 (± 0.1)	0.04
# 3	14.0 (± 0.8)	-1.4 (± 0.2)	0.2	-1.9 (± 0.1)	0.13	-0.4 (± 0.1)	0.17
# 4*	11.7 (± 0.1)	-1.2 (± 0.2)	0.02	-2.5 (± 0.2)	< 0.01	-1.2 (± 0.2)	0.02
# 5	12.1 (± 0.1)	-1.2 (± 0.3)	0.05	-1.7 (± < 0.1)	< 0.01	-0.5 (± < 0.1)	0.3
# 6	14.5 (± 0.2)	-3.3 (± 0.8)	0.04	-3.2 (± 0.3)	< 0.01	+0.1 (± 0.3)	0.95
# 7	13.0 (± 0.1)	-2.1 (± 0.2)	< 0.01	-2.6 (± 0.1)	< 0.01	-0.4 (± 0.1)	0.12
# 8*	12.5 (± 0.2)	-1.2 (± 0.1)	0.02	-2.0 (± 0.2)	< 0.01	-0.9 (± 0.2)	0.04
# 9	11.8 (± 0.2)	-0.7 (± 0.1)	0.1	+0.3 (± 0.3)	0.47	+0.1 (± 0.3)	0.08
# 10	12.6 (± 1.5)	-2.6 (± 1.2)	0.25	-1.1 (± 0.2)	0.56	+1.6 (± 0.2)	0.31
# 11	14.2 (± 0.2)	-0.2 (± 0.4)	0.73	-.9 (± 0.3)	0.08	-0.7 (± 0.3)	0.23

bioluminescence detection from cells that did not receive doxycycline treatment was determined to be 11,000 (± 205) p/s. Average total flux from cells treated with 10 ng doxycycline/ml was not increased significantly ($p = 0.06$), although it did trend upwards to 11,500 (± 200) p/s. Treatment with 100 ng doxycycline/ml, however, further increased the total flux to 12,500 (± 200) p/s, a significant increase over both the negative ($p = 1.1 \times 10^{-5}$) and over the 10 ng/ml treatment ($p = 9.2 \times 10^{-4}$). These values remained relatively constant over the full course of the assay (Figure 16), with ranges of only 2,010, 1,900, and 1,800 p/s for the negative control, 10 ng, and 100 ng doxycycline/ml treatments respectively following the initial evaluation at 1 h post treatment. It was possible to significantly distinguish the 100ng/ml treatment level from background at all but the 5 h post treatment time point. While it was possible to significantly distinguish the 10ng/ml treatment level at some of the time points, it was never consistently greater than that of the untreated control cells (Table 9). After it was discovered that bioluminescent production could be induced with treatment at 100 ng doxycycline/ml, but not at 10 ng doxycycline/ml, cells were treated with 500 ng doxycycline/ml to determine if higher treatment levels would be capable of inducing further increases in bioluminescent production. However, it was discovered that this treatment was not able to induce any further increase in bioluminescent output.

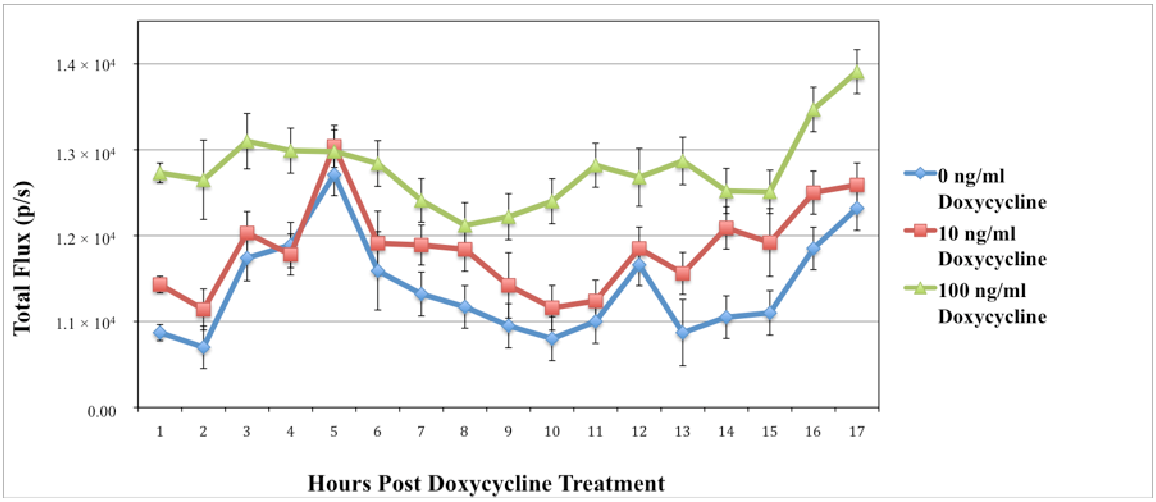

Figure 16. Bioluminescent production following treatment with varying levels of doxycycline.

Cells treated with 100 ng doxycycline/ml produced significantly greater bioluminescent flux ($p < 0.05$) than untreated cells at all time points except for 5 h post treatment, while cells receiving 10 ng doxycycline/ml produced greater bioluminescent flux only intermittently.

Table 9. Detection of significantly significant changes in bioluminescent production following doxycycline treatment.

HEK293 cells containing promoter sequences capable of regulating *luxC* and *luxE* gene expression in response to doxycycline levels can be used to report on exposure to increased levels of doxycycline in the media. Green boxes indicate time points where significant ($p < 0.05$) up regulation of bioluminescent production was detected. Hatched red boxes indicate that no significant ($p > 0.05$) increase in bioluminescent production was detected.

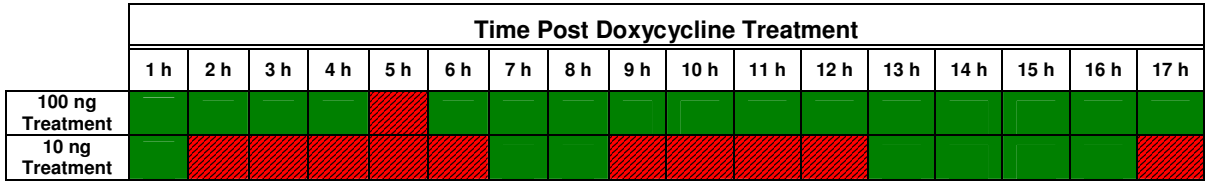

Use of constitutively bioluminescent cells as biosensors for n-decanal exposure

Constitutively bioluminescent HEK293 cells expressing $pLux_{AB}$/$pLux_{CDEfrp}$ were exposed to increasing levels of the cytotoxic aldehyde n-decanal and the rate and magnitude of bioluminescent production was monitored to determine the bioavailability of this toxicant to a mammalian cell line. It was observed that treatment with 0.1% n-decanal reduced bioluminescent output immediately following addition, with all of the surveyed time points displaying significantly down regulated production of light (Table 10). Treatment with 0.01% n-decanal also had deleterious effects on bioluminescent production, however, due to the reduced concentration, these effects were not consistently observable until 4 h after addition (Table 10). The remaining treatment levels, while not capable of inducing increases in bioluminescence, could not be statistically differentiated from cells not receiving treatment (Figure 17).

Discussion

These findings represent the first use of autonomous bioluminescent production from a mammalian cell line being harnessed to directly detect the bioavailability of compounds of interest. The unique ability of the *lux* genes to produce a bioluminescent signal that is practically background free, without exogenous stimulation, opens the door for future development of high

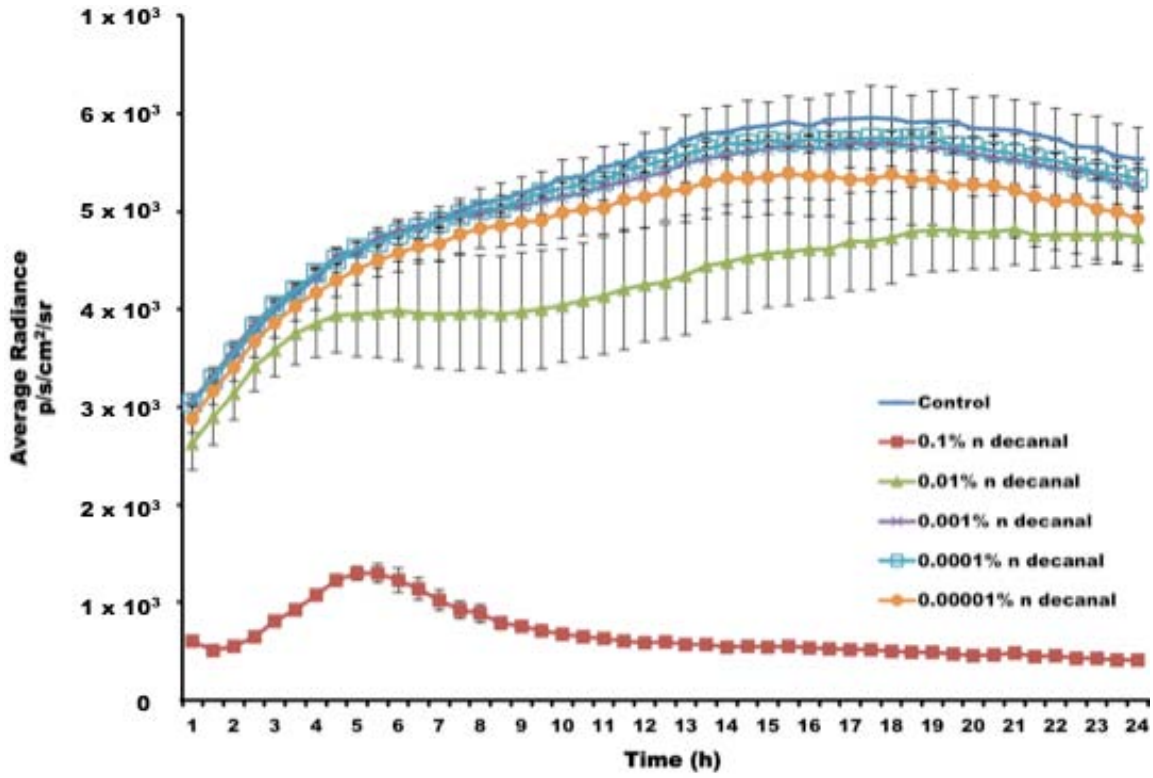

Figure 17. Bioluminescent profile of constitutively bioluminescent HEK293 cells following decanal treatment.

Treatment with 0.1% decanal leads to immediate reductions in bioluminescent output, while treatment with lower concentrations produces more subtle reductions in output. Only treatment with 0.1% and 0.01% decanal adversely effected bioluminescent production, while no treatment levels surveyed were capable of increasing bioluminescent production.

Table 10. Detection of significantly different changes in bioluminescent production following doxycycline treatment.

Hashed red boxes indicate bioluminescent profiles similar to control ($p > 0.05$). Green boxes represent bioluminescent profiles lower than untreated control cells ($p < 0.05$). At concentrations below 0.01% decanal it was not possible to differentiate the luminescent profile from that of the untreated control cell line. Intermittent deviation in bioluminescent flux was detected beginning at 40 min post decanal addition and became constant after 4 h at a concentration of 0.01%, while treatment with 0.1% decanal was able to be differentiated from control at all time points surveyed.

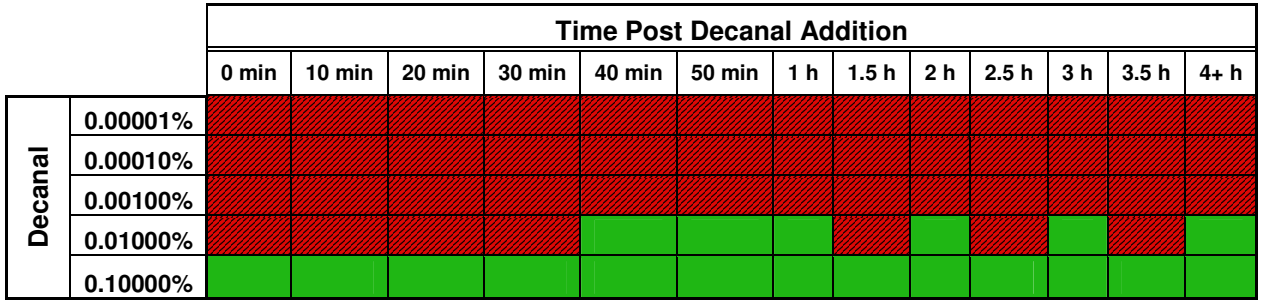

throughput, on-line monitoring systems. These types of screening systems have not previously been possible in the mammalian cellular background because of the photobleaching effects related to constant stimulation of fluorescent reporters or the prohibitively high cost of constant substrate profusion required for alternative bioluminescent reporters. With these barriers circumvented by the ability of the *lux*-expressing cells to produce light autonomously, there is now the potential to provide a facile method for screening large numbers of compounds simultaneously and directly relating the findings to human bioavailability.

The ability of *lux* expression to function as a traditional bioreporter by modulating the expression of the *luxC* and *luxE* genes under control of a tetracycline responsive promoter has been demonstrated in these experiments. The *luxC* and *luxE* genes were chosen as the regulatable genes because previously published literature has suggested that regulation of the *luxC* and *luxE* genes would provide the most digital control over bioluminescent expression using mathematical models (Welham and Stekel 2009). While this work has not demonstrated that this is in fact the most efficient method of regulation, it has validated that expression of the *luxC* and *luxE* genes can be used successfully to modulate bioluminescent expression at statistically significant levels ($p < 0.05$).

The *luxC* and *luxE* genes play a crucial role in the production and regeneration of the myristyl aldehyde substrate required by the *lux* luciferase enzyme in order to produce bioluminescence. The *luxE* gene encodes an acyl-protein syntetase that activates an intermediate fatty acid compound to provide the energy required for its future reduction to an aldhyde. It is the *luxC* gene,

which encodes a fatty acid reductase, that performs this reduction of the fatty acid precursor to form the alehyde that ultimately takes part in the bioluminescent reaction. Previous work has demonstrated that constitutive expression of the *luxA* and *luxB* genes that form the actual luciferase enzyme is not cytotoxic (Patterson, Dionisi et al. 2005) and that expression of these genes alone is not sufficient to elicit bioluminescent production without the function of the remainder of the *lux* cassette genes (Close, Patterson et al. 2010). It has also been shown that high levels of aldehyde expression can be toxic in organisms exogenously expressing the *lux* genes (Hollis, Lagido et al. 2001). Taken together, these data suggest that regulation of aldehyde production within the mammalian cell will be the most efficient means for controlling bioluminescent expression while simultaneously maintaining efficient conditions for cellular growth and metabolism.

While it may have been more efficient to control only a single gene (i.e. only *luxC* or *luxE*) rather than multiple genes to serve this purpose, it was necessary to simultaneously regulate two genes in order to properly mimic the polycistronic nature of the cassette within the mammalian host cells. Regulation of only one gene would have required re-engineering of the previously validated *lux* vectors, as well as the possible introduction of a third plasmid. This prospect would have been detrimental to transfection efficiency and significantly decreased the chances of successfully establishing a stable cell line expressing all three plasmid constructs.

Treatment of cells expressing the *luxC* and *luxE* genes under the control of the tetracycline responsive promoter with 100 ng doxycycline/ml was able to elicit a significant up regulation in bioluminescent output ($p = 1.1 \times 10^{-5}$) following a relatively short incubation period of 1 h (Figure 17). This time period is in line with previously published reports that have indicated the tetracycline responsive promoter is strong enough to produce detectable levels of its downstream gene product in as little as 30 min (Yarranton 1992; Gossen and Bujard 1993). It is not known why the bioluminescent levels of the control and 10 ng doxycycline/ml treated cells increased transiently during the 5 h time point (Figure 16). This anomalous increase in flux from the control cell line represents the only surveyed time point where it was not possible to statistically differentiate the signal from cells treated with 100 ng doxycycline/ml from the negative control, however, it maintained the trend of non-statistically differential expression between the control and 10 ng doxycycline/ml treated cell lines. The most parsimonious explanation is that there was a mechanical anomaly with the imaging equipment leading to false positive levels of photon acquisition counts over an area of the 24 well plate that contained both the negative control and 10 ng doxycycline/ml treated cells, as these were spatially adjacent during imaging. The 100 ng doxycycline/ml treated cells remained distal from this section of the plate, and therefore may not have been affected by the anomaly, explaining why there was not a corresponding increase in measured bioluminescent flux for all three treatment levels at the 5 h time point.

Levels of bioluminescent flux from cells treated with 100 ng doxycycline/ml were smaller than those detected from similar numbers of constitutively bioluminescent cells in culture. When the *luxC* and *luxE* genes were continuously expressed under the control of the EF1-α promoter the maximum level of radiance was measured at 4.5 (± 0.16) × 10^5 p/s, whereas, with the *luxC* and *luxE* genes placed under the control of the tetracycline responsive promoter and induced with 100 ng doxycycline/ml, the maximum measured flux was 1.3 (± 0.03) × 10^4 p/s. This is most likely due to a combination of the improved efficiency of the EF1-α promoter as compared to the tetracycline responsive promoter and the increases in transcriptional efficiency imparted during continuous expression.

Due to the discrepancy in luminescent flux between tetracycline responsive cell lines and those displaying constitutive expression, increases in treatment levels above 100 ng doxycycline/ml were attempted, however, none were shown to further increase bioluminescent output. These results indicate that the tetracycline responsive *lux* reporter cells have a relatively narrow detection range, and therefore would not make efficient laboratory reporter strains at this time. There are, however, further avenues that could be explored to improve their performance. The first steps in this direction would be the redesign of the plasmid vectors to regulate expression of only a single *lux* gene, or the choice of alternative *lux* genes as points of regulation for reporter function. General considerations for optimization of the *lux* system that could be applied as well will be discussed extensively in chapter V.

Due in part to the poor performance of *lux* expressing cells to act as a bioreporter for specific compound detection, it was further investigated whether or not constitutively bioluminescent mammalian cells could function as biosensors for toxicological screening. These unique cells are ideal platforms for real-time monitoring of the mammalian bioavailability of potentially toxic compounds, an assay that has not been previously available. To determine their effectiveness in this roll, cells were exposed to n-decanal, a cytotoxic aldehyde similar to the product of the bacterial bioluminescent reaction, and the minimum exposure level capable of reducing bioluminescent production was determined. Decanal was chosen for the initial assay because it can serve a three-fold purpose. As a similar product to that of the reaction catalyzed by the actions of the *luxCDE* genes (Meighen 1979), there have long been concerns over the potential cytotoxicity of these types of compound when the *lux* system is expressed in non-native organisms (Hollis, Lagido et al. 2001). By using changes in bioluminescence to monitor for the effects of n-decanal on the HEK293 cell line it was possible to determine 1) if small supplements of the compound can increase bioluminescent intensity, 2) at what level the compound becomes toxic to the cell, and ultimately, 3) if a constitutively bioluminescent mammalian cell line can function as a reporter system for toxic chemical exposure.

It was hypothesized that slight increases in n-decanal availability would lead to increased bioluminescent output. Previous work had indicated that when additional levels of n-decanal were made available to cell extracts containing the

lux proteins, it was possible to increase overall bioluminescent output *in vitro* (Close, Patterson et al. 2010). This effect was not observed during *in vivo* testing (Figure 17) however, and none of the time points surveyed produced a result whereby a cell population treated with any level of decanal produced significantly greater bioluminescent flux than the untreated control line. The small, aliphatic nature of n-decanal allows it to cross the membrane of Gram negative bacteria (Sizemore, Geissdorfer et al. 1993), and our data supports the hypothesis that the saturated ten carbon tail also allows the molecule to pass through the lipid bilayer of mammalian cells. Using the newly developed assay it was confirmed that n-decanal treatment is adversely toxic (high levels of the compound will fix cells in a manner similar to formaldehyde) and will become detrimental to cellular health at concentrations required to generate the diffusive force required to cross the membrane. It is possible, however, that there are alternative explanations for the failure of low level n-decanal treatment to increase bioluminescent flux. The cell could be reaching an equilibrium where the additional influx of aldehyde is boosting bioluminescent production levels, but simultaneously negatively effecting cellular metabolism, thereby reducing overall bioluminescent yield. This situation seems unlikely, given the observation that there is no effect over three orders of magnitude of aldehyde concentration. It is more parsimonious that the low levels of aldehyde concentration do not provide enough diffusive force to allow n-decanal to cross into the interior of the cell through the lipid bilayer.

Despite the inability of low levels of aldehyde treatment to stimulate bioluminescent production, it was clear that at and above concentrations of

0.01% the aldehyde became toxic to the HEK293 cell line (Table 10). While treatment with 0.1% decanal reduced bioluminescent output at all time points surveyed, treatment with 0.01% was not able to consistently reduce bioluminescence until 4 h after addition. These results are comparable with previously published reports that demonstrated the ability of aldehyde to diffuse into Gram negative bacteria at concentrations in the range of ~ $0.25 – 50 \times 10^{-5}$ M (Rogers and McElroy 1958). Our 0.01% decanal treatment corresponds to a concentration of ~64×10^{-5} M. While the previous experiments used the slightly longer dodecanal in place of decanal (C_{12} compared to C_{10}), less of that aldehyde is required to enter the cell in order to elicit a similar bioluminescent response because the longer chain aldehydes have been shown to produce a greater bioluminescent signal upon utilization in the *lux* reaction despite their slower penetration of the cell wall (Rogers and McElroy 1958). These data suggest that the concentration range of 10^{-5} M is the point where decanal is able to cross the cell wall at a rate greater then it is able to be cleared by aldehyde metabolizing enzymes.

The initial production of bioluminescence within error of the positive control indicates that for the first 0.5 h, a sufficient concentration of aldehyde has not entered into the cells to elicit a change in metabolism or cellular health. The fluctuations in bioluminescent production over the next 2 h indicate that aldehyde has entered into the cell, but is likely being processed by endogenous aldehyde metabolizing proteins, whereas the distinct reduction in bioluminescence

following the 4 h time point suggests that the concentration of aldehyde has become too great to be cleared and has begun causing cellular damage.

The clear distinction between concentrations of aldehyde that affect bioluminescent production, and those that do not have an affect, suggest that constitutively bioluminescent mammalian cells can be used as sensors for monitoring the bioavailability of toxic compounds in real time. Specifically the treatment of cells with 0.01% decanal shows that the real-time nature of the *lux* expression system can allow researchers to determine not only the presence or absence of an affect from their treatment of interest, but can also do so in a time-dependent manner. The autonomous nature of this reaction demonstrated by these results will allow for the development of biosentinel devices capable of acting remotely to detect and report directly on the mammalian bioavailability of a variety of biomedically relevant compounds in a way that is not feasible using substrate dependent luciferase systems.

CHAPTER V

Initial Optimization Of The Mammalian-Adapted Bacterial Bioluminescence System And Determination Of Objectives For Future Improvements

Introduction

The use of mammalian-adapted bacterial luciferase (*lux*) genes as a reporter system in human cells is still in its infancy. While the initial results detailed in this work are encouraging, the future of the mammalian *lux* system is still being written. As the newest of the mammalian-compatible reporter options, the *lux* system has not had the advantage of optimization that comes from widespread adoption and evaluation by multiple research groups.

Thus far, all of the popular genetic-based (i.e. those derived directly from living organisms) fluorescent and bioluminescent reporter systems currently being employed for small animal imaging have had the advantage of multiple refinements in order to increase their efficiency under standard laboratory conditions. Perhaps the best example of these incremental improvements has been with the widely used green fluorescent protein (GFP). Originally detailed in 1962 (Shimomura, Johnson et al. 1962), the GFP protein has undergone extensive modification from its native state in the last ~50 years in order to

compensate for the traits that make it less attractive for use as an imaging target. The genetic structure of the GFP protein has been altered repeatedly in order to allow it to fold properly in mammalian cells at the relatively increased temperature of 37°C (Crameri, Whitehorn et al. 1996), to prevent dimerization under the high levels of constitutive expression that are preferred for facile image acquisition (Zacharias, Violin et al. 2002), and mutated myriad times in order to alter the signal emission wavelength so that it can be used in tandem with other reporters, or detected with greater efficiency through living tissue (Heim, Prasher et al. 1994; Heim and Tsien 1996; Ormo, Cubitt et al. 1996). Each of these incremental changes have led to the development of a protein that, while the same in name, in some implementations, can not even be spectrally identified as its native precursor.

The same can be said for alternative bioluminescent proteins such as firefly luciferase (Luc). Recently there have been modifications engineered into the *luc* gene, leading to is commercial replacement with *luc2*, a modified version that has been designed to improve translational efficiency in the mammalian cellular background and has also been destabilized to promote lower background and increased induction levels (Promega 2009). As the use of optical imaging technologies continues to spread in the scientific community, there will continue to be an increasing drive for the development of new, enhanced versions of the Luc protein, just as there has for GFP, in order to fill the diverse requirements of new researcher's specific experimental designs.

If use of the *lux* reporter system spreads to even moderate levels among those actively engaged in optical imaging, there will no doubt be great interest in enhancing its bioluminescent characteristics, just as there has been with other widely adopted reporter systems. To this end, the groundwork for future development and optimization of the *lux* system has been laid out, with increasing the bioluminescent flux of the system as the primary goal. Under its current implementation, the mammalian-adapted *lux* system cannot produce levels of bioluminescent flux as high as any of the commercially available bioluminescent proteins can, following amendment with their luciferin substrates. Enhancing the bioluminescent flux of the *lux* system to achieve levels of flux on par with the alternative systems would overcome this deficiency, which is viewed as the main hurdle to its widespread use in the optical imaging community, and prevent it from being used solely as a niche-based reporter for experimental designs that require bioluminescent production without substrate amendment.

To determine points for future optimization of the *lux* system that could increase bioluminescent production, the function of the *lux* genes within the HEK293 mammalian cell line was first investigated. While the function of the *luxA* and *luxB* genes has previously been evaluated extensively (Patterson, Dionisi et al. 2005; Close, Patterson et al. 2010), the focus of these experiments was to evaluate the function of the remaining *luxC*, *luxD*, *luxE*, and *frp* genes that are responsible for establishment and regeneration of the aldehyde and $FMNH_2$ substrates required for bioluminescent production. The *luxC*, *luxD*, and *luxE* genes produce protein products that work together in a complex to supply the

myristyl aldehyde substrate (Meighen 1991). Their codependence allows them to be evaluated simultaneously, because a deficiency in any one will adversely effect the production of bioluminescence *in vivo*. The *frp* gene acts independently, and therefore was evaluated separately in order to determine its function in the regeneration of cytosolically available $FMNH_2$.

Because the function of these genes is in part dependent on the efficiency of their expression in the mammalian cellular environment, the translational efficiency imparted by the internal ribosomal entry site (IRES) elements that were included to spur translation of the *lux* genes while mimicking the polycistronic nature of the original bacterial operon was also investiagated. The use of a 2A linker site as an alternative to the IRES element was investigated and the resulting changes in *in vitro* bioluminescent production levels were compared. The 2A element was chosen because it performs the same basic function of the IRES element by generating multiple protein products from a single mRNA under the control of a single promoter element. However, the means by which the protein products are created are very different.

IRES elements are relatively large sequences of DNA that, upon transcription into mRNA, form a secondary structure capable of attracting and binding a ribosome to initiate translation of the downstream gene (Lupez-Lastra, Rivas et al. 2005). On the other hand, 2A elements are short, in-frame, linker regions that separate two in-frame ORF's driven off of a single promoter. During translation of the 2A sequence region the nascent amino acid sequence interacts with the exit tunnel of the ribosome, causing a "skipping" of the last peptide bond

at the C terminus of the 2A sequence. Despite this missing bond, the ribosome is able to continue translation, creating a second, independent protein product. The short nature of the sequence (they average 10 amino acids in length) and highly efficient 1:1 stoichiometry of these sequences give them many advantages over the more bulky IRES elements (de Felipe 2004).

By determining if increased efficiency of the aldehyde and/or $FMNH_2$ regulating genes increased bioluminescent output in the mammalian-adapted *lux* system, it allows future research to focus on improving the specific aspects of the *lux* system that can lead to the most beneficial improvements in the shortest amount of time. Likewise, the comparison of IRES-based polycistronic expression with a 2A-based expression system highlights if the exchange of these linker regions provides tangible advantages beyond the simple reduction in overall system size and repetition of large sequences of DNA in the plasmid vectors. It was not expected that these initial investigations would lead directly to the development of improved *lux* function in the mammalian cellular background, but instead, that they would provide the framework for moving forward with the first steps of what will hopefully one day be a rich history of *lux* development.

Materials And Methods

Replacement of IRES elements with 2A elements

Synthesis of 2A elements

To determine if the IRES element linking together the *luxA* and *luxB* genes in the original $pLux_{AB}$ construct was detrimental to transcriptional/translational efficiency, it was replaced with a synthetic 2A element. This sequence was previously characterized by Ibrahimi et. al (Ibrahimi, Velde et al. 2009), and was flanked by two identical sequences composed of three glycines, a serine, and three more glycines. The final construct was synthetically assembled as GGGSGGGEGRGSLLTCGDVEENPGPGGGSGGG and placed upstream of the *luxB* gene commercially (GeneArt). The purchased construct was cloned into $pLux_{AB}$ using the upstream EcoNI and downstream SalI restriction sites to replace the IRES element, creating the $pTa2A_{luxAB}$ plasmid, which contained a CMV promoter, the *luxA* gene, the Ta2A linker region, and the *luxB* gene.

Transfection of HEK293 cells

Transfection was carried out in six-well Falcon tissue culture plates (Thermo-Fisher). The day prior to transfection, HEK293 cells were passaged into each well at a concentration of approximately 1×10^5 cells/well and grown to 90 – 95% confluence in complete medium. The previously described $pLux_{CDEfrp}$:CO/$pLux_{AB}$ or $pLux_{CDEfrp}$:WT/$pLux_{AB}$ vectors (Close, Patterson et al. 2010) as well as the $pTa2A_{luxAB}$ plasmid were purified from a 100 ml overnight

culture of *E. coli* using the Wizard Purefection plasmid purification system (Promega). On the day of transfection, cell medium was removed and replaced and vector DNA was introduced using Lipofectamine 2000 (Invitrogen). Twenty-four h post-transfection, the medium was removed and replaced with complete medium supplemented with the appropriate antibiotic. Selection of successfully transfected clones was performed by refreshing selective medium every 4 – 5 d until all untransfected cells had died. At this time, colonies of transfected cells were removed by scraping, transferred to individual 25 cm^2 cell culture flasks, and grown in complete medium supplemented with the appropriate antibiotics.

***in vitro* bioluminescent measurement**

Total protein was extracted from co-transfected $pLux_{CDEfrp}$:CO/$pLux_{AB}$ or $pLux_{CDEfrp}$:WT/$pLux_{AB}$ cell lines (Close, Patterson et al. 2010) or the $pTa2A_{luxAB}$ transfected cell line using a freeze/thaw procedure. Cells were first grown to confluence in 75 cm^2 tissue culture flasks (Corning), then mechanically detached and resuspended in 10 ml of PBS. Following collection, cells were washed twice in 10 ml volumes of PBS, pelleted and resuspended in 1 ml PBS. These 1 ml aliquots of cells were subjected to three rounds of freezing in liquid nitrogen for 30 sec, followed by thawing in a 37°C water bath for 3 min. The resulting cell debris was pelleted by centrifugation at 14,000g for 10 min and the supernatant containing the soluble protein fraction was retained for analysis.

Bioluminescence was measured using an FB14 luminometer (Zylux) with a 1 sec integration time. To prepare the sample for *in vitro* bioluminescent

measurement, 400 μl of the isolated protein extract was combined with 500 μl of either oxidoreductase supplemented light assay solution containing 0.1 mM NAD(P)H, 4 μM FMN, 0.2% (w/v) BSA and 1 U of oxidoreductase protein isolated from *V. fischeri* (Roche), or oxidoreductase deficient light assay solution (distilled water substituted for the 1 U of oxidoreductase protein). Following the initial bioluminescent reading, samples were amended with 0.002% (w/v) n-decanal and the readings were continued to determine if additional aldehyde could increase light output. All bioluminescent signals were normalized to total protein concentration as determined by BCA protein assay (Pierce) and reported as relative light units (RLU)/mg total protein. All sample runs included processing of cell extracts from HEK293 cells stably transfected with $pLux_{AB}$ as a control for light expression upon amendment.

Results

in vitro supplementation assays to determine efficiency of gene function in vivo

Supplementation with NAD(P)H:flavin oxidoreductase protein

Previous work with the *lux* system in lower eukaryotes has shown the initial substrate, $FMNH_2$, to be a limiting reagent in the reaction (Gupta, Patterson et al. 2003). To determine if this was the case in HEK293 cells, *in vitro* supplementation assays were performed with the addition of 1 U of

NAD(P)H:Flavin oxidoreductase protein isolated from *Photobacterium fischeri*. Protein extracts from cells containing the *lux* genes in either their codon-optimized or wild-type forms were subjected to *in vitro* analysis to determine if the addition of oxidoreductase protein could improve light output. Upon addition of the flavin oxidoreductase protein, the average bioluminescent output increased from 1,400 (± 200) RLU/mg total protein to 111,500 (± 10,500) RLU/mg total protein in $pLux_{CDEfrp}$:WT containing cells (Figure 18A) and from 1,600 (± 200) RLU/mg total protein to 245,000 (± 20,500) RLU/mg total protein in $pLux_{CDEfrp}$:CO containing cells (Figure 18B).

Supplementation with aldehyde

The synthesized co-substrate required for light production in the *lux* system is a long chain aliphatic aldehyde that binds to the luciferase and is oxidized (Meighen 1991). The ability, conferred by the *luxCDE* genes, to produce and recycle the aldehyde substrate endogenously makes *lux* a uniquely beneficial reporter system. To assay for the production of aldehyde, cell extracts were supplemented with 0.002% (w/v) n-decanal, as this has previously been shown capable of functioning in place of the natural aldehyde substrate (Dunn, Michalis et al. 1973; Meighen, Bogacki et al. 1976; Gupta, Patterson et al. 2003; Szittner, Jansen et al. 2003; Patterson, Dionisi et al. 2005). When supplied with aldehyde, both the $pLux_{CDEfrp}$:WT and $pLux_{CDEfrp}$:CO containing cell extracts showed increases in bioluminescent output. Cell extracts from wild-type

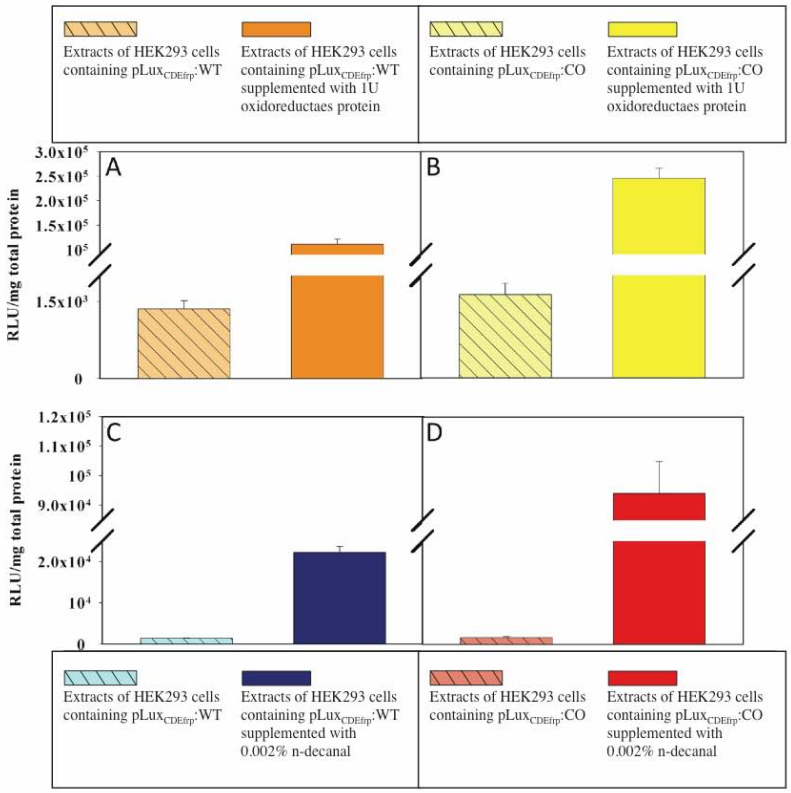

Figure 18. Supplementation assays demonstrating the functionality of the *luxCDEfrp* genes in the mammalian cell environment.

Supplementation with 1 U oxidoreductase protein significantly increased light output in cell extracts from (A) wild-type and (B) codon-optimized cell lines. Supplementation with 0.002% n-decanal resulted in increased bioluminescent output in both the (C) wild-type and (D) codon-optimized cell extracts as well, but at a lower magnitude than oxidoreductase supplementation. Values are the average of four trials, and are reported with the standard error of the mean. Originally published in (Close, Patterson et al. 2010).

containing cells showed an increase from 1,400 (± 200) RLU/mg total protein to 22,000 (± 1,500) RLU/mg total protein (Figure 18C). Extracts from codon-optimized cells increased from the baseline of 1,600 (± 200) RLU/mg total protein to 94,000 (± 10,800) RLU/mg total protein (Figure 18D).

Determination of bioluminescent output from HEK293 cells containing 2A linked luxAB genes

Five cell lines were recovered that stably expressed the 2A linked *luxAB* gene sequences following transfection with $pTa2A_{luxAB}$. These five lines were subjected to *in vitro* analysis to determine if they were capable of producing more light than approximately equal numbers of cells stably expressing the IRES linked *luxAB* gene sequences from $pLux_{AB}$. It was determined that the average bioluminescent signal from cells containing 2A linked *lux* genes was ~5500 (± 3700)% greater than that from cells with IRES linked *lux* genes. The major contributing factor to the large standard error of the mean was a single cell line that achieved 20,500% greater bioluminescent production than the $pLux_{AB}$ control (Table 11). When excluded from the calculations, this reduced the average bioluminescent production to ~1,800 (± 230)% over IRES linked gene expression.

Table 11. Bioluminescent expression from *in vitro* expression of *luxA* and *luxB* genes linked by 2A elements is consistently higher than that of IRES linked *luxA* and *luxB* genes.

	Bioluminescent Output (RLU/mg Protein)	% of Control
IRES linked *luxA* / *luxB*	1,719,940	N/A
2A linked *luxA* / *luxB* #1	21,103,893	1,227
2A linked *luxA* / *luxB* #2	35,885,713	2,087
2A linked *luxA* / *luxB* #3	29,711,493	1,728
2A linked *luxA* / *luxB* #4	352,781,297	20,511
2A linked *luxA* / *luxB* #5	38,499,816	2,238
HEK Neg	3,736	0

Discussion

Although the codon-optimized *lux* system is functioning at a level capable of producing bioluminescent detection under a wide array of conditions, it is clear that concentrations above the available levels of either the $FMNH_2$ (Figure 18 A and C) or aldehyde substrates (Figure 18 B and D) will result in increased bioluminescent output. However, an increase in aldehyde production can be cytotoxic, as has been demonstrated in *luxAB* containing *S. cerevisiae* and *Caenorhabditis elegans* cells (Hollis, Lagido et al. 2001). This may lead to a scenario where the *luxCDE* containing cells that most efficiently produce the aldehyde substrate are selected against during the initial period of growth following transfection with *luxCDEfrp* due to slowed growth and/or elevated cytotoxicity. The increased presence of aldehyde may therefore cause those cells capable of most efficiently producing aldehyde to inhibit their own growth, mimicking the effects of antibiotic selection and causing them to be out-competed in culture by cells expressing lower levels of aldehyde production. Mathematical models of the *lux* system have indicated that the production of light is much more sensitive to the aldehyde turnover rates modulated by the *luxCE* genes responsible for encoding the reductase and synthase that convert the myristyl acid to a myristyl aldehyde than it is to the concentration of luciferase dimer formed by the *luxAB* genes responsible for catalyzing the reaction and facilitating the production of light. The model predicts that a reduction in the concentration of the *luxC* or *luxE* gene products will lead to a drastic reduction in light output (Welham and Stekel 2009). If true, then it is hypothesized that the cytotoxicity of

aldehyde within the cell may be a non-issue in regards to selecting cell lines that can function in bioluminescent imaging assays. Cells with cytotoxic levels of aldehyde production will be removed early in the selection process due to slow growth rates and inability to compete with faster growing cell lines during the antibiotic selection phase following transfection. Similarly, cells with low levels of *luxCDE* expression will not generate high levels of bioluminescence during *in vitro* screening of *luxCDEfrp* containing cell lines. This would tend to encourage only the selection of cell lineages capable of producing just enough aldehyde to drive the *lux* reaction, but not enough to impair cellular growth and function, as platforms for biosensor development. Experiments aimed at determining if expression of the *lux* cassette genes (and, by extension, the products of their associated reactions) altered cellular metabolism and growth rates have supported these predictions.

As shown in Figure 18, the availability of $FMNH_2$ appears to contribute as a limiting reagent for the *lux* reaction in a mammalian cell environment. Supplementation with as little as 1 U of oxidoreductase protein *in vitro* led to relatively large (up to 151-fold) increases in bioluminescent output levels, while supplementation with 0.002% n-decanal produced less substantial (up to 58-fold) increases in light production. When supplemented with additional oxidoreductase protein to drive the turnover of FMN to $FMNH_2$, the average production of light increased by 82-fold in wild-type cell extracts (Figure 18A) and by 151-fold in extracts from cells containing codon-optimized *lux* genes (Figure 18B). The increases in light production attributed to additional $FMNH_2$ were

consistently of greater magnitude than those associated with aldehyde supplementation. The highest increase in light output achieved through addition of n-decanal was 58-fold in cells containing codon-optimized genes (Figure 18D), compared with only a 16-fold increase in light output from cell extracts co-transfected with the wild-type genes (Figure 18C). These results suggest that codon optimization of the remaining *luxCDE* genes from *P. luminescens* allows for more efficient processing of the available substrates in the mammalian cell environment, but does not allow for production levels that rival the ideal conditions of *in vitro* substrate supplementation where the bioluminescent output would be limited only by the efficiency of the LuxAB luciferase dimer. When supplemented with identical levels of aldehyde, cell extracts containing codon-optimized *luxCDEfrp* genes were able to produce over four times as much light as those containing the wild-type genes (Figure 18 C and D). A similar result was obtained under oxidoreductase supplementation, with extracts from the codon-optimized cell lines producing over twice as much light as their wild-type counterparts (Figure 18 A and B).

The data also indicate that the use of IRES elements is a contributing factor for inefficient bioluminescent expression in the mammalian cellular background. As demonstrated in Table 11, exchanging the IRES element for a 2A element lead to increased bioluminescent output in all cell lines that were stably isolated. It is important to note that during the process of Lipofectamine-based mammalian cell transfection, it is not possible to effectively control the location of gene insertion into the genome, nor is it possible to regulate the

number of integration events that take place. Taken together, these factors can help to explain the large discrepancy in bioluminescent output between clone number 4 and the remaining pTa2A$_{luxAB}$ transfected cell lines. It is conceivable that the resulting increase in bioluminescent production from cell line number 4 is the result of multiple *luxAB* gene insertions into the parental cell genome. Assuming all of these insertions remain under the control of the constitutively active CMV promoter, this will afford the cell with multiple locations for simultaneous production of LuxAB protein. Because all cell lines were tested *in vitro*, each was supplied with an identical level of the remaining required substrates for bioluminescent production. Under these circumstances, the cell line expressing the most LuxAB protein would be capable of producing the most light.

To compare and contrast the light output data, all readings are normalized to the total soluble protein concentration from each cell line. This method does not allow for determination of the total amount of Lux protein expression or even the ratio of Lux protein to endogenous protein available during the assay. As a result, there is no way to calculate if the increase in bioluminescent production is the result of multiple insertion events during the course of transfection, or if it is the result of increased up regulation of *luxAB* gene transcription due to their location within the genome. An additional explanation is that the *luxAB* genes transfected into clone number 4 were inserted into a euchromatic region of the genome as opposed to a more heterochromatic portion, or that they inserted near another strong promoter, which has caused them to be expressed at even

higher levels then would be found under the control of the CMV promoter alone. This explanation is less likely, however, because recent work has demonstrated that the CMV promoter is one of the most active promoters known in the HEK293 cellular environment (Qin, Zhang et al. 2010).

Regardless of the genetic reasons underlying the heightened bioluminescent production of clone number 4, it is important to note that the remaining 2A containing clones averaged ~1,800 (± 230)% over their IRES linked counterparts. This increase was relatively consistent (± 230%), indicating that increases in this range should be routinely achievable when IRES elements are exchanged for 2A elements. Although it is not yet known whether exchanging the IRES elements governing the expression of the remaining *lux* genes will have similar effects on autonomous bioluminescent expression, it is clear that the use of 2A elements are an attractive alternative due to their smaller size and increased efficiency at driving downstream gene expression.

CHAPTER VI

Summary And Conclusions

This investigation has lead to the development and documentation of the first published autonomously bioluminescent reporter system capable of functioning in the mammalian cellular environment. This type of system can be employed either in tandem or in replacement of traditional bioluminescent and fluorescent mammalian imaging systems such as firefly luciferase (Luc) and green fluorescent protein (GFP) to provide investigators with an additional tool for the interrogation of biological function in cell culture or small animal based imaging experiments. Although the mammalian-adapted bacterial luciferase (*lux*) system has not yet been subjected to enhancement and optimization, it can be deployed in its present state and used for the acquisition of data under protocols similar to those currently in place for alternative bioluminescent reporter proteins. The following conclusions have been drawn from this investigation in regards to the initial hypotheses:

Hypothesis 1: Through a process of poly-bicistronic expression of *Photorhabdus luminescence* genes codon-optimized for expression in mammalian cells it will be possible to autonomously produce a bioluminescent signal in the human HEK293 cell line.

It has been shown that poly-bicistronic expression of codon-optimized *P. luminescence lux* genes is capable of inducing constitutive bioluminescent production in the human HEK293 cell line. The codon optimization process was not shown to alter the pattern of bioluminescent expression over time as compared to expression of the wild-type genes, however, it has been demonstrated that the codon-optimization process leads to increased bioluminescent production. This increase is presumably due to the enhanced efficiencies in transcription and translation associated with the codon optimization process (Kim, Oh et al. 1997; Slimko and Lester 2003; Mechold, Gilbert et al. 2005; Barrett, Sun et al. 2006). Despite the production and regeneration of potentially cytotoxic substrates required for constitutive bioluminescent production, the expression of codon-optimized *lux* genes has not been shown to negatively effect the growth rate of their host cells as compared to untransfected control cells. The production of a stable bioluminescent signal without a corresponding reduction in cellular growth rate has confirmed our initial hypothesis that continuous bioluminescent production is possible in the HEK293 cell line using codon-optimized *lux* gene sequences.

Hypothesis 2: Bioluminescent expression driven by codon-optimized bacterial luciferase genes will allow improved temporal detection of signal compared to bioluminescent signal from firefly luciferase and fluorescent signal from green fluorescent protein in HEK293 cell culture and nude mouse models.

The bioluminescent signal resulting from expression of the mammalian-adapted *lux* genes is stable over prolonged time periods as compared to that of substrate dependent luciferase proteins and therefore allows for detection at multiple time points throughout the life of the host cell. While multiple signal detection is possible using repeated luciferin injections with alternative bioluminescent systems, the *lux* system allows for increased resolution by circumventing the requirement for luciferin clearance from the host prior to secondary image acquisition. This allows investigators using the *lux* system to achieve greater resolution of their visualized process by virtue of increasing the total amount of images they can obtain within a given time period. In addition, the substrate independent nature of the *lux* system provides investigators with a larger window for imaging small animal hosts by freeing them from the requirement of imaging at the same time point post substrate addition in order to accurately compare data obtained from multiple time point studies. These major considerations are all above and beyond the alleviation of standard concerns related to the efficiency and consistency of substrate injection that must be considered for any experiment utilizing conventional, exogenous luciferin-dependent bioluminescent systems.

While these concerns can also be avoided by imaging with a fluorescent imaging target, the *lux* system has the advantage of producing a bioluminescent signal with relatively low background in the mammalian cellular environment. As such, the *lux* system has proven to require a lower reporter cell population in order to successfully differentiate the signal from background light detection in

both cell culture and small animal imaging conditions than its fluorescent counterpart GFP. These combined advantages support our hypothesis that *lux*-based bioluminescent expression provides an improved system for temporal detection of signal as compared to the Luc and GFP systems, however, this statement must be considered in light of the relatively decreased bioluminescent flux of the *lux* system in its current state. Both the Luc and GFP systems display a greater photonic flux than does the *lux* system for an equal number of cells. When imaging in the mammalian cellular environment, this is especially important because the increased flux can overcome the negative effects of scattering and absorption of detection signal photons due to endogenous chromophoric material (Chance, Cope et al. 1998; Welsh and Kay 2005). For this reason, the *lux* system may not always be an ideal choice of reporter for mammalian imaging, especially if the detection signal is originating from depths lower than a few millimeters of tissue. Under these conditions the advantages of a higher flux system such as Luc may outweigh the disadvantages imposed by its requirement for exogenous substrate addition. The choice of an appropriate reporter system must therefore be made on a case-by-case basis at the discretion of the investigator.

Hypothesis 3: By regulating the expression of the *luxC* and *luxE* genes from the bacterial luciferase gene cassette it will be possible to construct a bioluminescent reporter capable of responding to changes in target analyte presence autonomously and in a near real-time manner.

This investigation has demonstrated the proof-in-principle work showing that regulation of the *luxC* and *luxE* genes under control of a tetracycline response element is capable of regulating bioluminescent production in a dose-response fashion, concurrent with administration of the activator chemical doxycyline. Unfortunately, the results did not demonstrate a relatively large increase in bioluminescent production in response to doxycyline treatment, nor did they show induction of bioluminescent production across a wide range of doxycycline concentrations. While the results obtained indicate that a tetracycline receptor-based, *luxC* and *luxE* regulated biosensor is not yet ready for routine laboratory use, they do show that regulating the production and regeneration of the myristyl aldehyde substrate within the mammalian cellular environment is a suitable method for controlling bioluminescent production from the host cell. These results can serve as a springboard for future optimization and design of *lux*-based bioreporters capable of responding to mammalian bioavailable target analytes.

Hypothesis 4: HEK293 cells constitutively expressing bioluminescence through expression of the codon-optimized bacterial luciferase genes will be capable of acting as real-time biosensors to determine the mammalian bioavailability of toxic chemicals.

Exposure of constitutively bioluminescent HEK293 cells to the cytotoxic aldehyde n-decanal demonstrated a reduced level of bioluminescent production from cells exposed to concentrations at or above 0.01% of the toxicant. This

level of treatment is in line with previously published reports for aldehyde toxicity (Rogers and McElroy 1958), supporting the hypothesis that continuously bioluminescent cell lines can be developed into successful screening tools for detection of mammalian bioavailable cytotoxic chemicals. The most important finding from this line of inquiry is that fluctuations in bioluminescent production can be detected during periods of transition from good to poor cellular health. The ability to detect these transition periods is intrinsic to the autonomous nature of the *lux* reaction. While it would be possible to visualize these fluctuations using other bioluminescent reporter systems such as Luc, the costs and logistical concerns related to the constant perfusion of luciferin would make these assays unfeasible for both basic and high throughput screening applications.

Similarly, detection of these transition periods would prove problematic using the commonly available fluorescent reporters, but for different reasons. The short time period repeated imaging necessary to obtain the resolution required for viewing small fluctuations in fluorescent production would entail repeated administration of fluorescent excitation signals. If not provided with a suitable recovery period between excitation signal applications, the fluorescent reporter system could succumb to photobleaching, thereby rendering the results suspect (Widengren and Rigler 1996).

In addition, both the fluorescent reporter proteins and the non-*lux* bioluminescent reporter proteins derive their resulting photon production signal from access to an exogenously supplied signal (either an excitation light signal for fluorescent reporters, or a chemical luciferin addition for bioluminescent

reporters). As a result, they would remain capable of producing an emission signal regardless of changes in cellular health and metabolism, so long as the reporter protein has not been degraded beyond use. This makes it challenging to link changes in their resulting light expression signals to changes in cellular health over relatively short time scales. Because the *lux* system is responsible for continuously producing and regenerating its substrates using endogenously available cellular materials it will be more adversely affected by changes in cellular function than the alternative reporter systems would be over the same time scale. This imparts a greater level of detection resolution to the *lux* system than would be available for a similarly designed Luc or GFP-based system. While additional work will be required before the mammalian-adapted *lux* system can be employed for high throughput mammalian bioavailability toxicology screening, the results demonstrated here suggest that it has excellent potential for use in this field.

List Of References

Airth, R. L., W. C. Rhodes, et al. (1958). "The function of coenzyme-A in luminescence." Biochim. Biophys. Acta **27**(3): 519-532.

Allen, M. S., J. R. Wilgus, et al. (2007). "A destabilized bacterial luciferase for dynamic gene expression studies." Syst. Synth. Biol. **1**: 3-9.

Almashanu, S., B. Musafia, et al. (1990). "Fusion of *luxA* and *luxB* and its expression in *Escherichia coli*, *Saccharomyces cerevisiae* and *Drosophila melanogaster*." J. Biolumin. Chemilumin. **5**(2): 89-97.

Ando, Y., K. Niwa, et al. (2007). "Firefly bioluminescence quantum yield and colour change by pH-sensitive green emission." Nature Photonics **2**(1): 44-47.

Angers, S., A. Salahpour, et al. (2000). "Detection of B_2-adrenergic receptor dimerization in living cells using bioluminescence resonance energy transfer (BRET)." Proc. Natl. Acad. Sci. U. S .A. **97**(7): 3684-3689.

Audigier, S., J. Guiramand, et al. (2008). "Potent activation of FGF-2 IRES-dependent mechanism of translation during brain development." RNA-Publ. RNA Soc. **14**(9): 1852-1864.

Baggett, B., R. Roy, et al. (2004). "Thermostability of firefly luciferases affects efficiency of detection by in vivo bioluminescence." Mol. Imaging **3**(4): 324-332.

Baker, M. (2010). "The whole picture." Nature **463**(7283): 977-980.

Baldwin, T. O., L. H. Chen, et al. (1987). Structural analysis of bacterial luciferase. Flavins and Flavoproteins Berlin, Walter de Gruyter & Co.**:** 621-631.

Baldwin, T. O., J. A. Christopher, et al. (1995). "Structure of bacterial luciferase." Curr. Opin. Struct. Biol. **5**(6): 798-809.

Barrett, J. W., Y. M. Sun, et al. (2006). "Optimization of codon usage of poxvirus genes allows for improved transient expression in mammalian cells." Virus Genes **33**(1): 15-26.

Belas, R., A. Mileham, et al. (1982). "Bacterial bioluminescence - isolation and expression of the luciferase genes from *Vibrio harveyi*." Science **218**(4574): 791-793.

Bhaumik, S. and S. S. Gambhir (2002). "Optical imaging of *Renilla* luciferase reporter gene expression in living mice." Proc. Natl. Acad. Sci. U. S. A. **99**(1): 377-382.

Bloch, S., F. Lesage, et al. (2005). "Whole-body fluorescence lifetime imaging of a tumor-targeted near-infrared molecular probe in mice." J. Biomed. Opt. **10**(5): Article #054003.

Boyle, R. (1666). "New experiments concerning the relation between light and air (in shining wood and fish)." Philos. T. R. Soc. **2**: 581-600.

Branchini, B. R., R. A. Magyar, et al. (1998). "Site-directed mutagenesis of histidine 245 in firefly luciferase: A proposed model of the active site." Biochemistry **37**(44): 15311-15319.

Branchini, B. R., M. H. Murtiashaw, et al. (2002). "Yellow-green and red firefly bioluminescence from 5,5-dimethyloxyluciferin." J. Am. Chem. Soc. **124**(10): 2112-2113.

Bumann, D. and R. H. Valdivia (2007). "Identification of host-induced pathogen genes by differential fluorescence induction reporter systems." Nat. Protocols **2**(4): 770-777.

Burdette, J. (2008). "*In vivo* imaging of molecular targets and their function in endocrinology." Journal of Molecular Endocrinology **40**(6): 253.

Caceres, G., X. Zhu, et al. (2003). "Imaging of luciferase and GFP transfected human tumours in nude mice." Luminescence **18**(4): 218-223.

Campbell, N. A., J. B. Reece, et al. (2007). Biology, Benjamin Cummings.

Campbell, Z. T., A. Weichsel, et al. (2009). "Crystal structure of the bacterial luciferase/flavin complex provides insight into the function of the beta subunit." Biochemistry **48**(26): 6085-6094.

Chalfie, M., Y. Tu, et al. (1994). "Green fluorescent protein as a marker for gene expression." Science **263**: 802-805.

Chance, B., M. Cope, et al. (1998). "Phase measurement of light absorption and scatter in human tissue." Review of scientific instruments **69**(10): 3457-3481.

Chang, S. T., H. J. Lee, et al. (2004). "Enhancement in the sensitivity of an immobilized cell-based soil biosensor for monitoring PAH toxicity." Sens. Actuators B **97**: 272-276.

Chattoraj, M., B. A. King, et al. (1996). "Ultra-fast excited state dynamics in green fluorescent protein: Multiple states and proton transfer." Proc. Natl. Acad. Sci. U. S. A. **93**(16): 8362-8367.

Choi, O., K. K. Deng, et al. (2008). "The inhibitory effects of silver nanoparticles, silver ions, and silver chloride colloids on microbial growth." Water Res. **42**(12): 3066-3074.

Choy, G., S. O Connor, et al. (2003). "Comparison of noninvasive fluorescent and bioluminescent small animal optical imaging." Biotechniques **35**(5): 1022-1031.

Close, D. M., S. S. Patterson, et al. (2010). "Autonomous bioluminescent expression of the bacterial luciferase gene cassette (*lux*) in a mammalian cell line." PLoS ONE **5**(8): e12441.

Close, D. M., S. Ripp, et al. (2009). "Reporter proteins in whole-cell optical bioreporter detection systems, biosensor integrations, and biosensing applications." Sensors **9**(11): 9147-9174.

Colepicolo, P., K. W. Cho, et al. (1989). "Growth and luminescence of the bacterium *Xehorhabdus luminescens* from a human wound." Appl. Environ. Microbiol. **55**(10): 2601-2606.

Contag, C. H. and M. H. Bachmann (2002). "Advances in *in vivo* bioluminescence imaging of gene expression." Annu. Rev. Biomed. Eng. **4**: 235-260.

Contag, C. H., P. R. Contag, et al. (1995). "Photonic detection of bacterial pathogens in a living host." Molec. Micro. **18**: 593-603.

Conti, E., N. P. Franks, et al. (1996). "Crystal structure of firefly luciferase throws light on a superfamily of adenylate-forming enzymes." Structure **4**(3): 287-298.

Crameri, A., E. Whitehorn, et al. (1996). "Improved green fluorescent protein by molecular evolution using DNA shuffling." Nature Biotechnology **14**(3): 315-319.

Cubitt, A. B., R. Heim, et al. (1995). "Understanding, improving and using green fluorescent proteins." Trends Biochem. Sci. **20**(11): 448-455.

Daniel, R., R. Almog, et al. (2008). "Modeling and measurement of a whole-cell bioluminescent biosensor based on a single photon avalanche diode." Biosens. Bioelectron. **24**(4): 882-887.

Daniel, R., R. Almog, et al. (2009). "Development of a quantitative optical biochip based on a double integrating sphere system that determines absolute photon number in bioluminescent solution: application to quantum yield scale realization." Appl. Optics **48**(17): 3216-3224.

de Felipe, P. (2004). "Skipping the co-expression problem: the new 2 A" CHYSEL" technology." Genetic Vaccines and Therapy **2**(1): 13.

DeLuca, M. (1969). "Hydrophobic nature of active site of firefly luciferase." Biochemistry **8**(1): 160-166.

DeLuca, M., J. Wannlund, et al. (1979). "Factors affecting the kinetics of light emission from crude and purified firefly luciferase." Anal. Biochem. **95**(1): 194-198.

Denburg, J. L., R. T. Lee, et al. (1969). "Substrate-binding properties of firefly luciferase. I. Luciferin binding site." Arch. Biochem. Biophys. **134**(2): 381-394.

Deroose, C. M., A. De, et al. (2007). "Multimodality imaging of tumor xenografts and metastases in mice with combined small-animal PET, small-animal CT, and bioluminescence imaging." Journal of Nuclear Medicine **48**: 295-303.

Dorn, J. G., M. K. Mahal, et al. (2004). "Employing a novel fiber optic detection system to monitor the dynamics of in situ *lux* bioreporter activity in porous media: system performance update." Anal. Chim. Acta **525**(1): 63-74.

Doudoroff, M. (1942). "Studies on the luminous bacteria II. Some observations on the anaerobic metabolism of facultatively anaerobic species." J. Bacteriol. **44**(4): 461 - 467.

Drepper, T., T. Eggert, et al. (2007). "Reporter proteins for in vivo fluorescence without oxygen." Nat. Biotechnol. **25**(4): 443-445.

Dunn, D. K., G. A. Michalis, et al. (1973). "Conversion of aldehyde to acid in bacterial bioluminescent reaction." Biochemistry **12**(24): 4911-4918.

Ehrmann, M. A., C. H. Scheyhing, et al. (2001). "In vitro stability and expression of green fluorescent protein under high pressure conditions." Lett. Appl. Microbiol. **32**(4): 230-234.

Ekwall, B., V. Silano, et al. (1990). Toxicity Tests with Mammalian Cell Cultures. Short-term Toxicity Tests for Non-genotoxic Effects. P. Bourdeau, John Wiley & Sons Ltd**:** 75 - 98.

Elman, N. M., H. Ben-Yoav, et al. (2008). "Towards toxicity detection using a lab-on-chip based on the integration of MOEMS and whole-cell sensors." Biosens. Bioelectron. **23**(11): 1631-1636.

Eltoukhy, H., K. Salama, et al. (2006). "A 0.18-um CMOS bioluminescence detection lab-on-chip." IEEE J. Solid-State Circuit **41**(3): 651-662.

Engebrecht, J., K. Nealson, et al. (1983). "Bacterial bioluminescence: isolation and genetic analysis of functions from *Vibrio fischeri*." Cell **32**: 773-781.

Escher, A., D. J. Okane, et al. (1989). "Bacterial luciferase alpha-beta fusion protein is fully active as a monomer and highly sensitive *in vivo* to elevated temperature." Proc. Natl. Acad. Sci. U. S. A. **86**(17): 6528-6532.

Fisher, A. J., F. M. Raushel, et al. (1995). "Three-dimensional structure of bacterial luciferase from *Vibrio harveyi* at 2.4. ANG. resolution." Biochemistry **34**(20): 6581-6586.

Fontes, R., B. Ortiz, et al. (1998). "Dehydroluciferyl-AMP is the main intermediate in the luciferin dependent synthesis of Ap(4)A catalyzed by firefly luciferase." FEBS Lett. **438**(3): 190-194.

Fraga, H. (2008). "Firefly luminescence: A historical perspective and recent developments." Photochem. Photobiol. Sci. **7**(2): 146-158.

Freundlieb, S. (2007). The tet system: powerful, inducible gene expression. Clontechniques. Clontech. Mountain View, CA, Clontech Laboratories Inc. **4:** 14-15.

Giepmans, B. N. G., S. R. Adams, et al. (2006). "Review - The fluorescent toolbox for assessing protein location and function." Science **312**(5771): 217-224.

Gossen, M. and H. Bujard (1993). "Anhydrotetracycline, a novel effector for tetracycline controlled gene expression systems in eukaryotic cells." Nucleic Acids Research **21**(18): 4411.

Gould, S. J. and S. Subramani (1988). "Firefly luciferase as a tool in molecular and cell biology." Anal. Biochem. **175**(1): 5-13.

Gupta, R. K., S. S. Patterson, et al. (2003). "Expression of the *Photorhabdus luminescens lux* genes (*luxA*, *B*, *C*, *D*, and *E*) in *Saccharomyces cerevisiae*." FEMS Yeast Research **4**: 305-313.

Gvakharia, B. O., P. J. Bottomley, et al. (2009). "Construction of recombinant *Nitrosomonas europaea* expressing green fluorescent protein in response to co-oxidation of chloroform." Appl. Microbiol. Biotechnol. **82**(6): 1179-1185.

Hakkila, K., T. Green, et al. (2004). "Detection of bioavailable heavy metals in EILATox-Oregon samples using whole-cell luminescent bacterial sensors in suspension or immobilized onto fibre-optic tips." J. Appl. Toxicol. **24**(5): 333-342.

Hanazono, Y., J. M. Yu, et al. (1997). "Green fluorescent protein retroviral vectors: Low titer and high recombination frequency suggest a selective disadvantage." Human Gene Ther. **8**(11): 1313-1319.

Hartung, T. (2009). "Toxicology for the twenty-first century." Nature **460**(7252): 208-212.

Hastings, J. W., W. D. McElroy, et al. (1953). "The effect of oxygen upon the immobilization reaction in firefly luminescence." J. Cell. Compar. Physl. **42**(1): 137-150.

Hastings, J. W. and K. H. Nealson (1977). "Bacterial bioluminescence." Annu. Rev. Microbiol. **31**: 549-595.

Heikkila, J. E., M. J. V. Vaha-Koskela, et al. (2010). "Intravenously administered alphavirus vector VA7 eradicates orthotopic human glioma xenografts in nude mice." PLoS ONE **5**(1): e8603. doi:8610.1371/journal.pone.0008603.

Heim, R., D. Prasher, et al. (1994). "Wavelength mutations and posttranslational autoxidation of green fluorescent protein." Proceedings of the National Academy of Sciences of the United States of America **91**(26): 12501.

Heim, R. and R. Tsien (1996). "Engineering green fluorescent protein for improved brightness, longer wavelengths and fluorescence resonance energy transfer." Current Biology **6**(2): 178-182.

Heitzer, A., K. Malachowsky, et al. (1994). "Optical biosensor for environmental on-line monitoring of naphthalene and salicylate bioavailability with an immobilized bioluminescent catabolic reporter bacterium." Appl. Environ. Microbiol. **60**: 1487-1494.

Hilderbrand, S. and R. Weissleder (2009). "Near-infrared fluorescence: application to *in vivo* molecular imaging." Current Opinion in Chemical Biology **14**(1): 71-79.

Hollis, R. P., C. Lagido, et al. (2001). "Toxicity of the bacterial luciferase substrate, n-decyl aldehyde, to *Saccharomyces cerevisiae* and *Caenorhabditis elegans*." FEBS Letters **506**(2): 140-142.

Honma, S., T. Yoshikawa, et al. (2010). Bioluminescent imaging for assessing heterogeneous cell functions in the mammalian central circadian clock. Molecular Imaging for Integrated Medical Therapy and Drug Development. N. Tamaki and Y. Kuge. New York, NY, Springer**:** 189-196.

Horry, H., T. Charrier, et al. (2007). "Technological conception of an optical biosensor with a disposable card for use with bioluminescent bacteria." Sens. Actuator B-Chem. **122**(2): 527-534.

Ibrahimi, A., G. Velde, et al. (2009). "Highly efficient multicistronic lentiviral vectors with peptide 2A sequences." Human Gene Therapy **20**(8): 845.

Inoue, Y., S. Kiryu, et al. (2009). "Comparison of subcutaneous and intraperitoneal injection of D-luciferin for *in vivo* bioluminescence imaging." European Journal of Nuclear Medicine and Molecular Imaging **36**(5): 771-779.

Islam, S., R. Vijayaraghavan, et al. (2007). "Integrated circuit biosensors using living whole-cell bioreporters." IEEE Transactions **54**(1): 89-98.

Ivask, A., T. Green, et al. (2007). "Fibre-optic bacterial biosensors and their application for the analysis of bioavailable Hg and As in soils and sediments from Aznalcollar mining area in Spain." Biosens. Bioelectron. **22**(7): 1396-1402.

Johnson, B. T. (2005). Microtox acute toxicity test. Small-Scale Freshwater Toxicity Investigations. C. Blaise and J. F. Ferard. Netherlands, Springer**:** 69-105.

Jung, G., J. Wiehler, et al. (2005). "The photophysics of green fluorescent protein: Influence of the key amino acids at positions 65, 203, and 222." Biophys. J. **88**(3): 1932-1947.

Kalchenko, V., S. Shivtiel, et al. (2006). "Use of lipophilic near-infrared dye in whole-body optical imaging of hematopoietic cell homing." J. Biomed. Opt. **11**(5): Article #050507.

Kelly, C. J., C. A. Lajoie, et al. (1999). "Bioluminescent reporter bacterium for toxicity monitoring in biological wastewater treatment systems." Water Environ. Res. **71**: 31-35.

Kim, C. H., Y. Oh, et al. (1997). "Codon optimization for high-level expression of human erythropoietin (EPO) in mammalian cells." Gene **199**(1-2): 293-301.

Kim, J., K. Urban, et al. (2010). "Non-invasive detection of a small number of bioluminescent cancer cells *in vivo*." PLoS One **5**(2): e9364.

Kirchner, G., J. L. Roberts, et al. (1989). "Active bacterial luciferase from a fused gene expression of a *Vibrio harveyi luxAB* translational fusion in bacteria, yeast and plant cells." Gene **81**(2): 349-354.

Knight, A. W., N. J. Goddard, et al. (1999). "Development of a flow-through detector for monitoring genotoxic compounds by quantifying the

expression of green fluorescent protein in genetically modified yeast cells." Meas. Sci. Technol. **10**(3): 211-217.

Koncz, C., O. Olsson, et al. (1987). "Expression and assembly of functional bacterial luciferase in plants." Proc. Natl. Acad. Sci. U. S. A. **84**(1): 131-135.

Lee, J. H. and M. B. Gu (2005). "An integrated mini biosensor system for continuous water toxicity monitoring." Biosens. Bioelectron. **20**(9): 1744-1749.

Lee, K., S. Byun, et al. (2003). "Cell uptake and tissue distribution of radioiodine labelled D-luciferin: implications for luciferase based gene imaging." Nuclear Medicine Communications **24**(9): 1003.

Leth, S., S. Maltoni, et al. (2002). "Engineered bacteria based biosensors for monitoring bioavailable heavy metals." Electroanalysis **14**(1): 35-42.

Lewis, S. M. and C. K. Cratsley (2008). "Flash signal evolution, mate choice, and predation in fireflies." Annu. Rev. Entomol. **53**: 293-321.

Liu, H. S., M. S. Jan, et al. (1999). "Is green fluorescent protein toxic to the living cells?" Biochem. Biophys. Res. Commun. **260**(3): 712-717.

Lorenz, W., R. McCann, et al. (1991). "Isolation and expression of a cDNA encoding Renilla reniformis luciferase." Proceedings of the National Academy of Sciences of the United States of America **88**(10): 4438.

Lupez-Lastra, M., A. Rivas, et al. (2005). "Protein synthesis in eukaryotes: the growing biological relevance of cap-independent translation initiation." Biological Research **38**: 121-146.

Markova, S., S. Golz, et al. (2004). "Cloning and expression of cDNA for a luciferase from the marine copepod Metridia longa: a novel secreted bioluminescent reporter enzyme." Journal of Biological Chemistry **279**(5): 3212.

Matz, M. V., A. F. Fradkov, et al. (1999). "Fluorescent proteins from nonbioluminescent Anthozoa species." Nature Biotechnol. **17**(10): 969-973.

McCapra, F. (1976). "Chemical mechanisms in bioluminescence." Accounts Chem. Res. **9**(6): 201-208.

McCapra, F., Y. C. Chang, et al. (1968). "Chemiluminescence of a firefly luciferin analogue." Chem. Commun.(1): 22-&.

McCapra, F., D. J. Gilfoyle, et al. (1994). The chemical origin of color differences in beetle bioluminescence. Bioluminescence and Chemiluminescence: Fundamental and Applied Aspects. A. K. Campbell, L. J. Kricka and P. E. Stanley. Chichester, Wiley.

McElroy, W. D. (1947). "The energy source for bioluminescence in an isolated system." Proc. Natl. Acad. Sci. U. S. A. **33**(11): 342-345.

McElroy, W. D., J. W. Hastings, et al. (1953). "The requirement of riboflavin phosphate for bacterial luminescence." Science **118**(3066): 385-386.

McElroy, W. D. and B. L. Strehler (1954). "Bioluminescence." Bacteriol. Rev. **18**(3): 177-194.

McMillin, D. W., J. Delmore, et al. (2010). "Tumor cell-specific bioluminescence platform to identify stroma-induced changes to anticancer drug activity." Nat. Med. **16**(4): 483-U171.

Mechold, U., C. Gilbert, et al. (2005). "Codon optimization of the BirA enzyme gene leads to higher expression and an improved efficiency of biotinylation of target proteins in mammalian cells." Journal of Biotechnology **116**(3): 245-249.

Meighen, E. A. (1979). "Biosynthesis of aliphatic aldehydes for the bacterial bioluminescent reaction stimulation by ATP and NADPH." Biochemical and Biophysical Research Communications **87**(4): 1080-1086.

Meighen, E. A. (1991). "Molecular biology of bacterial bioluminescence." Microbiological Reviews **55**(1): 123-142.

Meighen, E. A., I. G. Bogacki, et al. (1976). "Induction of fatty aldehyde dehydrogenase activity during development of bioluminescence in *Beneckea harveyi*." Biochemical and Biophysical Research Communications **69**(2): 423-429.

Mohler, S. (2010). "Tips on Buying and Working with Luciferin." Genetic Engineering and Biotechnology News **30**(4): 20-21.

Naylor, L. H. (1999). "Reporter gene technology: The future looks bright." Biochem. Pharmacol. **58**(5): 749-757.

Nemtseva, E. V. and N. S. Kudryasheva (2007). "The mechanism of electronic excitation in the bacterial bioluminescent reaction." Russ. Chem. Rev. **76**(1): 91-100.

Nivens, D. E., T. E. McKnight, et al. (2004). "Bioluminescent bioreporter integrated circuits: potentially small, rugged and inexpensive whole-cell biosensors for remote environmental monitoring." J. Appl. Microbiol. **96**(1): 33-46.

Niwa, H., S. Inouye, et al. (1996). "Chemical nature of the light emitter of the *Aequorea* green fluorescent protein." Proc. Natl. Acad. Sci. U. S. A. **93**(24): 13617-13622.

O'Neill, K., S. Lyons, et al. (2010). "Bioluminescent imaging: a critical tool in pre-clinical oncology research." The Journal of Pathology **220**(3): 317-327.

Olson, H., G. Betton, et al. (2000). "Concordance of the toxicity of pharmaceuticals in humans and in animals." Regulatory Toxicology and Pharmacology **32**(1): 56-67.

Olsson, O., A. Escher, et al. (1989). "Engineering of monomeric bacterial luciferases by fusion of *luxA* and *luxB* genes in *Vibrio harveyi*." Gene **81**(2): 335-347.

Ormo, M., A. Cubitt, et al. (1996). "Crystal structure of the *Aequorea victoria* green fluorescent protein." Science **273**(5280): 1392-1392.

Oshiro, M. (1998). "Cooled CCD versus intensified cameras for low-light video - Applications and relative advantages." Methods in Cell Biology **56**: 45-62.

Patterson, G. H., S. M. Knobel, et al. (1997). "Use of the green fluorescent protein and its mutants in quantitative fluorescence microscopy." Biophys. J. **73**(5): 2782-2790.

Patterson, S. S., H. M. Dionisi, et al. (2005). "Codon optimization of bacterial luciferase (*lux*) for expression in mammalian cells." Journal of Industrial Microbiology & Biotechnology **32**(3): 115-123.

Paulmurugan, R., Y. Umezawa, et al. (2002). "Noninvasive imaging of protein-protein interactions in living subjects by using reporter protein complementation and reconstitution strategies." Proc. Natl. Acad. Sci. U. S. A. **99**(24): 15608-15613.

Pazzagli, M., J. H. Devine, et al. (1992). "Use of bacterial and firefly luciferases as reporter genes in DEAE-dextran-mediated transfection of mammalian cells." Anal. Biochem. **204**(2): 315-323.

Polyak, B., E. Bassis, et al. (2001). "Bioluminescent whole cell optical fiber sensor to genotoxicants: system optimization." Sens. Actuator B-Chem. **74**(1-3): 18-26.

Prasher, D. C., V. K. Eckenrode, et al. (1992). "Primary structure of the *Aequorea victoria* green fluorescent protein." Gene **111**(2): 229-233.

Promega. (2009). "Technical Manual: pGL4 Luciferase." 2010, from http://www.promega.com/tbs/tm259/tm259.pdf.

Qin, J., L. Zhang, et al. (2010). "Systematic Comparison of Constitutive Promoters and the Doxycycline-Inducible Promoter." PLoS One **5**(5): e10611.

Ripp, S. (2009). Bacteriophage-based pathogen detection. Advances in Biochemical Engineering/Biotechnology: Whole Cell Sensing Systems. S. Belkin and M. B. Gu. New York, NY, Springer. **DOI 10.1007/10_2009_7**.

Ripp, S., K. A. Daumer, et al. (2003). "Bioluminescent bioreporter integrated circuit sensing of microbial volatile organic compounds." J. Ind. Microbiol. Biotechnol. **30**(11): 636-642.

Ripp, S., M. L. DiClaudio, et al. (2009). Biosensors as environmental monitors. Environmental Microbiology. R. Mitchell and J. D. Gu, John Wiley & Sons**:** 219-239.

Rogers, P. and W. D. McElroy (1958). "Enzymic determination of aldehyde permeability in luminous bacteria. 1. Effect of chain length on light emission and penetration." Archives of Biochemistry and Biophysics **75**(1): 87-105.

Rothert, A., S. K. Deo, et al. (2005). "Whole-cell-reporter-gene-based biosensing systems on a compact disk microfluidics platform." Anal. Biochem. **342**: 11-19.

Sanseverino, J., R. Gupta, et al. (2005). "Use of *Saccharomyces cerevisiae* BLYES expressing bacterial bioluminescence for rapid, sensitive detection of estrogenic compounds." Applied and Environmental Microbiology **71**(8): 4455.

Seliger, H. and W. McElroy (1960). "Spectral emission and quantum yield of firefly bioluminescence." Archives of Biochemistry and Biophysics **88**(1): 136-141.

Shetty, R. S., S. Ramanathan, et al. (1999). "Green fluorescent protein in the design of a living biosensing system for L-arabinose." Anal. Chem. **71**(4): 763-768.

Shimomura, O., F. Johnson, et al. (1962). "Extraction, purification and properties of aequorin, a bioluminescent protein from the luminous hydromedusan, *Aequorea*." Journal of cellular and comparative physiology **59**(3): 223-239.

Sizemore, C., W. Geissdorfer, et al. (1993). " Using fusions with *luxAB* from *Vibrio harveyi* MAV to quantify induction and catabolite repression of the *xyl* operon in *Staphylococcus carnosus* TM300." FEMS Microbiology Letters **107**(2-3): 303-306.

Slimko, E. M. and H. A. Lester (2003). "Codon optimization of *Caenorhabditis elegans* GluCl ion channel genes for mammalian cells dramatically improves expression levels." Journal of Neuroscience Methods **124**(1): 75-81.

Strehler, B. L., E. N. Harvey, et al. (1954). "The luminescent oxidation of reduced riboflavin or reduced riboflavin phosphate in the bacterial luciferin-luciferase reaction." Proc. Natl. Acad. Sci. U. S. A. **40**(1): 10-12.

Szittner, R., G. Jansen, et al. (2003). "Bright stable luminescent yeast using bacterial luciferase as a sensor." Biochemical and Biophysical Research Communications **309**(1): 66-70.

Thompson, E., S. Nagata, et al. (1989). "Cloning and expression of cDNA for the luciferase from the marine ostracod Vargula hilgendorfii." Proceedings of the National Academy of Sciences of the United States of America **86**(17): 6567.

Thouand, G., P. Daniel, et al. (2003). "Comparison of the spectral emission of lux recombinant and bioluminescent marine bacteria." Luminescence **18**(3): 145-155.

Troy, T., D. Jekic-McMullen, et al. (2004). "Quantitative comparison of the sensitivity of detection of fluorescent and bioluminescent reporters in animal models." Imaging **3**(1): 9-23.

Tsien, R. Y. (1998). "The green fluorescent protein." Annu. Rev. Biochem. **67**: 509-544.

Ugarova, N. N. (1989). "Luciferase of *Luciola mingrelica* fireflies - kinetics and regulation mechanism." J. Biolumin. Chemilumin. **4**(1): 406-418.

Vaupel, P., F. Kallinowski, et al. (1989). "Blood-flow, oxygen and nutrient supply, and metabolic microenvironment of human tumors - a review." Cancer Res. **49**(23): 6449-6465.

Verhaegen, M. and T. Christopoulos (2002). "Recombinant Gaussia luciferase. Overexpression, purification, and analytical application of a bioluminescent reporter for DNA hybridization." Anal. Chem **74**(17): 4378-4385.

Vervoort, J., F. Muller, et al. (1986). "Bacterial luciferase - A C-13, N-15, and P-31 nuclear magnetic resonance investigation." Biochemistry **25**(24): 8067-8075.

Vijayaraghavan, R., S. Islam, et al. (2007). "A bioreporter bioluminescent integrated circuit for very low-level chemical sensing in both gas and liquid environments." Sensors and Actuators B: Chemical **123**(2): 922-928.

Viviani, V. R. (2002). "The origin, diversity, and structure function relationships of insect luciferases." Cell. Mol. Life Sci. **59**(11): 1833-1850.

Vo-Dinh, T., Ed. (2003). Biomedical Photonics Handbook. Boca Raton, FL, CRC Press.

Wang, Y., Y. John, et al. (2008). "Fluorescence proteins, live-cell imaging, and mechanobiology: seeing is believing." Annual Review of Biomedical Engineering **10**(1): 1-38.

Ward, W. W. and M. J. Cormier (1978). "Energy transfer via protein-protein interaction in Renilla bioluminescence." Photochem. Photobiol. **27**(4): 389-396.

Welham, P. A. and D. J. Stekel (2009). "Mathematical model of the *Lux* luminescence system in the terrestrial bacterium *Photorhabdus luminescens*." Molecular Biosystems **5**(1): 68-76.

Wells, M. (2006). "Advances in optical detection strategies for reporter signal measurements." Curr. Opin. Biotechnol. **17**(1): 28-33.

Welsh, D. and S. Kay (2005). "Bioluminescence imaging in living organisms." Current Opinion in Biotechnology **16**(1): 73-78.

White, E. H. and B. R. Branchini (1975). "Modification of firefly luciferase with a luciferin analog - red light producing enzyme." J. Am. Chem. Soc. **97**(5): 1243-1245.

White, E. H., G. F. Field, et al. (1961). "Structure and synthesis of firefly luciferin." J. Am. Chem. Soc. **83**(10): 2402-2403.

White, E. H., E. Rapaport, et al. (1969). "Chemi- and bioluminescence of firefly luciferin." J. Am. Chem. Soc. **91**(8): 2178-2180.

White, E. H., M. G. Steinmetz, et al. (1980). "Chemi-luminescence and bioluminescence of firefly luciferin." J. Am. Chem. Soc. **102**(9): 3199-3208.

Widengren, J. and R. Rigler (1996). "Mechanisms of photobleaching investigated by fluorescence correlation spectroscopy." Bioimaging **4**(3): 149-157.

Wood, K., Y. Lam, et al. (1989). "Introduction to beetle luciferases and their applications." Journal of Bioluminescence and Chemiluminescence **4**(1): 289-301.

Wood, K., Y. Lam, et al. (1989). "Complementary DNA coding click beetle luciferases can elicit bioluminescence of different colors." Science **244**(4905): 700.

Yarranton, G. (1992). "Inducible vectors for expression in mammalian cells." Current Opinion in Biotechnology **3**(5): 506-511.

Yokoe, H. and T. Meyer (1996). "Spatial dynamics of GFP-tagged proteins investigated by local fluorescence enhancement." Nat. Biotechnol. **14**(10): 1252-1256.

Yotter, R. A., M. R. Warren, et al. (2004). "Optimized CMOS photodetector structures for the detection of green luminescent probes in biological applications." Sens. Actuator B-Chem. **103**(1-2): 43-49.

Yotter, R. A. and D. M. Wilson (2003). "A review of photodetectors for sensing light-emitting reporters in biological systems." IEEE Sens. J. **3**(3): 288-303.

Zacharias, D., J. Violin, et al. (2002). "Partitioning of lipid-modified monomeric GFPs into membrane microdomains of live cells." Science **296**(5569): 913.

Zhao, H., T. C. Doyle, et al. (2005). "Emission spectra of bioluminescent reporters and interaction with mammalian tissue determine the sensitivity of detection in vivo." J. Biomed. Opt. **10**(4): Article #041210.

Zimmer, M. (2002). "Green fluorescent protein (GFP): Applications, structure, and related photophysical behavior." Chem. Rev. **102**(3): 759-781.

Vita

Daniel Michael Close was born in Elgin, IL on December 10th, 1980. He grew up in Geneva, IL, where he attended Fox Ridge Elementary School, Geneva Middle School, and Marmion Military Academy. Upon successful completion of his primary education, Daniel enrolled in the School of Arts and Sciences at the University of Saint Louis, St. Louis, MO in the fall of 1999. He received a bachelors of science degree in biology and a certification in forensic science while graduating Suma Cum Laude in May of 2003.

Following graduation, Daniel worked for one year at a clinical laboratory in St. Charles, IL and two years as the acting laboratory manager for Dr. Toshio Narahashi at Northwestern University Medical School in Chicago, IL before beginning his graduate education at the Center for Environmental Biotechnology at The University of Tennessee, Knoxville under the direction of Dr. Gary Salyer in August of 2006.

Daniel will begin working as a post-doctoral fellow at the Joint Institute for Biological Sciences at Oak Ridge National Laboratory in Oak Ridge, TN in April, 2011.